



University
of Glasgow

Dobson, Helen Louise (1997) *The interaction of pulsed Nd:YAG laser irradiation with human enamel.*

PhD thesis

<http://theses.gla.ac.uk/4312/>

Copyright and moral rights for this thesis are retained by the author

A copy can be downloaded for personal non-commercial research or study, without prior permission or charge

This thesis cannot be reproduced or quoted extensively from without first obtaining permission in writing from the Author

The content must not be changed in any way or sold commercially in any format or medium without the formal permission of the Author

When referring to this work, full bibliographic details including the author, title, awarding institution and date of the thesis must be given

**THE INTERACTION OF PULSED ND:YAG LASER IRRADIATION
WITH HUMAN ENAMEL**

Helen Louise Dobson

Presented for the Degree of Doctor
of Philosophy in the Faculty of
Medicine, University of Glasgow

Oral Sciences, Dental Hospital
University of Glasgow
April 1997

© H L Dobson 1997

ABSTRACT

The aim of the work presented in this thesis was to investigate the interaction of pulsed Nd:YAG laser irradiation with both sound and artificially carious human enamel. More specifically, the aims were to characterise the effect of Nd:YAG laser irradiation on artificially created white spot enamel lesions (to simulate the effect of lasing carious enamel); to quantify the effects of pulsed Nd:YAG laser irradiation on enamel demineralisation; to investigate whether there is synergy between the action of pulsed Nd:YAG laser irradiation and fluoride in terms of imparting acid resistance to enamel; and finally to clarify the mechanism by which pulsed Nd:YAG laser irradiation physically interacts with enamel to induce acid resistance.

Laser irradiation of artificial white spot lesions, at 50 mJ and 100 mJ (10 pps, 2 or 5 sec), was found to ablate tissue, causing crater formation. Ablation depth, as determined by microdensitometry, was correlated only with the power used, being greater at 100 mJ than at 50 mJ. SEM examination of the surface morphology of lased enamel, and the surrounding unlased area, was consistent with a process of melting and recrystallisation. It is evident, from this investigation, that in order to remove carious enamel selectively, while leaving sound enamel intact, successive applications of low power irradiation (50 mJ) are the most suitable.

It is clear from this investigation, that Nd:YAG laser irradiation imparts a significant degree of acid resistance to the tooth surface. Laser irradiation of a single spot on a tooth surface, at 100 mJ or 150 mJ (30 sec, 10 and 20 pps respectively) led to a 60 % lower mineral loss than non-lased enamel, upon exposure to a demineralising regime. Irradiation at these parameters caused cratering of the enamel surface. A laser application of 150 mJ (20 pps) for 30 sec, over a measured area of a tooth, caused a 30 % inhibition of mineral loss. The surface of the enamel lased at this power also exhibited increased surface roughness and opacity. Enamel lased at 100 mJ (20 pps) was not significantly

different from non-lased enamel in terms of acid resistance, and had no visible surface changes.

Microradiography of single sections was a very good quantitative technique to analyse lased and non-lased enamel, and this *in vitro* model would be ideal for the further investigation of other laser parameters pertaining to acid resistance, and of combined preventive protocols.

There was no evidence that topical fluoride varnish (Duraphat®) acts in synergy with laser irradiation, to increase acid resistance. This is in contrast to previous research. This may be because lesions were formed in a manner which is more suitable as a model to reflect oral conditions, compared with the acid etching methods used by other researchers. The basis of the investigation in this thesis was its clinical relevance.

Finally, the infrared spectroscopy carried out in this project did not clarify the mechanism by which enamel exposed to laser irradiation gains a degree of acid resistance. It was difficult to draw any conclusions regarding carbonate content from this study, both because the number of samples was low and as the changes induced in enamel upon laser irradiation (melting and recrystallisation), suggest that it no longer conforms to a carbonate/phosphate structure compatible with this quantitative method.

The work presented in this thesis has indicated the versatility of the Nd:YAG laser as a dental instrument. The laser can be used to ablate carious enamel and has potential as a prophylactic treatment for caries. The most significant aspect of the laser as a strategy to prevent caries, is that it seems to physically alter the structure of enamel so may, therefore, be a method of permanently increasing tooth resistance to decay.

LIST OF CONTENTS

	PAGE
TITLE PAGE	I
ABSTRACT	II
TABLE OF CONTENTS	V
INDEX OF FIGURES	IX
INDEX OF TABLES	XIII
INDEX OF APPENDICES	XIV
PUBLICATIONS	XV
ACKNOWLEDGEMENTS	XVI
DECLARATION	XVII

Errata

Page IX, Figure 2.5; delete '51' and insert '49'

Page 5, line 8; delete 'Ca:P' and insert 'Ca:PO₄'

Page 7, line 11; delete 'refinable' and insert 'refined'

Page 23, line 16; after '(by diffusion and scattering)' insert 'of the light'.

Page 29, Table 1.1; substitute 'MHDP' for 'methyl hydroxy diphosphonate'

Page 29, Table 1.1; delete 'wrt HA' and insert 'with respect to hydroxyapatite'

Page 30, lines 4 and 24; delete 'photographic' and insert 'radiographic'

Page 30, line 9; delete 'kg.m³' and insert 'kg.m⁻³'

Page 35, line 12; delete 'technique' and insert 'techniques'

Page 44, line 4; delete 'Durpahat' and insert 'Duraphat'

Page 46, line 24; insert 'USA' after 'California'

Page 51, line 6; delete 'developed' and insert 'processed'

Page 59, line 2; delete 'Detre' and insert 'Detrey'

Page 60, line 3; insert 'UK' after 'Manchester'

Page 60, line 24; insert 'Poole' after 'Sigma Chemical'

Page 64, line 3; delete 'above (Section 6.2.1)' and insert 'in Section 6.2.1'

Page 66, line 23; insert '(10 pps)' after '5 sec'

Page 73, line 7; insert 'least squares' before 'r=0.33'

Page 90, line 5; delete 'table' and insert 'Tables'

Page 105, line 10; delete 'fluorine' and insert 'fluoride'

Page 132, line 12; delete 'calculated' and insert 'calculated'

Page 134, line 19; insert 'has' after 'which'

Page 135, line 13; delete 'enable exact determination of' and substitute 'ascertain from'

Page 135, line 14; delete 'from'

Page 166, line 5; delete 'phenomenain' and insert 'phenomena in'

Page 170, line 31; delete 'Californian Dental Association Journal' and substitute with 'Journal of the Californian Dental Association'



30114007327672

TABLE OF CONTENTS

CHAPTER 1 - Introduction and Literature Review		PAGE
1.1	Introduction and Aims	1
1.2	Enamel Development and Structure	2
1.2.1	Introduction	2
1.2.2	Enamel Development	2
1.3.2	The Structure of Mature Enamel	5
1.3	Dental Caries	7
1.3.1	Introduction	7
1.3.2	The Caries Process	7
1.4	Fluoride and its Influence on Caries Dynamics	12
1.4.1	Introduction	12
1.4.2	The Effect of Fluoride on Demineralisation	13
1.4.3	The Effect of Fluoride on Remineralisation	14
1.4.4	The Effect of Fluoride on Bacteria	15
1.4.5	Methods of Fluoride Administration	16
1.5	Lasers in Dentistry - An Overview	18
1.5.1	Introduction	18
1.5.2	Mechanism of Action (Laser Definition and Types)	20
1.5.3	Tissue Effects	22
1.6	Artificial White Spot Lesions	27
1.6.1	Introduction	27
1.6.2	Methods of Artificial White Spot Lesion Creation	28
1.7	Methods of Analysis of Mineral Changes	28
1.7.1	Introduction	28
1.7.2	Transverse (Contact) Microradiography	28
1.7.3	Longitudinal Microradiography	30
1.7.4	Wavelength Independent Microradiography	31
1.7.5	Polarized Light Microscopy	31
1.7.6	Microhardness	32
1.7.7	Scanning Electron Microscopy	33
1.7.8	Infrared Spectroscopy	34
1.7.9	Chemical Analysis	35

1.7.10 Iodine Permeability Testing	35
CHAPTER 2 - Materials & Methods (general)	36
2.1 Introduction	36
2.2 Tooth Selection, Preparation and Tissue Sampling	36
2.2.1 Introduction	36
2.2.2 Tooth Selection	37
2.2.3 Section Cutting	37
2.2.4 Section Grinding	39
2.3 Artificial White Spot Lesion Creation	39
2.3.1 Introduction	39
2.3.2 Whole Teeth	41
2.3.3 Sections	41
2.3.4 Demineralisation	41
2.4 Topical Fluoride Application	42
2.4.1 Introduction	42
2.4.2 Duraphat® Application	45
2.4.3 Fluoride Ion Measurement	46
2.5 The Nd:YAG Dental Laser	46
2.5.1 Introduction	46
2.5.2 Laser Treatment	48
2.6 Microradiography and Microdensitometry	50
2.6.1 Introduction	50
2.6.2 Microradiography	50
2.6.3 Microdensitometry	51
2.6.4 Measured Parameters	57
2.7 Scanning Electron Microscopy (SEM)	58
2.7.1 Introduction	58
2.7.2 Replica Creation	58
2.7.3 Sputter Coating	59
2.7.4 Scanning Electron Microscopy	59
2.8 Infrared Spectroscopy	60

2.8.1	Introduction	60
2.8.2	Production of a Standard Curve	60
2.8.3	Enamel Samples	63

CHAPTER 3 - The Effect of Pulsed Nd:YAG Laser Irradiation on Artificial White Spot Enamel Lesions

3.1	Introduction	65
3.2	Method and Materials	66
3.3	Results	68
	3.3.1 Microradiography	69
	3.3.2 SEM Analysis	73
3.4	Discussion	82

CHAPTER 4 - The effect of Pulsed Nd:YAG Laser Irradiation (Alone and in Conjunction with Fluoride Varnish), on Human Enamel Demineralisation

4.1	Introduction	85
4.2	Method and Materials	86
	4.2.1 Tooth Selection and Preparation	86
	4.2.2 Fluoride Application and Laser Parameters	86
	4.2.3 Section Preparation and Lesion Creation	87
	4.2.4 Microradiography and Microdensitometry	87
4.3	Results	88
	4.3.1 General Observations	88
	4.3.2 Lased versus Non-Lased Enamel	90
	4.3.3 Fluoride versus Non-Fluoride	99
	4.3.4 100 mJ versus 150 mJ	100
	4.3.5 Lased versus Non-Lased Enamel at Baseline	101
	4.3.6 Summary	101
4.4	Discussion	102

**CHAPTER 5 - The Effect of Pulsed Nd:YAG Laser Irradiation,
Applied in a Continuous Motion, on Human
Enamel Demineralisation**

5.1	Introduction	109
5.2	Method and Materials	110
	5.2.1 Tooth Selection and Preparation	110
	5.2.2 Laser Application	110
	5.2.3 Section Preparation and Lesion Creation	110
	5.2.4 Microradiography and Microdensitometry	112
5.3	Results	112
	5.3.1 General Observations	112
	5.3.2 Lased versus Non-Lased Enamel	113
	5.3.3 100 mJ versus 150 mJ	118
	5.3.4 Lased versus Non-Lased Enamel at Baseline	119
	5.3.5 Summary	119
5.4	Discussion	119

**CHAPTER 6 - An Investigation, by Infrared Spectroscopy, of Enamel
Exposed to Pulsed Nd:YAG Laser Irradiation**

6.1	Introduction	121
6.2	Method and Materials	122
	6.2.1 To Produce a Standard Curve	122
	6.2.2 Enamel Samples	123
6.3	Results	124
	6.3.1 Standards	124
	6.3.2 Enamel Samples	125
6.4	Discussion	129

CHAPTER 7 - Conclusions and Discussion 137

APPENDICES 142

BIBLIOGRAPHY 162

INDEX OF FIGURES

FIGURE	PAGE
1.1	10
<p>The pore structure of a carious lesion in human enamel. The translucent zone shows relatively large pores, numbers of which increase as the dark zone is approached. However, in the dark zone a micropore system is present in addition to the large pores. The body of the lesion shows an increased pore volume, with large pores which freely accept all imbibition media. The surface zone shows a low pore volume with a number of very small pores in addition to moderately large ones, similar to those of the translucent zone (from Silverstone <i>et al.</i>, 1981).</p>	
1.2	21
<p>Schematic diagram of a laser. The external energy source is pumped into an excited medium where it stimulates the atoms to an excited state. The photons which are subsequently emitted, resonate back and forwards between the two mirrors, inducing further photon emission, before leaving the tube in the form of a laser beam.</p>	
2.1	38
<p>The Labcut hard tissue saw for cutting 700 μm sections through the experimental sections.</p>	
2.2	40
<p>Ground glass plate, with Bauxilite powder slurry and gauze covered brass plate used for section grinding. The Mitutoyo digital micrometer for determination of section thickness.</p>	
2.3	43
<p>Artificial white spot enamel lesions which are an opaque white colour, with surface shine and integrity maintained.</p>	
2.4	47
<p>The Nd:YAG American Dental Laser, model dLase-300, and the optic fibre handpiece.</p>	
2.5	51
<p>The laser handpiece held stationary, in contact with, and perpendicular to the surface to be treated, by an adjustable jig.</p>	

Index of Figures (Contd)

FIGURE	PAGE	
2.6	Sections mounted in clingfilm covering the glass photographic plate. The aluminium step-wedge is placed alongside the sections. The sections, plate and step-wedge are placed in a photographic plate holder.	52
2.7	Black and white photograph of a developed microradiographic plate showing sections with artificial carious lesions and the aluminium step-wedge.	53
2.8	The Leitz microdensitometry system, incorporating a Leitz microscope, a video camera, an image analyser unit (ASBA) and a computer to process and store the information obtained.	54
2.9	The Advice Image Analysis Unit.	56
2.10	Measurement of baseline transmittance (automatically calculated by the computer). For the peak of interest of maximum absorbance at frequency ν , a baseline is drawn through ν_1 and ν_2 . The baseline is measured at the same frequency (ν) as the peak of interest.	62
3.1	Four lased spots on the artificial white spot lesion strips. The enamel was carbonised around the periphery of the crater. The craters formed using 100 mJ pulses (left hand side craters) were slightly larger than those formed at 50 mJ (right hand side craters).	67
3.2	The maximum depth (μm) of the craters formed by laser irradiation at 50 or 100 mJ, for 2 or 5 secs.	71
3.3	A typical microradiograph of a crater formed by lasing at 100 mJ for 2 sec. The original lesion on the enamel (seen here at the left of the lased crater) has been completely ablated, and the underlying enamel has been disrupted.	72
3.4	The width (μm) of the craters formed by laser irradiation at 50 or 100 mJ, for 2 or 5 secs.	74
3.5	Regression graphs of the lased crater widths against the original lesion characteristics.	75

Index of Figures (Contd)

FIGURE	PAGE
3.6 Regression graphs of the lased crater depths against the original lesion characteristics.	76
3.7 Typical SEMs of lased craters, which were arbitrarily scored into three groups a) group 1 - slight superficial melting over a diffuse, large area.	77
b) Group 2 - A distinct central crater shaped area, with well defined melting around the periphery of the crater onto non-ablated enamel.	78
c) Group 3 - A central area of deep ablation, with extensive surface melting. Layers of molten enamel are seen and there is little peripheral melting.	79
4.1 Enamel lased at 150 mJ often appeared smoother than the surrounding enamel and had a white opacity.	89
4.2 The mean measured parameters (± 1 sd) of the lased and non-lased enamel, of the non-fluoride treated samples.	95
4.3 The mean measured parameters (± 1 sd) of the lased and non-lased enamel, of the fluoride treated samples	96
4.4 A typical example of lesions formed on enamel which has been lased in a specific area. In both cases the lased enamel (150 mJ) is in the centre of the microradiograph, where the thicker surface zone and decreased demineralisation are clearly seen.	97
4.5 The release of fluoride ions from Duraphat [®] applied to enamel surfaces. A thin coat of Duraphat [®] was applied to windows on tooth surfaces (approx. 5 mm x 5 mm), then wiped off and rinsed with de-ionised water (as described in Section 2.4.2). Half of the samples were exposed to Nd:YAG laser irradiation across the whole of the Duraphat [®] covered area. All samples were placed in individual aliquots of de-ionised water and left for measured amount of time over a 24 hr period. The fluoride concentration of the water was measured after the samples were removed. The controls had no Duraphat [®] applied.	106

Index of Figures (Contd)

FIGURE	PAGE
5.1 The method used to prepare samples for the acid resistance experiment. Laser irradiation was applied in a continuous manner across the tooth surface.	111
5.2 The mean measured parameters (± 1 sd) of the lased and non-lased enamel samples.	117
6.1 Typical infrared spectra of the a) lased and b) non-lased enamel samples. The carbonate content of the enamel was calculated using the extinction ratio of the carbonate bands at 2340 cm^{-1} and the phosphate bands at 575 cm^{-1} .	128

INDEX OF TABLES

TABLE	PAGE
1.1 A summary of the methods used for artificial white spot lesion creation.	29
3.1 The mean microradiographic values for each measured parameter of the lesions and lased craters.	70
3.2 SEM scores of damage to white spot lesions, with the corresponding laser powers and depth measurement from each crater (whereby group 1 is superficial damage, group 2 is moderate ablation, and group 3 is extensive ablation - as described in Section 3.3.2)	81
4.1 Mineral content changes of each sample, after demineralisation, for the 100 mJ laser treatment, a) ΔZ , b) SZ, c) LB, d) LD (non-lased data is the mean of the upper and lower non-lased enamel).	91
4.2 Mineral content changes of each samples, after demineralisation, for the 150 mJ laser treatment, a) ΔZ , b) SZ, c) LB, d) LD (non-lased data is the mean of the upper and lower non-lased enamel).	92
4.3 The mean difference between baseline and demineralised enamel for each measured parameter of the lesions, at the a) 100 mJ and b) 150 mJ laser treatment (non-lased values are the mean of the upper and lower non-lased areas of enamel, adjacent to the lased area).	94
5.1 Change in mineral content parameters of each sample, after demineralisation, for the 100 mJ laser treatment, ΔZ (%Vol.min. μm), SZ (%Vol.min.), LB (Vol.min.) and LD (μm).	114
5.2 Change in mineral content parameters of each sample, after demineralisation, for the 150 mJ laser treatment, ΔZ (%Vol.min. μm), SZ (%Vol.min.), LB (Vol.min.) and LD (μm).	115
5.3 The mean difference between baseline and demineralised enamel for each measured parameter of the lesions, at the a) 100 mJ and b) 150 mJ laser treatment.	116

Index of Tables (Contd)

TABLE		PAGE
6.1	The mean extinction values (and the percentage error of the mean) of the ten successive readings, from each disc of the three blends.	126
6.2	The mean extinction values (and the percentage error of the mean) of the four discs from each blend, and the mean of the values from all three of the blends, at each standard.	127
6.3	The carbonate content of the enamel samples, calculated from their IR spectra.	130

INDEX OF APPENDICES

APPENDIX		PAGE
I	Derivation of the equation by Angmar <i>et al.</i> (1963)	142
II	The microradiographic measurements of crater depth, and width, lesion ΔZ , lesion body, lesion depth and surface zone, at each laser condition.	143
III	Microradiographic measurements of lesions on each area of enamel:	145
	Table 1: 100 mJ, non-fluoride treated samples.	145
	Table 2: 100 mJ, fluoride treated samples.	146
	Table 3: 150 mJ, non-fluoride treated samples.	148
	Table 4: 150 mJ, fluoride treated samples.	151
IV	Microradiographic measurements of lesions in a) the lased areas and b) the non-lased areas:	153
	Table 1: 100 mJ samples	153
	Table 2: 150 mJ samples	155
V	Extinction ratios of the carbonate:phosphate bands (E_{1415}/E_{575} - see Section 6.2.2), for three blends of the standard weight ratios (1:20, 1:10, 1:6, 1:5, 1:3, 2:5), four pressings from each blend, four discs per blend and the mean value.	157

PUBLICATIONS

- Dobson, H.L., Whitters, C.J., Creanor, S.L., Strang, R. & Foye, R.H. (1997)
Effects of an Nd:YAG laser & Duraphat® on enamel demineralisation.
Journal of Dental Research, 76, 213.
- Dobson, H.L., Whitters, C.J., Creanor, S.L., Strang, R. & Foye, R.H. (1996)
The effect of an Nd:YAG laser on human enamel demineralisation.
Journal of Dental Research, 75, 1182.
- Dobson, H.L., McGadey, J., Foye, R.H., Payne, A.P., Creanor, S.L. & Strang, R. (1995) The effect of an Nd:YAG laser on artificial white spot enamel lesions. *Journal of Dental Research*, 74, 872.

ACKNOWLEDGEMENTS

There are many people who have given me invaluable help during the past three years and to whom I would like to express my gratitude; here are just a few of them.

My supervisors, Dr. Ronnie Strang and Dr. Steve Creanor, for their advice, encouragement and guidance throughout this project. Mr. Richard Foye and Dr. John Whitters, who have provided help and suggestions during the three years, and Mr. Harper Gilmour, Mr. Jimmy McGadey and Dr. Ray Bailey for their expertise with technical aspects of this thesis.

Thanks must also go to my parents for their support - when they weren't on holiday - to Dr. Chris Fee, Alison Singley and Iain Macpherson for the many late night discussions, and Dr. Mark Sanderson for being some sort of role-model. Finally, thanks must go, of course, to Stuart Young, particularly for his ability to glaze over at any mention of my thesis, and direct the conversation onto other things.

I also acknowledge the financial support of the MRC.

DECLARATION

This thesis is the work of the author.

A handwritten signature in black ink, appearing to read "H. D. Ober." with a period at the end. The signature is written in a cursive style.

CHAPTER 1 - Introduction and Literature Review

1.1 Introduction & Aims

In western countries there has been a dramatic decline in dental caries over the past decade. This has been attributed to fluoride uptake in the form of water fluoridation and the increased use of topical fluoride agents. In economically developing countries, however, caries prevalence is increasing as dietary habits of industrialised nations are adopted. As treatment of caries does not confer immunity from subsequent attack, it is clear that the main focus of caries reduction must be on prevention. Existing preventive strategies, such as the use of fluoride agents, will, however, usually only delay the onset of caries and must be part of a continuous treatment regime.

Lasers have been used in dental research since 1963, and have potential for application in a range of dental procedures. Two main avenues of current laser research are the precise and efficient removal of enamel and dentine for cavity preparation (replacement of the dental drill), and the use of laser irradiation to impart acid resistance to enamel (as a caries preventive strategy). In determining safe and effective laser treatment modalities there are many variables which must be considered. These include differences between laser systems, wavelengths, treatment regimes and powers, tissue optical and thermal properties, and variations in patient healing and immune responses. Any particular combination of these factors must be tested before a treatment can be advocated.

The Nd:YAG American Dental Laser (dLase 300) was the first laser system to be designed specifically for use in dentistry. There is, however, little quantitative data regarding the efficacy and viability of this laser for various dental procedures.

The overall aim of this thesis was to investigate the interaction of pulsed Nd:YAG laser irradiation with both sound and artificially carious enamel. Specifically, the aim was to characterise the ablative effect of the laser on artificially created white spot enamel lesions (to simulate the effect of lasing carious enamel). Secondly, to quantify the effects of Nd:YAG irradiation on enamel demineralisation and investigate whether there is synergy between lasers and fluoride in terms of imparting acid resistance to enamel. The final aim was to clarify the mechanism by which laser irradiation physically interacts with enamel to induce acid resistance.

1.2 Enamel Development and Structure

1.2.1 Introduction

Tooth enamel is the hardest and most highly mineralised tissue in the body. It is made up of an inorganic mineral component and an organic component in the form of a protein matrix. Understanding how enamel is formed and acquires its high mineral content is fundamental in the understanding of its structural arrangement and behaviour under changing environmental conditions. There are two major processes in enamel formation (amelogenesis). First is the secretion of a protein matrix by ameloblasts (enamel forming cells); this is followed by the immediate mineralisation of the matrix and subsequent maturation of the enamel.

1.2.2 Enamel Development

During the bell stage of enamel development, under the influence of the internal enamel epithelium (IEE), some of the cells on the surface of the dental papilla differentiate into odontoblasts and begin to deposit a layer of dentine on the papillary side of the basal lamina. This is followed by differentiation of other IEE cells into pre-ameloblasts. With the increasing accumulation of pre-dentine, the basal lamina begins to disintegrate, through

lysosomal enzyme action. The distal surfaces of the pre-ameloblasts develop cytoplasmic processes, which push through the predentine and make contact with the odontoblastic processes. This is linked to the polarisation and further differentiation of the pre-ameloblasts into ameloblasts, which begin to secrete enamel matrix after dentine mineralisation begins.

The enamel matrix is a complex mixture of non-collagenous proteins, peptides, citric acid, carbohydrates (as glycoproteins and glycosaminoglycans) and lipids. Enamel proteins are glycosylated peptides, probably synthesised and secreted by ameloblasts. There are two classes of enamel proteins: amelogenins - (hydrophilic proline-rich glycoproteins) and enamelin (acidic glycoproteins with a high concentration of glycine, aspartic acid, serine and glutamic acid). Amelogenin is secreted first. The proteins are synthesised by the ameloblasts and contained within small cellular granules. On fusion of these granules with the ameloblast membrane the matrix is excreted from the cell onto the mineralised dentine, where it exists as an amorphous mass. The ameloblasts then decrease in length, withdrawing away from the dentine, and develop a 4 μm long conical extension (the Tomes process) at their distal ends. Initially, matrix is secreted from the entire distal surface of an ameloblast, but later it only occurs from the cervically inclined surfaces of the Tomes process.

The secreted matrix layer becomes invaded immediately by apatite crystal seeds. Calcium and phosphate travel from the capillary network of the follicle via ameloblasts and the stratum intermedium, which together control the influx of calcium through a Ca-adenosine triphosphatase pump. The mineralising front begins only 0.05 - 0.1 μm from the Tomes process. As soon as the crystallite nuclei appear, part of the matrix forms into elliptical tubuli (20 - 40 nm diameter) which surround the crystallites.

Before the Tomes processes have developed, the crystallites lie parallel to each other and no prism structure is apparent. Formation of the Tomes

processes enables the ameloblast to package the enamel crystallites into prisms, with a characteristic 'keyhole structure' (see Section 1.2.3). Four ameloblasts contribute to the formation of one prism. Each Tomes process is formed and directed such that the axes of the developing enamel rods begin with a slight deviation from the perpendicular to the plane of the first enamel layer, causing displacement between the horizontal rows of enamel. The ameloblasts move obliquely away from the forming tissue.

Mineralisation of the enamel prisms occurs in several phases. In the initial phase, immediately after secretion of the matrix, crystal seeds are deposited as described above. This is followed by an increase in mineral density through individual crystal growth; the crystallites increase in thickness and width. This mineral increase begins at the surface of the initially mineralised enamel that has reached its final thickness, and spreads toward the ADJ. When the mineralising front reaches the innermost layer of enamel, mineralisation proceeds back towards the outer enamel surface. The incisal and occlusal portions of enamel reach the fully matured condition first and the cervical portions last.

The advancing front of enamel formation lags behind that of dentine. The amelo-dentinal junction (ADJ) is the surface which separates the enamel from the coronal dentine. It is the region of the tooth where the enamel and dentine begin to form first; dome-shaped proturbances of the under surface of the enamel fit into depressions in the dentine surface. It is of clinical interest since it is an area where caries can spread laterally at an accelerated pace (see Section 1.3.2).

When immature enamel reaches its final, pre-determined thickness, the ameloblasts become shortened, their cytoplasmic structure is altered and their Tomes processes disappear (hence outer enamel has an aprismatic appearance). They are transformed into resorbing cells which draw water and excess matrix material out of the maturing enamel. The protein may be

actively removed by enzyme breakdown or squeezed out due to its thixotropic nature; remaining organic material exists between the prisms as the prism sheath. The rate of enamel formation and maturation varies from tooth to tooth and between different areas of a tooth; the average rate of formation is 4 μm per day.

1.2.3 The Structure of Mature Enamel

The inorganic component of enamel is an apatitic calcium phosphate, closely related to hydroxyapatite - $\text{Ca}_{10}(\text{PO}_4)_6(\text{OH})_2$. The Ca:P ratio varies between 1.8 and 2.4 (compared with 1.667 for hydroxyapatite). Small amounts of sodium, magnesium and potassium are present, and fluorine or chlorine can be substituted for the hydroxyl groups in the lattice. Enamel also contains 2 - 5 % wt carbonate which has replaced phosphate and hydroxyl groups in the lattice (Nelson & Featherstone 1982). The carbonate level rises markedly from the surface to the ADJ, whereas the concentrations of Ca and P tend to fall. Carbonate distribution appears to be fixed before the tooth erupts and is not substantially affected by exposure in the mouth (Weatherell *et al.*, 1968). There is a great deal of variation in composition between the teeth within the same mouth and also between different regions of a single tooth (principally with distance from the surface).

The mineral is arranged as hexagonal crystallites packed together into individual prisms or rods, covered occlusally by the prism sheath and embedded in the organic matrix (1 - 2 % of the mature enamel volume). In cross-section, prisms show a 'keyhole' appearance, and can be divided, descriptively, into a head and a tail portion. Within the head of the prisms crystallites are arranged with their long axes parallel to the long axis of the prism, but this orientation gradually alters throughout the prism and in the tail they lie at an angulation of 65 - 70 ° away from the prism axis. There are, therefore, abrupt changes in crystallite angulation between prisms which causes light diffraction and shows up the prism boundaries (the

interprismatic region). The unit volume mineral content in the head region is higher than average due to better organisation of the individual crystallites here, and the absence of organic material.

Enamel prisms extend continuously from a position near to the ADJ almost to the tooth surface, in a direction roughly perpendicular to the dentine surface. Individual prisms follow a tortuous, undulating course, especially in the cuspal area, which allows the otherwise brittle enamel to withstand a certain amount of compression force, as occurs during occlusion. Surface enamel is the last part of the enamel prism to form; it is harder and less soluble than the subsurface enamel and contains higher concentrations of fluoride and carbonate. In deciduous teeth, and 70 % of permanent teeth, this layer (30 µm wide) is aprismatic and the crystallites lie with their optical axes perpendicular to the enamel surface. The average width of a prism is 4 - 5 microns, but it enlarges as it approaches the enamel surface; the undulating course has a periodicity of 4 - 8 microns. The cross striations and Striae of Retzius seen on histological examination of enamel are probably due to rest phases during enamel formation, where there is a local change in crystallite orientation. Most of the water in mature enamel is bound to apatite crystals as a hydration shell.

Deciduous enamel is less mineralised than permanent enamel. Optically it is more opaque, which may represent greater porosity, it gives the clinical impression of wearing more quickly and it is less resistant to caries *in vitro* (Featherstone & Mellberg 1981; Shellis 1984a). During early mineralisation of human deciduous enamel, the innermost layer achieves relatively high levels of mineralisation rapidly, before the full thickness of enamel has been secreted. Shellis (1984a) indicated formation times of around 1 year for deciduous teeth compared with 3 - 5 years for the permanent dentition. Deciduous enamel is thinner than permanent enamel, and the relatively low mineral levels attained may be linked to the reduced time available for maturation - this may account for the different physical properties observed

(Wilson & Beynon, 1989).

1.3 Dental Caries

1.3.1 Introduction

Dental caries involves the progressive destruction of dental enamel by dissolution of mineral from the outer surface towards the dentine. It is a disease of bacterial origin; microorganisms on the surface of the tooth produce organic acids which dissolve the tooth mineral. Caries lesion formation is the cumulating effect of alternating mineral dissolution at low pH, and partial reprecipitation when the pH rises. The caries process is a complex interplay between teeth and factors in the oral environment, such as saliva, plaque and the availability of refinable carbohydrates.

1.3.2 The Caries Process

Bacteria in the plaque adhering to the tooth surface will ferment carbohydrates to produce organic acids, such as lactic and acetic acids. These acids cause a local drop in pH (also caused directly by the intake of acidic fruits or drinks) which is only partially counteracted by oral buffer systems (eg., saliva-phosphate, bicarbonate and protein systems; dissolution of organic material in plaque and calculus).

The acid will diffuse through plaque into the interprismatic channels in enamel where it dissociates into H^+ ions and anions; the dissociation rate is determined by the acid strength. The physico-chemical equilibrium between enamel and the intercrystallite fluid is disrupted, resulting in mineral dissolution and initiating lesion formation. Carbonate and magnesium-rich mineral will dissolve first (Hallsworth *et al.*, 1973, Robinson *et al.*, 1983), accumulate in the intercrystallite fluid and then migrate down a concentration gradient towards the enamel surface. The H^+ ions are adsorbed

onto the surfaces of the enamel crystallites and react with OH^- and PO_4^{3-} groups in the lattice to form H_2O and HPO_4^{2-} (Weatherell *et al.*, 1983). The resultant charge imbalances in the lattice and intercrystalline fluid render the lattice unstable. A loss of calcium and less strongly bound protonated phosphate groups from the lattice will convert it to a more stable, non-apatitic structure (Weatherell *et al.*, 1983).

The rate of diffusion of acid into the lesion, and solubilised mineral ions out, is usually the limiting factor of the demineralisation rate under a given acidogenic challenge (Vogel *et al.*, 1987, 1988). The composition of the lesion fluid will govern the driving force of diffusion for the various ions, and ultimately the rate of demineralisation. Dissolution of mineral ions from enamel crystallites produces a high concentration of dissolved ions in the surrounding intercrystalline fluid, and hence a steep concentration gradient of the mineral ions at the lesion front. As more enamel dissolves and the surface area for dissolution increases, so the inter-crystallite volume increases at a faster rate. The mineral ion concentration of the intercrystalline fluid will therefore become lower at the dissolution site than in the body of the lesion, thus encouraging lesion penetration into enamel (Robinson *et al.*, 1982). Featherstone & Rodgers (1981) showed lesion progression as a function of the unionised acid concentration and the acid dissociation constant. The increase in magnesium and carbonate concentrations towards the ADJ (Weatherell *et al.*, 1968; Robinson *et al.*, 1981) will accelerate lesion progression in this direction.

As the advancing lesion approaches the ADJ, the more rapid dentine demineralisation spreads towards the pulp and laterally under the sound enamel beneath the initial lesion. At this stage the surface enamel is intact and a lesion is only detected radiographically. After further demineralisation, however, the enamel and dentine become weakened and cavitate - giving bacteria deeper access to enamel and dentine. Breakdown of the enamel organic matrix by bacterial enzymes releases glutamic and aspartic acid -

leading to further mineral dissolution. These proteolytic enzymes may also remove the dentine collagen. Chelation of Ca^{2+} at neutral pH by carboxylic acid anions or carbohydrate derivatives produced by bacteria may have a minor contribution in mineral removal (Schatz, 1955). Bacteria may penetrate subsurface lesions and grow along dentinal tubules into mineralised areas (Brannström *et al.*, 1980). Eventually, if the process is unchecked, the lesion breaks into the pulp chamber which consequently becomes infected. The ensuing acute inflammatory response may result in non-vitality of the pulp or abscess formation.

The white spot lesion is the earliest macroscopic evidence of carious progress. It is a small, opaque white region seen when the tooth has dried; its optical appearance is due to increased light scattering within the porous enamel. There are four principal histological zones of the white spot lesion, as described by Darling (1956) using polarizing microscopy (see figure 1.1). The relatively intact surface zone is approximately 20 - 100 μm thick. The dark zone is the zone positioned deep beneath the body of the carious lesion, superficial to the translucent zone - the advancing front of the lesion. These zones are not distinct entities, but represent a continuum of changes as caries progresses. A clinical white spot is not a 'defined' enamel defect and may have various mineral distributions, including subsurface demineralisation and surface softening (Arends & ten Cate, 1981).

Subsequent mineral loss, and lesion progression, results in the formation of a surface zone overlying an area of subsurface demineralisation (Arends & Christofferson, 1986). The surface zone is a porous, but mineral rich, zone which forms after initial surface softening and, once formed, changes thickness slowly in comparison with the demineralisation period. When the natural enamel surface is removed prior to artificial caries attack, demineralisation is faster than in unabraded enamel (Kidd *et al.*, 1978). This has been explained by the higher mineral content, narrower diffusion pathways, different crystal orientation and/or by the lower carbonate

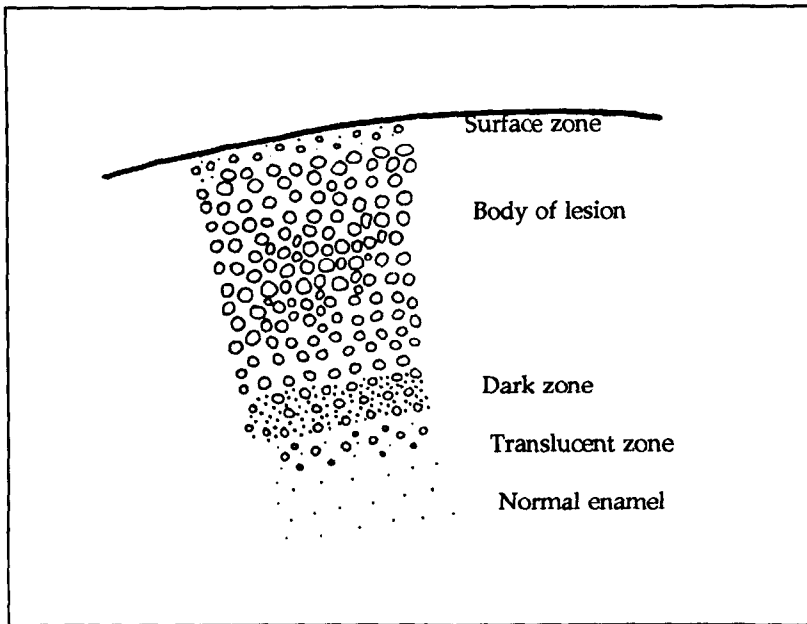


Figure 1.1. The pore structure of a carious lesion in human enamel. The translucent zone shows relatively large pores, numbers of which increase as the dark zone is approached. However, in the dark zone a micropore system is present in addition to the large pores. The body of the lesion shows an increased pore volume, with large pores which freely accept all imbibition media. The surface zone shows a low pore volume with a number of very small pores in addition to moderately sized ones, similar to those of the translucent zone (from Silverstone *et al.*, 1981).

concentration, and higher fluorapatite concentration in the surface compared with subsurface enamel.

The surface layer seems to be maintained by an equilibrium in which surface enamel is first partially dissolved, then continuously regenerated by dissolved calcium and phosphate ions diffusing from the subsurface enamel. Surface conditions may favour precipitation of fluorapatite and a solid phase of dicalcium phosphate dihydrate. Factors in the oral environment, such as the pellicle and acquired fluoride adsorbed onto the enamel surface, may also inhibit surface enamel dissolution while allowing acid penetration to the underlying enamel (Zahradnik *et al.*, 1976). Development of the surface zone appears to be due to the fluoride in saliva rather than in the enamel surface layers (Arends & Christoffersen, 1986).

The main factors governing the stability of enamel apatites are the concentrations of calcium, phosphate and fluoride in solution, and pH. If a solution is undersaturated with respect to these ions the solid will dissolve, but if the solution is supersaturated, the solid will precipitate. As pH decreases, the solubility of apatites increases. The implicit assumption in most studies of enamel solubility is that enamel is a hydroxyapatite with a higher solubility than synthetic hydroxyapatite. Although an oversimplification, this is useful in predicting enamel solubility and allowing the development of demineralisation models (Margolis & Moreno, 1985; Patel & Brown, 1975; Larsen & Jenson, 1989). The critical pH is that at which saliva is exactly saturated with respect to enamel apatite. When saliva is undersaturated with respect to hydroxyapatite but supersaturated with respect to fluorapatite, caries-like lesions with intact surfaces are formed; subsurface dissolution of hydroxyapatite occurs with simultaneous reprecipitation of fluorapatite.

The incidence of caries at specific sites on the tooth surface, rather than as widespread decalcification, indicates the importance of local conditions.

Plaque bacterial content will vary between areas and is a determining factor in the local occurrence of caries. Caries in different locations may be caused by different bacteria or combinations of bacteria. It is well established that the mineral content and caries susceptibility of human enamel varies greatly (Shellis, 1984b; Borsboom *et al.*, 1985; Strang *et al.*, 1986).

1.4 Fluoride and its Influence on Caries Dynamics

1.4.1 Introduction

The reduction of caries in the western world has been attributed to fluoride uptake in the form of water fluoridation, fluoride dentifrices and other topical agents. Armstrong & Brekhas (1938) suggested a link between the mottling of enamel and its high fluoride content; mottled enamel was stronger and more caries resistant than normal enamel. The work of Dean *et al.* (1942) further established fluoride as an agent for caries protection. Backer Dirks (1974), in a review of epidemiological studies, found a concentration of 1 ppm fluoride in water supplies led, in most cases, to over a 50 % reduction in caries, with higher fluoride concentrations resulting in only slightly lower caries scores. Although it is well established that fluoride is incorporated into dental apatite crystals during tooth development, the role of this systemic fluoride in caries prevention is debatable (Fejerskov *et al.*, 1981, Larsen & Jensen, 1985). Some studies found no relationship between the fluoride content of enamel, and caries (Shern *et al.*, 1977, Schamschula *et al.*, 1979). Others, however, indicate that low concentrations of fluoride in acid solution reduce enamel demineralisation (Arends *et al.*, 1983, ten Cate & Duijsters 1982, 1983). It is now known that fluoride acts in three main ways to inhibit caries - by inhibition of demineralisation, enhancement of remineralisation and effects on bacteria (ten Cate & Duijsters 1983a, 1983b).

1.4.2 The Effect of Fluoride on Demineralisation

Early assumptions were that the observed decrease in caries was due to the presence of fluoride during tooth formation, its incorporation into enamel and the associated decreased solubility of fluoride-containing crystallites (Frazier *et al.*, 1967). Ingested fluoride (from water, food and drinks, or supplements) may enter the tissue fluid surrounding the dental follicle and become incorporated into the apatite crystal lattice during amelogenesis. Fluoride ions replace hydroxyl (OH⁻) ions to form fluorapatite (FA), and a range of fluorohydroxyapatites (FHA) with various degrees of fluoride substitution. Strong binding of the fluoride ions to adjacent calcium ions gives fluorapatite a more compact and stable structure than hydroxyapatite (HA), making it less acid soluble (Brown *et al.*, 1977).

However, Nelson *et al.* (1983), found that structurally incorporating fluoride (up to 1000 ppm) into synthetic carbonated apatite did not influence its rate of dissolution, whereas concentrations of 1 ppm in the dissolution medium reduced the rate by 20 - 30 %. Similarly, Wong *et al.* (1987) found that 5 ppm fluoride in solution was more effective in reducing the rate of apatite dissolution than 1000 ug/g of fluoride either adsorbed on, or incorporated into the enamel mineral. Furthermore, low levels of fluoride in solution (1 - 2 ppm) have been shown to inhibit enamel demineralisation *in vitro* (ten Cate & Duijsters, 1983a, 1983b, Margolis *et al.*, 1986).

Tanaka *et al.* (1993) demonstrated that fluoride enrichment of enamel by exposure to acid buffers of relatively low fluoride concentrations, retards or prevents the formation of caries-like lesions. They found, however, that the fluoride incorporation involves dissolution of enamel and the reprecipitation of fluoridated apatite (Margolis *et al.*, 1986) rather than its exchange for hydroxyl ions on the surface of enamel crystals. The enamel became enriched with fluoride more than would occur from simple ion exchange. There was an inverse relationship between fluoride enrichment and the

extent of demineralisation when the enamel was exposed to acidic (non-fluoride) demineralising buffers.

Fluoride in the aqueous phase around enamel crystallites decreases their dissolution and is more important than fluoride incorporation in the crystal lattice. This may come from fluoride-rich apatite in the lesion area or the topical addition of fluoride. In a medium undersaturated with respect to enamel, enamel will dissolve at a given rate. However, in the presence of fluoride, the medium becomes more highly supersaturated with respect to fluorapatite, and the deposition of a fluoridated apatitic phase within the partially dissolved surface enamel will be accelerated (remineralisation), so reducing the net rate of mineral loss. When the rate of fluorapatite deposition is greater than the simultaneous rate of mineral loss, demineralisation will be inhibited.

1.4.3 The Effect of Fluoride on Remineralisation

There is some conflicting evidence as to the effect of fluoride on remineralisation. Amjad & Nancollas (1979) found low concentrations of fluoride (< 1 ppm) to inhibit apatite crystal growth, whilst at concentrations of 1 - 5 ppm, remineralisation was enhanced. Koulourides *et al.*, (1965), found remineralisation of surface softened enamel was enhanced *in vitro* when the remineralising solutions contained fluoride concentrations as low as 10^{-5} mol.L⁻¹. It is now generally established that fluoride enhances initial remineralisation of subsurface lesions *in vitro* (ten Cate, 1990; Varughese & Moreno, 1981). There are indications, from intra-oral models, that this also occurs *in vivo* (reviewed by Wefel, 1990).

Apatite crystal growth is accelerated in the presence of fluoride, and there is formation of fluorapatite and fluoridated hydroxyapatite (Amjad *et al.*, 1982). As these compounds have a lower solubility product than hydroxyapatite, remineralisation will, therefore, impart the greatest acid resistance to enamel

when it occurs in the presence of fluoride (Shellis, 1994). Fluorapatite can precipitate from a solution undersaturated with respect to hydroxyapatite (Larsen *et al.*, 1976), therefore when fluoride is present, remineralisation can occur at a lower pH.

As remineralisation of subsurface lesions is diffusion controlled, the low porosity of the surface layer may limit the rate of mineral uptake. It is important that the driving force for remineralisation (high supersaturation and fluoride concentration) is not too large, as crystal growth which is too rapid may cause blockage of the surface pores through which diffusion occurs. In this case the lesion would be arrested rather than remineralised (Arends & ten Cate, 1981; ten Cate, 1990). It is, therefore, considered optimal to maintain a constant, relatively low, fluoride concentration in the oral fluids, rather than increase the remineralisation rate excessively. Silverstone (1983) found maximum remineralisation occurred at a concentration of 0.05 mmol/L (1 ppm) at enamel surfaces.

1.4.4 The Effects of Fluoride on Bacteria

Fluoride present in an oral environment can be taken up and concentrated by the plaque microflora. It diffuses across bacterial membranes as hydrogen fluoride (HF), which then dissociates to H^+ and F^- . Fluoride uptake increases as external pH drops (Eisenberg & Marquis, 1980); the fluoride becomes bound within the bacterial cells. Most detrimental to bacteria, at a normal plaque fluoride concentration, is the action of fluoride in directly inhibiting the ATP-ase associated with proton expulsion. The resultant accumulation of H^+ within the cell may decrease the pH to below the optimum for catabolic and biosynthetic enzyme activity, preventing acid production. The fluoride does not need to enter the cell to act (Marquis, 1990). Entry of extra H^+ ions into the cells in the form of HF will further disrupt bacterial growth and metabolism (Hamilton, 1990).

1.4.5 Methods of Fluoride Administration

Water fluoridation has still not been widely implemented in most countries, its requirements of a reliable mains water supply and grid electricity system are not always able to be fulfilled. Other means of community-based fluoridation have, therefore, been investigated. Marthalar (1969) reported a 47 % caries reduction over an 8 yr period when tablets were given daily at school. In contrast, Stephen & Campbell (1978) reported an 81.3 % caries reduction in first permanent molars when school children were asked to let 1 mg F tablets slowly dissolve in the saliva, enabling fluoride concentrations of around 1000 ppm fluoride to be achieved, within the saliva. Drops and tablets, however, need good subject cooperation to maximise the benefit. Addition of fluoride to food, sweets and beverages eg. salt, is a means of both systemic and topical fluoridation (Wespi, 1948; Toth, 1976). Fluoridated salt has been introduced in Switzerland, Columbia and Hungary (350 mg fluoride per Kg). Although caries reductions as great as 60 % have been reported in trials (Toth, 1976), western countries tend to prefer more controlled methods of fluoride administration. Fluoridated milk has been proposed as a means of delivering fluoride, since it is consumed by those in greatest need of fluoride exposure (children and pregnant women), and has the added benefit of containing vitamins, calcium and phosphorous. Stephen *et al.* (1981) demonstrated a caries reduction of 73 % in erupting first permanent molars, but, overall, the 5 yr benefit of school based distribution was 38 %. Implementation on a wide scale would, however, be expensive and the logistics of quality control would be difficult. Hamberg (1971) demonstrated the 50 % caries inhibiting potential, up to 6 years of age, of fluoride combined with vitamin supplements. As most people appreciate the importance of vitamin supplements during pregnancy and childhood, this method of fluoride implementation appears to have been somewhat neglected.

The exact pre-eruptive fluoride concentration requirement is a matter of

debate, but any dosage regime must take into account the fluoride present, even at trace levels, in domestic water supplies, to prevent the occurrence of low-grade fluorosis.

The most commonly used topical fluoride preparations are dentifrices and mouthwashes, both of which provide frequent fluoride exposure (formulations differ only in fluoride source, concentration and pH). Professionally applied fluoride agents have historically included varnishes, gels and solutions; they contain a higher concentration of fluoride and are discussed in Section 2.4.

For topical fluoride treatments to be most effective, the fluoride should be present at its site of action for as long as possible. The majority of fluoride introduced into the mouth by a topical application, such as toothpaste, is cleared within an hour by salivary wash-out. Remaining fluoride, initially retained in oral reservoirs, is then released slowly into the saliva and cleared within a few hours (Duckworth & Morgan, 1991). Accumulation of fluoride has been demonstrated in both saliva and plaque using fluoride dentifrices or mouthwashes (Duckworth & Morgan, 1991; Geddes & McNee, 1982), indicating the existence of more stable fluoride reservoirs where fluoride remains after the second clearance phase (possibly stagnation zones on and between teeth, and plaque). As demineralised, porous enamel takes up significantly more fluoride than adjacent sound enamel, it can also act as a fluoride ion reservoir (Nelson *et al.*, 1983; Joyston-Bechal & Kidd, 1980; Koulourides *et al.*, 1965). The amount of fluoride taken up by early lesions and present at a cariogenic site will determine the efficacy of a product. Fluoride uptake, reaction and release into the enamel is dependent on contact duration with the agent.

Application of acidified agents to a tooth surface were known to dissolve some enamel but were thought to benefit enamel through the precipitation of fluoride-containing reaction products. A globular calcium fluoride-like

layer is formed on the enamel surface and within the pores of the enamel lesion; this releases fluoride over a long period (Mellberg *et al.*, 1966; Kirkegaard, 1977; ten Cate & Duijsters, 1982). As calcium fluoride is more stable, in terms of solubility, than fluorapatite, some acid protection will be given simply by its formation on the enamel surface (Rölla & Saxegaard, 1990). The stability of calcium fluoride in plaque appears to be due to surface adsorption of secondary phosphate ions (HPO_4^{2-}) to calcium (Rölla *et al.*, 1993). This occurs at neutral pH and renders the calcium fluoride crystals insoluble. At lower pH, the secondary phosphate is converted to singly charged primary phosphate, dissolution of the calcium fluoride is no longer inhibited, and fluoride ions are released. The calcium fluoride thus acts as a pH-controlled reservoir of fluoride ions, increasing the fluoride concentration around the enamel crystallites at times of acid challenge, and specifically adsorbs fluoride ions at cariogenic sites (Arends and Christoffersen, 1990; Rölla *et al.*, 1991). Fluoride may, therefore, be maintained at low concentrations for long periods between topical applications (Shellis & Duckworth, 1994).

1.5. Lasers in Dentistry - an overview

1.5.1 Introduction

The ruby laser was developed by Maiman (1960), and was used soon after in the first dentistry-related laser research. Early studies demonstrated glass-like fusion, and cratering, of enamel exposed to ruby laser irradiation (Stern & Sognaes, 1964). Stern *et al.* (1966) found a decreased permeability of lased enamel to acidic oral fluids, suggesting a possible role for the laser in caries prevention. The CO_2 laser was also found to induce resistance to acid demineralisation of enamel (Stern & Sognaes, 1972). The clinical application of the CO_2 laser for the vaporisation of caries was also investigated. Melcer *et al.* (1984) reported successful clinical trials of caries removal by the laser. Most investigations which have focused on lasers as replacements for

conventional dental drills found, however, that the high energy densities needed for hard tissue removal by CO₂ and ruby lasers caused shattering and cracking of the enamel surface (Taylor *et al.*, 1965), with irreversible pulp damage (Gordon, 1967; Sognaes & Stern, 1965). Pulpal necrosis was found after ruby laser irradiation even at low power levels (Adrian, 1971).

The Nd:YAG laser was the first laser system to be designed specifically for use in dentistry. Its use was reported by Yamamoto & Ooya (1974), who determined that the Nd:YAG laser was an effective tool for inhibiting the formation of incipient caries *in vitro*, and *in vivo* (Yamamoto & Sato, 1980) reducing subsurface demineralisation and acid solubility. The poor absorption of the Nd:YAG laser wavelength means that at a low power it could remove the organic and inorganic debris found in pits and fissures, prior to sealant therapy, without damaging the surrounding enamel (Bahar & Tagomori, 1994). Myers & Myers (1988) found the Nd:YAG laser to be highly effective in the selective removal of caries in enamel. More recently there has been evidence of a synergistic effect between lasers and fluoride in terms of imparting increased acid resistance to enamel (Tagomori and Morioka, 1989; Fox *et al.*, 1992). It is difficult, however, to make direct comparisons between studies as different lasers (in terms of wavelength and mode of operation) have been used, with a range of exposure parameters.

The clinical application of lasers in dentistry requires two important considerations. Firstly, the use of a minimum energy density - to avoid damaging the oral soft tissue, especially the dental pulp; and secondly, the laser beam must be guided easily (with a flexible optic fibre, for example) to the tooth surface. For years, many laser systems required a bulky, articulated arm system to transmit the energy beam and so were impractical for use in the oral cavity. The Nd:YAG American Dental Laser has a beam which can readily be transmitted along a silica optical fibre system, providing more versatility and the flexibility to reach most areas of the mouth.

1.5.2 Mechanism of Action (Laser Definition and Types)

Laser is an acronym for Light Amplification by Stimulated Emission of Radiation. Lasers consist of three basic elements - an active medium, an excitation mechanism and a resonator cavity, all secured within an outer console (see figure 1.2). An external energy source, which may be optical (a xenon or krypton lamp) or electrical (high voltage or radio frequency current), is pumped into the active medium of the laser. Absorption of this energy alters the electronic structure of atoms in the active medium; orbiting electrons are excited to a higher energy level. Some of these atoms in the excited state will return, spontaneously, to their original energy level, emitting as they do so, energy in the form of a photon of electromagnetic radiation. Some of these spontaneously emitted photons will then strike atoms that are still at the higher energy level, stimulating the emission of a second photon, propagated in the same direction and phase. The atom, on returning to ground state, may re-enter the cycle. Population inversion occurs when more atoms are in the excited state than in the ground state and it is a prerequisite for laser operation.

The resonator cavity, containing the active medium, has mirrors placed at each end. The emitted photons of light travel the length of the tube and resonate back and forth by reflection from these mirrors. As the distance between the mirrors is a multiple of the wavelength of the light emitted, the reflected light remains exactly in phase, re-enters the active medium and stimulates further photon emission. The rate of stimulated emission increases rapidly by this cascade process, the light in the tube amplifying in intensity. As one mirror is partially transparent, some light leaves the tube in the form of a laser beam. This beam is highly coherent (the light wavefronts travelling in phase), monochromatic (of one wavelength) and collimated (all rays are parallel).

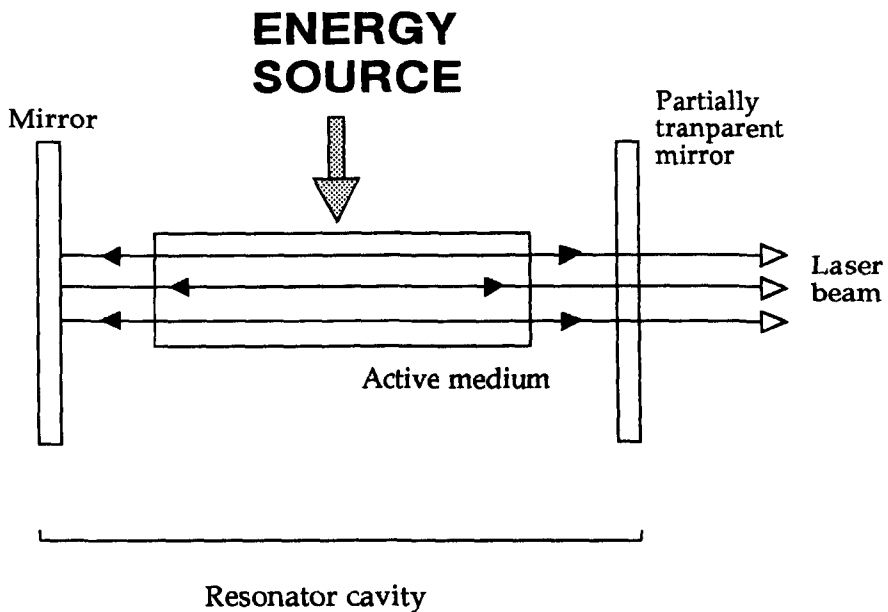


Figure 1.2 Schematic diagram of a laser. The external energy source is pumped into the active medium where it stimulates the atoms to an excited state. The photons which are subsequently emitted, resonate back and forwards between the two mirrors, inducing further photon emission, before leaving the tube in the form of a laser beam.

Large amounts of energy are required to maintain the lasing process, efficiency ranging from fractions of a percent to as great as 30 %. The remaining energy generates heat. Although the actual amount of light emitted by a laser is relatively small, it can be focused to a very high intensity.

Lasers are characterised by the composition and structure of the active medium as the output wavelength of each element is unique. The characteristic wavelength of Nd:YAG lasers is 1.064 μm .

1.5.3 Tissue effects

On irradiation of a tooth surface, a laser beam can be reflected, scattered or absorbed within the tooth, or transmitted into surrounding tissue. On absorption, the light energy may be converted into heat; thermal changes are responsible for most of the laser-induced tissue effects seen in dentistry. Absorption can also cause fluorescence, phosphorescence and dissociation of molecules. The properties of a tissue determine whether absorption of a particular wavelength occurs and to what extent (individual laser wavelengths produce unique tissue effects). Energy density and pulse duration are also considerations in the overall effect of the laser on tissues.

In the case of the Nd:YAG laser, more than 40 % of the beam is reflected by tooth enamel (Bohem *et al.*, 1977); it is preferentially absorbed by pigmented tissues. Due to inter and intra tooth variability, in composition and structure, the effect of this laser on enamel may be inconsistent. The use of absorptive coatings has been found to increase the energy absorption of this laser (Morioka, 1984). Tagomori & Iwase (1995) used black ink as an absorptive mediator before lasing enamel three times successively, reapplying the ink between each laser irradiation. The black ink burned away within the first 10 pulses of the laser, and was reapplied. On re-lasing, the enamel was heated not only in the surface as normal but also deeper inside, where the

ink had penetrated into the pits and cracks of the lased area.

Nd:YAG laser ablation of dental tissue is due to the heating and evaporation of interstitial water. On laser irradiation, enamel absorbs energy and becomes heated locally at the surface. During this time, large amounts of energy are also being transmitted to deeper areas of the tissue. At a critical temperature, the water in the surface tissue vaporizes, creating sufficient pressure to cause microscopic tissue fragments to erupt and form a crater. If light scattering is small, the crater will advance into the tooth before side tissue is vaporised. Once the water is evaporated, any remaining organic and inorganic material continues to absorb heat, undergoing carbonisation and pyrolysis, either melting or vaporising. The optical properties of the tissue may change with prolonged heating; for example, dark charring can cause a sudden increase in light absorption. The most efficient ablation occurs when using a short pulse duration, compared to the thermal relaxation time, and a high intensity beam, to ablate tissue before there is significant heat loss to the remaining tissue (by diffusion and scattering).

In continuous mode, the laser beam energy is constant for the length of the exposure. In pulsed mode, a flash-lamp is used to pump the lasing medium and the beam is rapidly switched on and off for the exposure period. This creates pulses with a high peak power intensity, whilst the overall energy is kept constant. Continuous and pulsed outputs of a particular laser can have different effects on tissues even if the overall amount of energy applied is comparable.

The high intensity irradiation of pulsed lasers, focused into a small volume of material, may cause formation of a plasma (a super-heated gas), due to very brief ionisation of the surface material. As the surface temperature increases rapidly, intense bright light is released, along with sound, as the tissue surface rapidly expands then contracts. If generated just underneath the tissue surface, the pressure front blows out fragments of tissue. Pulsed

lasers do have advantages, however, in that heat build-up can be reduced, with enamel melting and re-crystallization confined to the enamel surface layer (5 - 10 μm) (Featherstone & Nelson, 1987, Tasev *et al.*, 1990).

Suzuki *et al.* (1982) estimated the temperature rise of surface enamel, fused and melted by exposure to a normal pulsed Nd:YAG laser (50 J/cm²), to be 1000 °C. At relatively high energy levels it is possible to produce a surface melt while producing only a 4 °C increase in pulpal temperature (Anic *et al.*, 1992; Launey *et al.*, 1987). Stresses in enamel due to expansion, contraction and shockwaves associated with a laser beam's localised heating, may form cracks (Ferreira *et al.*, 1989). Tagomori & Iwase (1995) used SEM examination to examine enamel subjected to successive doses of pulsed Nd:YAG laser irradiation. They observed the process of formation of hexagonal columns in the lased enamel surface, as a sequence through melting, recrystallisation and growth of large and stable hexagons during repeated laser irradiation.

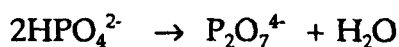
The mechanism by which lased enamel becomes resistant to acid demineralisation has not been fully determined. The melting of enamel on irradiation suggests a surface microfusion of lased enamel, with a corresponding decrease in permeability and hence acid penetration (Sato, 1983; Stern *et al.*, 1972). However, Borggreven *et al.* (1980) found CO₂ laser irradiation (10 J/cm²) to actually increase the permeability of bovine enamel, suggesting laser-induced chemical modifications in enamel, rather than structural reorganisation, to be responsible for the induced acid resistance.

The rapid melting of surface enamel crystals, induced by laser irradiation, is followed by recrystallisation, where larger crystals are formed and prism boundaries eliminated (Ferreira *et al.*, 1989). As dissolution rates are inversely proportional to crystal surface area, it follows that lased enamel should have a much lower solubility than nonlased enamel (Ferreira *et al.*, 1989; Palamara *et al.*, 1992). Recrystallisation products include calcium phosphate phases other than apatite, with carbonate content considerably

lower than the original surface enamel and hence lower solubility. The loss of water and CO₂ from enamel on Nd:YAG laser irradiation (Yamamoto & Ooya, 1974; Yamamoto & Sato, 1980), appears to cause microspaces in the lased enamel which are potential sites for deposition of ions (such as Ca²⁺) released by an acid attack (Oho & Morioka, 1990). This would also account for the observed acid resistance in lased enamel; in nonlased enamel these ions would diffuse to the surrounding solution.

The occurrence of compositional phase changes in the inorganic material of dental enamel upon lasing has been suggested as another possible explanation of acid resistance. These changes have been inferred from studies of thermally heated enamel, and are summarized below (Fowler & Kuroda, 1986):

As enamel is heated, there is the formation of pyrophosphate from the acid phosphate groups in enamel.



This starts at 300 °C and reaches a maximum at approximately 700°C. Above this temperature, pyrophosphate reacts with apatitic hydroxyl ions to form β-tri-calcium phosphate (β-TCP) and possibly α-TCP (depending on the Ca/P ratio of the enamel). There is also a loss of constitutional water at > 1000 °C, while the integrity of the lattice is maintained.

At temperatures between 650 - 1100 °C, as well as β-TCP formation, the Ca/P ratio of the apatitic phase becomes more stoichiometric - its carbonate and water contents are lower, and hydroxide content higher, than the original enamel. Fluoride is dispersed and hydrogen bonded to hydroxide. As this apatite phase has less defects and impurities than the original enamel, it should also be less soluble.

At temperatures > 1100 °C, there is formation of α -TCP, β -TCP, an apatitic phase with decreased carbonate and water, and tetracalcium phosphate monoxide (TetCP).

The following trends in solubility are generally accepted (Patel & Brown, 1975):

$\text{TetCP} \geq \alpha\text{-TCP} > \beta\text{-TCP} > \text{enamel} > \text{hydroxyapatite}$
(where TetCP is the most soluble and hydroxyapatite is the least).

The high temperature products formed would be detrimental to the tooth as they have higher solubilities than normal enamel. However, between 650 - 1100 °C, the reduced solubility of the modified apatite towards that of hydroxyapatite could offset the increased solubility of the β -TCP phase, provided that the amount of β -TCP is low enough, such that this mixture of modified enamel apatite and β -TCP and/or α -TCP could be less soluble than the original enamel.

It is well known that pyrophosphate ions adsorbed on a hydroxyapatite (HA) crystal surface markedly reduce the HA dissolution rate (Evans *et al.*, 1980; Christoffersen & Christoffersen, 1981), so it is probable that the pyrophosphate formed in enamel at low temperatures would contribute to a reduction in solubility rate (Fowler & Kuroda, 1986). The long term stability of pyrophosphate in enamel has not been reported, but it is known to hydrolyse to HPO_4 (Fleisch *et al.*, 1966). Calcium ions increase, and magnesium ions decrease the rate of hydrolysis.

Minor amounts of α -TCP and TetCP have been identified in lased enamel at powers of $15 - 10^5 \text{ J.cm}^{-2}$ and 10^4 J.cm^{-2} respectively (Kantola, 1973; Kuroda & Fowler, 1984). Nelson *et al.* (1987), using infrared spectroscopy, found TetCP at much lower energy densities and for short irradiation times (ie. $10 - 51 \text{ J.cm}^{-2}$). However Ferreira *et al.* (1989) were unable to detect TetCP or α -TCP using electron diffraction. As they used very short irradiation times ($6 - 520$

µs) they suggested therefore, that the absence of α -TCP and TetCP may be due to a faster growth rate of apatite relative to these minor phases. This is consistent with Brune (1980) who used X-ray diffraction for crystal identification. The tetracalcium diphosphate monoxide may thus only be present in very small amounts.

Obviously on lasing a tooth, high temperature phases would be formed at the point of impact of the laser, with a decreasing temperature gradient and associated compositional changes towards the dentine. Below the surface melt zone there is a region, approximately 10 - 40 µm deep, where the temperature rise is insufficient for the melting process but induces some compositional changes to the crystals. Therefore, depending on the energy used, internal regions of the enamel may gain more acid resistance than the external contact area (Fowler & Kuroda, 1986).

Nelson *et al.* (1987) proposed that the improved acid resistance of lased enamel is due to a combination of reduced enamel permeability together with reduced enamel solubility. It is not known, however, which of these is the most significant. The number of contributing factors to the acid resistance of dental enamel makes it difficult to interpret and determine a definitive mechanism of laser action.

1.6 Artificial White Spot Lesions

1.6.1 Introduction

It is difficult to obtain natural white spot lesions, suitable for experimental purposes, in sufficient numbers. Also, as natural lesions will have undergone both de-and re-mineralisation in the oral environment, their history will be ambiguous. In order to standardise experimental procedures it is, therefore, preferable to use artificial white spot lesions as they can be created with pre-determined characteristics. Silverstone (1973) found areas in artificial white

spot lesions corresponding to all the areas in natural lesions. Each lesion should have a well defined, intact surface zone, and lesion body, and there should be no cracks or other artifacts on the anatomical surface of the experimental lesion.

1.6.2 Methods of Artificial White Spot Lesion Creation

There are many different methods for the creation of artificial lesions, including the use of natural plaque (Clarkson *et al.*, 1984, Geddes *et al.* 1986), acidified gels (Silverstone, 1966), buffered solutions (Featherstone *et al.*, 1978), and acid vapour (Weatherell *et al.*, 1983). The relative merits of each technique are summarised in table 1.1. below.

The method of artificial lesion creation affects the extent of demineralisation (Strang *et al.*, 1988, ten Cate *et al.*, 1992) and subsequent remineralisation (ten Cate *et al.*, 1992). There can be considerable variation in demineralisation within different areas of the same tooth (Strang *et al.*, 1986, Larsen, 1990). Lesions which exhibit a large initial loss of mineral have a greater capacity for remineralisation (Strang *et al.*, 1987). Creanor *et al.* (1989) found that enamel near the cervical margin of the tooth demineralised faster than enamel at the cusp.

1.7 Methods of Analysis of Mineral Changes

1.7.1 Introduction

This section will discuss the variety of methods used to assess lesion progress and determine changes in the mineral content of enamel.

1.7.2 Transverse (Contact) Microradiography

The principle of this technique is to quantify the absorption of

Table 1.1 A summary of the methods used for artificial white spot enamel lesion creation.

Technique	Description	Advantages / Disadvantages
Natural plaque	Application of human, day old plaque to enamel surface. Supply with a carbohydrate substrate, incubate for 24 hrs at 37 °C	Rate of mineral loss is difficult to control, lesions often fail to exhibit the characteristics of natural lesions. Tedious procedure, & unsuitable for large scale production of lesions. Potentially useful in investigation of foodstuffs. Lesion production in 5 - 10 days.
Acidified gel	Immersion in acidified gel for up to 12 weeks. Gel made from gelatin hydroxymethylcellulose or methylcellulose, with a Ca and P source, and lactic acid.	Long periods required for lesion creation & results in an unpredictable impurity content in the lesions. But, lesions are usually similar to natural carious lesions.
Buffered solutions	A surface dissolution inhibitor (ie. MHDP) is used, in a lactate buffered solution, or buffer solution alone (with a specific level of saturation wrt HA).	Excellent control of pH and contaminants. However, the solution must be changed frequently due to crystal formation - increased laboratory handling time.
Acid Vapour	Expose enamel to a moist acid vapour for set periods of time. A vapour droplet forms on the tooth surface, with a subsurface lesion below.	There is crystal formation within the vapour droplet resulting in a net loss of mineral from the tooth, due to supersaturation. This minimises background contamination. Radiographically similar to natural lesions.

monochromatic X-rays by a tooth sample, compared with a simultaneously exposed standard - usually an aluminium step-wedge. Planoparallel tooth slices, cut perpendicular to the anatomical tooth surface, are placed on photographic film, or plates, together with the step-wedge, and irradiated. The optical density of the developed film is directly proportional to the amount of X-ray absorption at any point which is, in turn, related to the mineral density of the tissue. Computerised microdensitometry measurements are taken of the microradiographs and Angmar's formula is used to calculate the mineral content of the enamel, in Vol% or kg.m^3 (Angmar *et al.*, 1963). By this procedure, mineral loss, gain and distribution may be quantified with reasonable accuracy; resolution is $3 \mu\text{m}$. Lesion progression can be observed by taking serial measurements on demineralised samples. Due to specimen curvature, however, and a finite densitometer slit width, the outer $10 \mu\text{m}$ of the tooth section may not be measured accurately. Also, the presence of ions with a very high x-ray absorption coefficient may distort the results; the presence of tin ions for example, after SnF_2 application, could be mistaken for remineralisation (Arends & ten Bosch, 1992). Enamel sections should be homogeneous in thickness - a difficult criteria to satisfy (White *et al.*, 1992). This problem and others, such as the assumption of uniform elemental composition of enamel, have been assessed extensively by De Josselin de Jong & ten Bosch (1985).

1.7.3 Longitudinal Microradiography

In this case longitudinal, planoparallel tooth slabs (up to 0.5 mm thick) are irradiated together with a two-dimensional step-wedge, the photographic film placed parallel to the demineralizing surface. Following computerised densitometry, changes in calcium or mineral content of the sample are calculated per unit area ($\text{Vol}.\mu\text{m}$, kg.m^{-2}). The procedure does not distinguish between types of lesions, cannot determine mineral depth distribution and may be subject to systematic errors of up to 20 % (De Josselin de Jong 1987b). It is, however, an accurate method to investigate

mineral changes as a function of position and time. Being non-destructive, the technique can be repeated enabling consecutive changes to be determined. The technique allows a relatively large surface area (3 mm x 3 mm) to be studied at one time and slabs with natural surfaces can be used if their thickness varies by less than 200 μm .

1.7.4 Wavelength Independent Microradiography.

Wavelength independent microradiography uses polychromatic high-energy x-rays (< 60 kV) to determine the amount of mineral per unit area in enamel and dentine samples (Herkstroter & ten Bosch, 1990). The reference step-wedge is made of an alloy with a mass attenuation coefficient that has a wavelength-independent ratio to the mass attenuation coefficients of enamel and dentine. The technique can be used to study thick sections or whole teeth with or without natural curved surfaces (accuracy is about 0.01 $\text{kg}\cdot\text{m}^{-2}$ or 310 Vol% $\cdot\mu\text{m}$).

1.7.5 Polarized Light Microscopy

Dental enamel, being anisotropic, will resolve a plane-polarized beam of light into two component rays. The birefringence of a sample is the difference in the refractive index of these two rays. Enamel exhibits both the intrinsic birefringence of apatite crystals and form birefringence due to inter-crystalline microscopic spaces. The difference between intrinsic and form birefringence indicates the mineral porosity of an enamel lesion.

Specimens, in the form of thin sections (approximately 80 μm thick), are imbibed with a variety of media of known refractive indices, such as quinoline or Thoulet's solution. Each results in a different form birefringence observation. The volume fraction of pores can be calculated using the Wiener equation (Darling, 1958). However, this method has been found to underestimate pore volume by failing to take into account pores which are

too large to contribute to form birefringence (Shellis & Poole, 1985). For the purpose of calculations it is also assumed that the optical axis is in the tooth section plane, which is improbable (Carlstrom, 1964), and that imbibition is complete even in the smallest pores (Poole *et al.*, 1961).

Polarizing microscopy can be used to determine qualitatively mineral changes and lesion characteristics of enamel sections but, due to the number of unknown variables, is best used in conjunction with a quantitative technique such as microradiography. Multiple imbibition of sections is a time-consuming procedure. Polarizing microscopy has been used extensively in investigations of lesion histology enabling Silverstone (1966, 1967, 1968) and Kidd (1983) to describe in detail the four distinct zones discussed in Section 1.3.2. It has also been used in lesion depth measurements, and histological investigations of lased enamel (Oho & Morioka, 1990; Flaitz *et al.*, 1995). The immersion of lesion sections in imbibition media may affect their subsequent de- or remineralisation (White *et al.*, 1992).

1.7.6 Microhardness

Microhardness testing involves the pressing of a standard diamond, under a defined load, onto a test specimen for a given time. The resultant permanent indentation is measured using a microscope; the extent of surface deformation indicates the sample hardness. In dental research the Knoop diamond is usually used to investigate carious lesions. The diamond is cut with a longitudinal angle of 172.5 ° and transverse angle of 130 °. When applied to a tooth sample under a specific load, cutting occurs mainly across the l axis, to a maximum depth of approximately 3 µm. Hardness is then expressed in Knoop units (KHN) given by the formula:

$$\text{KHN} = 1430.L.lk^{-2}$$

lk is the length of the indentation in µm, L is the load in gramforce - gf (Knoop *et al.*, 1939).

Early hardness testing of enamel caries was carried out on anatomical surfaces (Caldwell *et al.*, 1958) or adjacent parallel sections (Koulourides & Pigman, 1960). This method, however, will not detail any hardness changes below the surface or in different regions of the lesion, as indentations transect the surface zone and lesion body. More informative, therefore, is cross-sectional testing whereby the diamond is placed perpendicular to the anatomical surface at intervals across a transverse lesion section (Davidson *et al.*, 1974; Arends *et al.*, 1980). Featherstone *et al.* (1983) found a direct relationship between the KHN of enamel specimens and their mineral content, as measured microradiographically and this technique was used by Nelson *et al.* (1986), to compare the effect of different laser treatments on enamel demineralisation. Microhardness testing of enamel has accuracy within 5 % (Purdell-Lewis, 1976) but, at 25 μm , the spatial resolution is less than that of microradiography. As flat, highly polished specimens are required, the technique is time-consuming and samples are unlikely to be re-usable.

1.7.7 Scanning Electron Microscopy

The scanning electron microscope (SEM) has been used extensively to investigate the mechanism of enamel lesion formation - as reviewed by Shellis and Hallsworth (1987). The technique enables the examination of enamel structure at all levels from the whole tooth to a single enamel crystal; it is not restricted by the resolution of visible light. Ingram & Fejerskov (1986) concluded that there were no measurable differences in surface morphology between normal and carious enamel, but the interprismatic region of fractured enamel may show demineralisation (Brannström *et al.*, 1980). The SEM has been used to demonstrate the ultrastructural and crystallographic changes - such as surface melting and prism fusion - of enamel surfaces subjected to Nd:YAG laser irradiation (Yamamoto & Ooya, 1974; Quintana *et al.*, 1992). The technique is, however, only of limited quantitative value and is destructive because the specimen has to be coated

before examination within the SEM vacuum (as described in Section 2.7.2).

The SEM has been used in conjunction with the electron probe in a number of studies to assess lesion progress (Purdell-Lewis *et al.*, 1976; Clarkson *et al.*, 1981; Clarkson *et al.*, 1984b). This technique allows measurement of specific ions such as fluoride, calcium and phosphorous (Rentsch *et al.*, 1990) but again it is a destructive method and extremely time-consuming.

1.7.8 Infrared Spectroscopy

An infrared spectrometer contains a source of infrared light which emits radiation covering the whole frequency range. This light is split into two beams of equal intensity and one beam is passed through the sample to be examined. Certain wavelengths are absorbed by the sample molecule, while others are reflected; if the frequency of a vibration in the sample molecule is within the range of the instrument, the molecule may absorb energy of this frequency and undergo rotational and vibrational energy level transitions (stretching and bending deformation of bonds). Comparing the intensity of the two light beams, after one has passed through the sample, produces an interference pattern (interferogram) that is the sum of the absorption and reflection (interference pattern) of each wavelength in the beam.

The interferogram is analysed mathematically by Fourier Transform techniques to determine individual absorption frequencies and their intensities. The finished spectrum is a chart showing downward peaks, corresponding to absorption, plotted against wavenumbers (ν) which are expressed in reciprocal centimetres (cm^{-1}). The infrared spectrum of a compound is characteristic for that compound and may be used for identification, and determining the presence of specific bonds.

Quantitative analysis by infrared spectroscopy (as described in Section 2.7.8) has been used to estimate the carbonate concentration of enamel samples to

better than $\pm 10\%$ (Featherstone *et al.*, 1984; Nelson *et al.*, 1987). As carbonate is preferentially dissolved in lesion formation (Hallsworth *et al.*, 1973) quantifying it may indicate the stage of sample demineralisation. Considerations of this technique and its potential use in the analysis of enamel will be discussed further in Chapter 6.

1.7.9 Chemical Analysis

This generally involves the dissolution of samples of hard tissue in acid and subsequent analysis, for certain inorganic ions, by atomic absorption spectrophotometry (calcium ions) or other colorimetric techniques (phosphate ions). Samples of enamel may be obtained by microdrilling, sequential acid etching (Weatherell & Hargreaves, 1991) or abrasion (Weatherell *et al.*, 1985). Although these are very sensitive techniques for detecting mineral changes, they are time-consuming, destructive and do not usually provide a mineral profile through a tooth.

1.7.10 Iodine Permeability Testing

This technique, developed by Bakhos *et al.* (1977), measures changes in tooth surface permeability to iodine (I_p) and in principle will give an estimate of the state of de- and remineralisation of a tooth; the amount of iodide which permeates a tooth is related to its pore volume. A moderate correlation has been found between I_p measurements and the amount of calcium lost from a tooth (ten Bosch and Angmar-Mansson, 1991) or surface microhardness measurements (Zero *et al.*, 1990) following an acid challenge. Again, however, the technique does not provide a tooth profile and may be affected by surface zone pore blockage, especially if used *in vivo* or *in situ* (Arends & ten Bosch, 1992).

CHAPTER 2 - Materials & Methods (general)

2.1 Introduction

This Chapter will describe the experimental methods involved in Chapters 3, 4 and 5: tooth collection and preparation, artificial lesion creation, laser irradiation, topical fluoride application, mineral quantification and SEM analysis. Chapter 3 involved the cutting of sections from whole teeth on which lesions had already been formed. Chapters 4 and 5 involved a single section technique, with sections produced at the start of the experimental procedure. The use of a single section protocol should overcome the variability between different sections cut from the same tooth, or even the same lesion (Creanor *et al.*, 1986). Also, as each single section can be analysed at both the start and end of the experiment (or at any point in between), it can act as its own control (Harvey *et al.*, 1982). The methods used in this study were all standard techniques, modified by the author for the purposes of this project.

2.2 Tooth Selection, Preparation and Tissue Sampling

2.2.1 Introduction

Human premolar teeth were used in this project since it has been shown that artificial lesions formed in enamel from other sources such as bovine and ovine samples, progress at varying rates (Featherstone & Mellberg, 1981). Potential disadvantages, however, include the difficulty of obtaining an adequate quantity and quality of material and the variable age and composition of human enamel, which may lead to large variations in treatment response. Bovine enamel is an alternative to human enamel (Mellberg, 1992), with the advantages of large flat surfaces, lower fluoride concentrations (Mellberg & Loertscher, 1974) greater porosity resulting in

faster lesion formation (Featherstone & Mellberg, 1981), and no prior caries experience. Human enamel is, however, the obvious substrate for the study of human enamel caries (Mellberg, 1992).

2.2.2 Tooth Selection

The teeth used were human premolars extracted for orthodontic purposes in the Oral Surgery Department of Glasgow Dental Hospital (water fluoride <0.03 ppm). After drying in air, the teeth were inspected under x 10 magnification to ensure they were caries-free; any teeth with obvious flaws, cracks or incipient lesions were discarded. The selected teeth were lightly polished with a slurry of pumice and water, washed in warm soapy water then wiped with an isopropyl alcohol-saturated tissue (Azo-Wipe, Vernon-Carus Limited, Preston, England) to ensure a grease-free surface. The teeth were kept in 0.12 % thymol solution until required for experiments.

2.2.3 Section Cutting

The root was removed from each tooth by hacksaw, cutting approximately 1 - 2 mm below the cervical margin. The crowns of teeth on which lesions were already formed (see Section 2.3.1), and which had been subsequently lased, were embedded in sticky wax (Kemdent, Associated Dental Products Ltd. UK) and mounted on a chuck. The chuck was placed into a Labcut Hard Tissue Saw (Agar Scientific, Cambridge - see figure 2.1) such that the tooth was perpendicular to the peripheral, diamond-coated cutting blade. The blade operated at a speed of approximately 350 revolutions per min. Sections were cut such that the centre of each lased crater was positioned in the centre of the section, which was approximately 700 µm wide.

The crowns of teeth to be used for the single section experiments (Chapter 4) were first bisected longitudinally (using the Labcut) in a mesiodistal direction. Two longitudinal sections, approximately 700 µm wide, were cut

from each half in a bucco-lingual direction. Sections were numbered using a pen, 1 to record the tooth from which they were derived, and the cutting order. The sections were then laid in two spots on the natural enamel surface, as described in Section 4.2.2.



thickness and degree of paraodontal resorption. The sections were ground to a thickness of between 140 - 160 μm . The sections which had previously been laid were checked continuously during grinding, using a dissecting microscope (Zeiss Stereo-microscope 4; Zeiss, Wetzlar, Germany) x 10 magnification) to ensure that the centres of the lesion craters were included in the section - as shown in figure 4.1. Sections were stored in ethanol prior to microradiography.

2.3 Artificial white spot lesion creation

Figure 2.1 The Labcut hard tissue saw for cutting 700 μm sections through the experimental samples.

The many different methods for creation of artificial white spot lesions are discussed in Section 1.6. The buffered solution method was used in this study.

from each half in a bucco-lingual direction. Sections were numbered using a pencil to record the tooth from which they were derived, and the cutting order. The sections were then lased in two spots on the natural enamel surface, as described in Section 4.2.2.

In both cases, the sections produced at this stage were too thick for microradiography and had cutting marks on either side. They were subsequently hand ground to a suitable thickness for microradiography.

2.2.4 Section Grinding

Each side of the section was carefully ground with a slurry of 1200 grade Bauxilite (Al₂O₃) (Raymond Lamb, London, England) and water, on a large glass plate. The section was held in place by a heavy brass plate covered with damp gauze (figure 2.2). The section thickness was measured regularly using a digital micrometer (figure 2.2) (Mitutoyo, Tokyo, Japan). Readings were taken along the edge of the section near the enamel surface at approximately 1 mm intervals; this allowed estimation of the overall section thickness and degree of planoparallelity. All sections were ground to a thickness of between 140 - 160 µm. The sections which had previously been lased were checked continuously during grinding, using a dissecting microscope (Zeiss Stereo-microscope 4, Zeiss, Wetzlar, Germany)(x 10 magnification) to ensure that the centres of the lased craters were included in the section - as shown in figure 4.1. Sections were stored in thymol prior to microradiography.

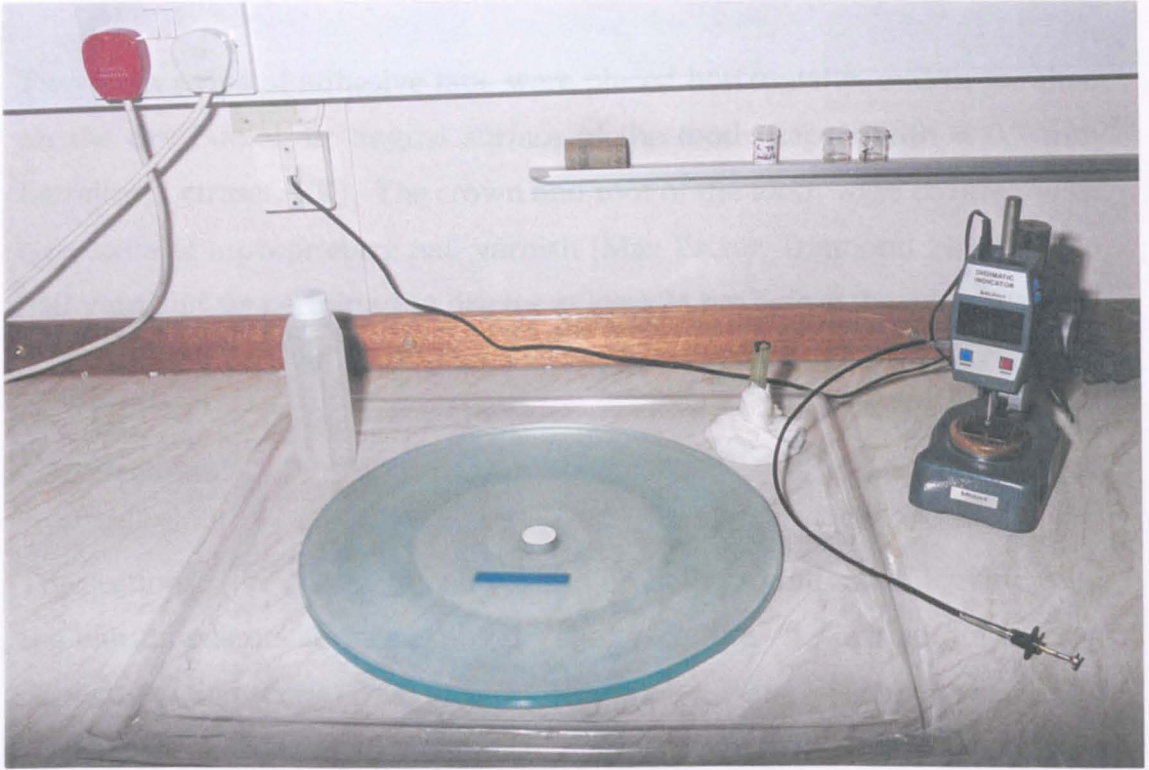
2.3 Artificial white spot lesion creation

2.3.1 Introduction

The many different methods for creation of artificial white spot lesions are discussed in Section 1.6. The buffered solution method was used in this study

due to its ability to produce artificial lesions rapidly, which conforms to accepted parameters in terms of their surface morphology and consistency in re- or demineralisation (Strang et al., 1988).

2.1.2 Whole Teeth



dry for 24 hrs before the sections were placed in the demineralising solution.

2.1.4 Demineralisation

The buffered solution used contained 7.0 mmol/L calcium as anhydrous calcium chloride, 20 mmol/L phosphate as anhydrous sodium dihydrogen orthophosphate and 0.53 mmol/L fluoride as sodium fluoride. The pH was adjusted to 4.05 by the addition of glacial acetic acid and sodium hydroxide. The teeth were suspended in this demineralising solution.

Figure 2.2 Ground glass plate with Bauxilite powder slurry and gauze covered brass plate used for section grinding. The Mitutoyo digital micrometer for determination of section thickness.

due to its ability to produce artificial lesions rapidly, which conformed to accepted parameters in terms of their surface morphology and consistency in re- or demineralisation (Strang *et al.*, 1988).

2.3.2 Whole Teeth

Two 1 cm strips of adhesive tape were placed horizontally, and in parallel, on the dry buccal, or lingual surface of the tooth (tape width = 0.7 mm Letraline, Letraset, UK). The crown and root of the tooth were covered with two coats of a proprietary nail varnish (Max Factor, Diamond Hard). The nail varnish was permitted to dry for at least 24 hrs before the adhesive tape was removed and the tooth placed into demineralising solution.

2.3.3 Sections

The sections were coated in nail varnish on both ground sides, leaving only the natural enamel surface exposed. The procedure was carried out using a dissecting microscope (Zeiss Stereo-microscope 4, Zeiss, Wetzlar, Germany)(x 10 magnification) to ensure accuracy of application. The varnish was left to dry for 24 hrs before the sections were placed in the demineralising solution.

2.3.4 Demineralisation

The buffered solution used contained 2.0 mmol/L calcium as anhydrous calcium chloride, 2.0 mmol/L phosphate as anhydrous sodium dihydrogen orthophosphate and 0.53 μ mol/L fluoride as sodium fluoride. The pH was adjusted to 4.65 by the addition of glacial acetic acid and sodium hydroxide. Varnished teeth were suspended in this demineralising solution (approximately 100 ml of solution per tooth), which was stirred slowly at regular intervals (Magnetic Stirrer, H1304N, Jencons Scientific Limited, England), and changed every 24 hrs. The teeth were inspected regularly for signs of demineralisation.

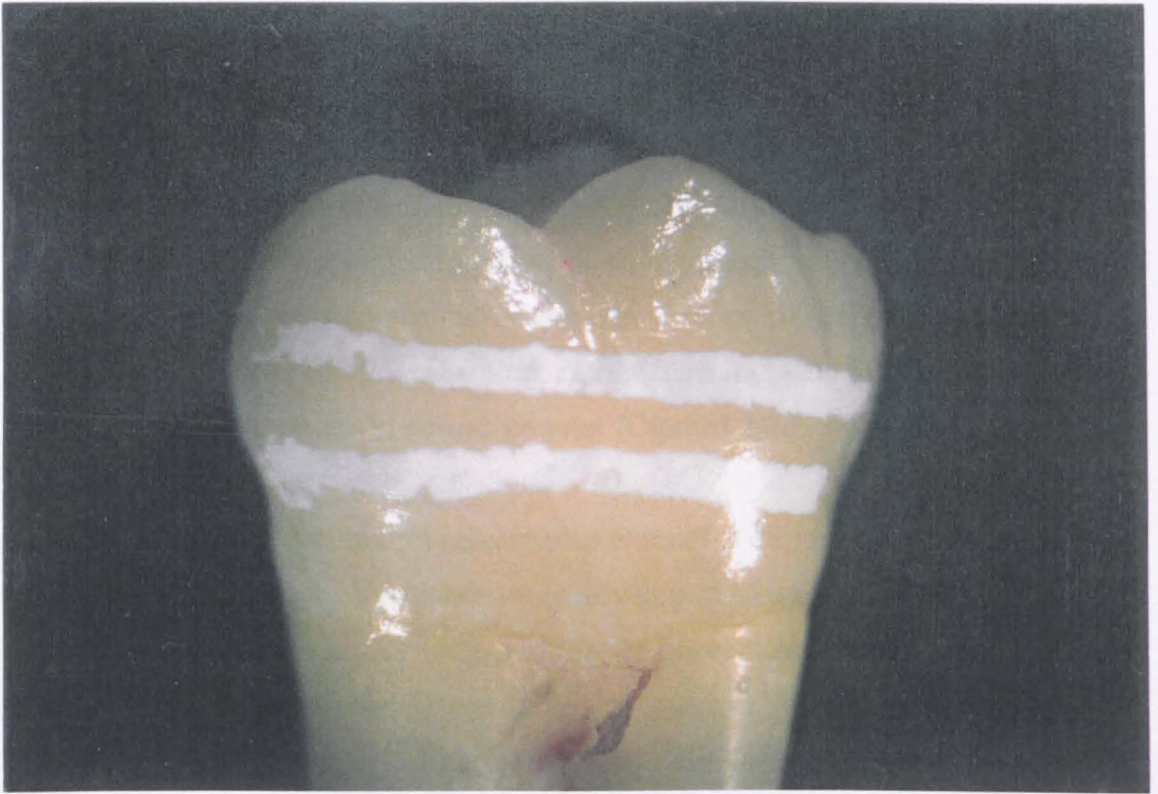
Lesion creation usually took between 4 and 7 days. After this time, the air-dried enamel appeared to be an opaque, dense white colour whilst surface shine and integrity were maintained (figure 2.3). Specimens which had cavitated or failed to demineralise during this period were discarded. Those on which suitable lesions had formed had the nail varnish removed by swabbing the tooth surface with acetone; the teeth were then washed in ethanol and stored in 12 % thymol solution until used for further experimentation.

2.4 Topical Fluoride Application

2.4.1 Introduction

The mechanism of caries prevention by fluoride is discussed in Section 1.4. The cariostatic effects of fluoride varnishes (ie. Duraphat® and Fluor Protector®), solutions (2 % NaF) and gels (acidulated phosphate fluoride (APF), stannous fluoride and amine fluoride), have been demonstrated in clinical studies (reviewed by De Bruyn & Arends, 1987; Ripa, 1990). Although fluoride concentrations and pH's vary, there is no significant difference between these topical application vehicles in terms of caries inhibition. Choice of fluoride vehicle, therefore, depends on cost, convenience, patient acceptance and safety. APF gel is the most widely used topical application in the USA. In Europe, however, fluoride varnishes are most common due to their ease and control of application (Bennett & Murray, 1973). De Bruyn and Arends (1987) recommended normal patient toothbrushing, followed by drying and varnish application; varnishes set in saliva and patients can leave immediately after the application. Fluoride solutions and gels are applied by a paint-on or tray technique; they are less convenient and require more chair time than varnishes. APF gel has a detrimental effect on certain porcelain and composite restorations (Ripa, 1990).

There is conflicting information as to the amount and duration levels of fluoride retained on sound and demineralized enamel after application of varnishes. Neele *et al.* (1983) found that the main reaction product in sound enamel after in vivo application of Duraphat[®] was fluorapatite. More recent research, however, indicates that calcium fluoride is the major or even the



(Vivodent, Leichensdorf). Duraphat[®] contains 5 %wt sodium fluoride (2.25 %wt F) in an alcoholic suspension of natural resins. Fluor Protector[®] is a polyurethane-based lacquer consisting of 5 %wt difluorosilane (0.7 %wt F). The pH of Duraphat[®] was measured in this study as 4.17; Fluor Protector[®] is also acidic (Ogaard *et al.*, 1994). Although having very high fluoride concentrations, the safety of these varnishes is acceptable due to the fast-setting bases, the slow release of fluoride over time, and the relatively small amount of varnish required (Ogaard *et al.*, 1994). Peak values of fluoride in plasma appear to remain much lower after an application of Duraphat[®] or

Figure 2.3 Artificial white spot enamel lesions which are an opaque white colour, with surface shine and integrity maintained.

of (1977) the tooth was stored in artificial saliva for one week. Dijkman & Arends (1986), found that after one week in situ

There is conflicting information as to the amount and chemical form of fluoride retained on sound and demineralised enamel after application of varnishes. Retief *et al.* (1983) found that the main reaction product in sound enamel after *in vitro* application of Duraphat® was fluorapatite. More recent research, however, indicates that calcium fluoride is the major or even the only product formed when enamel is treated with fluoride agents (Bruun & Givskov, 1991; Cruz *et al.*, 1992). This calcium fluoride acts as a slow-releasing fluoride reservoir in the mouth (as discussed in Section 1.4.5), the fluoride being redeposited in areas of demineralisation, reducing the loss of mineral by promoting reprecipitation of stable apatitic structures. Topical fluoride treatment may thus enhance remineralisation of early carious lesions, and prevent further demineralisation, rather than increase the content of the more stable fluorapatite in sound enamel (Ögaard *et al.*, 1984).

Fluoride uptake, reaction and release into enamel is dependent on its contact duration with enamel. Varnishes were developed to maximise this contact - they adhere to the tooth for long periods, so preventing immediate fluoride loss. The two most readily available commercial fluoride varnishes are Duraphat® (Woelm ICN Pharmaceutical, FRG) and Fluor Protector® (Vivadent, Leichtenstein). Duraphat® contains 5 %wt sodium fluoride (2.26 %wt F) in an alcoholic suspension of natural resins; Fluor Protector® is a polyurethane-based lacquer consisting of 5 %wt difluorosilane (0.7 %wt F). The pH of Duraphat® was measured in this study as 4.12; Fluor Protector® is also acidic (Ögaard *et al.*, 1994). Although having very high fluoride concentrations, the safety of these varnishes is acceptable due to the fast-setting bases, the slow release of fluoride over time, and the relatively small amounts of varnish required (Ögaard *et al.*, 1994). Peak values of fluoride in plasma appear to remain much lower after an application of Duraphat® or Fluorprotector®, than after fluoride gels (Ekstrand *et al.*, 1980). Edenholt *et al.* (1977) demonstrated a rapid and extensive loss of fluoride from topical fluoride agents if, after application, the tooth was stored in artificial saliva for one week. Dijkman & Arends (1988), found that after one week *in situ*,

Duraphat® treated enamel had lost significant amounts of the fluoride originally precipitated in the enamel, and the CaF₂ layer on the enamel surface was at levels similar to non Duraphat® treated samples. Comparable results have been obtained with Fluor Protector® (reviewed by Ögaard *et al.*, 1994); although it initially deposits more fluoride both on and in enamel than Duraphat®, it has been shown to be no more effective clinically (Clark *et al.*, 1985).

Attin *et al.* (1995) carried out an investigation into the retention of fluoride in incipient lesions after topical application of Duraphat® and a new varnish - Bifluorid® (2.71 %wt fluoride as sodium fluoride and 2.92 %wt as calcium fluoride; VOCO Chemie GmbH, Cuxhafen, Germany). Although initially, the deposited fluoride was greater from Bifluorid® than Duraphat®, the pure calcium fluoride in the Bifluorid® did not bind efficiently to the enamel surface and leached away with the varnish, leading to no long-term difference in the amount of deposited fluoride between the two varnishes.

2.4.2 Duraphat® Application

Duraphat® was chosen due to it having superseded APF gel in clinical use in the UK. Although treatment times of one minute and less have been tested, the usual recommended time is 4 minutes (Wei, 1988). In a study by Saxegaard and Rølla (1988), the amount of soluble fluoride formed following topical fluoride application to sound enamel did increase with treatment time, but significant increases (1 - 24 hrs) took too long to be clinically practical. Fluoride reacts more rapidly with demineralised enamel than sound enamel *in vivo* (Ögaard *et al.*, 1984), so exposure time may be less important in clinical situations than during *in vitro* studies. Drying of teeth before application of fluoride solutions and gels avoids dilution of the agent (Ripa, 1990) and enhances fluoride uptake in enamel (Koch *et al.*, 1988).

A thin layer of topical fluoride varnish (Duraphat®; Woelm ICN

Pharmaceutical, FRG) was applied by means of a cotton swab to the dry, natural enamel surface. It was left on for 5 min, then wiped off with a tissue and the section rinsed several times with de-ionised water. Most of the Duraphat® was removed in order to standardise Duraphat® application between sections and to minimise any physical influence of the fluoride varnish on the laser-enamel interaction. Duraphat® is, however, known to be difficult to remove, and would still be present to some extent. Sorvari *et al.* (1994), by scanning electron microscopy, revealed remnants of Duraphat® varnish on the tooth surface even following vigorous sonication in acetone.

2.4.3 Fluoride Ion Measurement

Fluoride analysis (see Chapter 4) was carried out using a combination ion-selective fluoride electrode (Orion Research Electrode No. 9609BN) and ionanalyser (Orion Research Expendable Ion Analyzer EA940, Boston, USA). 1 ml samples of the de-ionised water, in which teeth had been left for specific periods of time, were mixed with equal parts of low level total ionic strength adjustment buffer (TISAB, which standardises the pH to between 5 and 5.5). The electrode was placed in the samples and allowed to stabilise for 5 min before a reading was taken. The electrode was rinsed with de-ionised water between each measurement.

2.5 The Nd:YAG Dental Laser

2.5.1 Introduction

The laser used in this study was an Nd:YAG laser - designed specifically for use in dentistry (American Dental Laser, model dlase 300, Sunrise Technology Inc., Fremont, California) (figure 2.4). The active medium of the laser (see Section 1.5.2) is a crystal rod made of yttrium, aluminium and garnet which has been seeded with neodymium. Since the Nd:YAG laser wavelength (1064 nm) is not in the visible part of the spectrum, a low energy



Figure 2.4 The Nd:YAG American Dental Laser, model dLase-300, and the optic fibre handpiece.

He-Ne laser is incorporated into the instrument as a visible aiming beam. A timer in the energy source (a xenon lamp) gives the laser output in pulse mode (as described in Section 1.5.3); the pulse duration is 150 μ s. The pulse rate ranges from 10 to 30 pulses per second (pps) and the energy per pulse ranges from 30 to 150 mJ - both are adjustable by the operator. By varying the pulse rate and the pulse energy output, average power settings of 0.3 W to 3 W can be achieved. The laser energy is transmitted through a flexible optic fibre (inner diameter - 320 μ m), to which an adjustable handpiece is fitted. The beam divergence at the end of the fibre is 23 degrees. The laser operation is controlled by a foot pedal. As the Nd:YAG laser energy is readily transmitted through transparent eye tissues all laser operators must wear protective spectacles. All laser procedures were carried out under local rules determined by the laser protection supervisor.

2.5.2 Laser Treatment

In Chapters 3 and 4, an adjustable jig was used to hold the laser handpiece stationary, in contact with, and perpendicular to, the surface to be treated (see figure 2.5). The use of a stationary handpiece allowed a standard and repeatable dose of laser energy to be applied to the tissue. In Chapters 5 and 6, the laser was moved continuously over a relatively large surface area, in contact with, and perpendicular to, the enamel surface.

The tip of the optic fibre was cleaved between each laser treatment to remove any melted or damaged fibre which would affect the beam integrity. The image of the red aiming beam on a flat surface was examined to ensure the fibre gave a uniform circular beam.

The laser treatment settings were chosen from the results of a pilot study in which laser irradiation was applied to artificial white spot enamel lesions and normal enamel. It was found that even at the lowest dose of energy (30 mJ, 10 pps for a few seconds) the surface zones of the lesions were damaged,

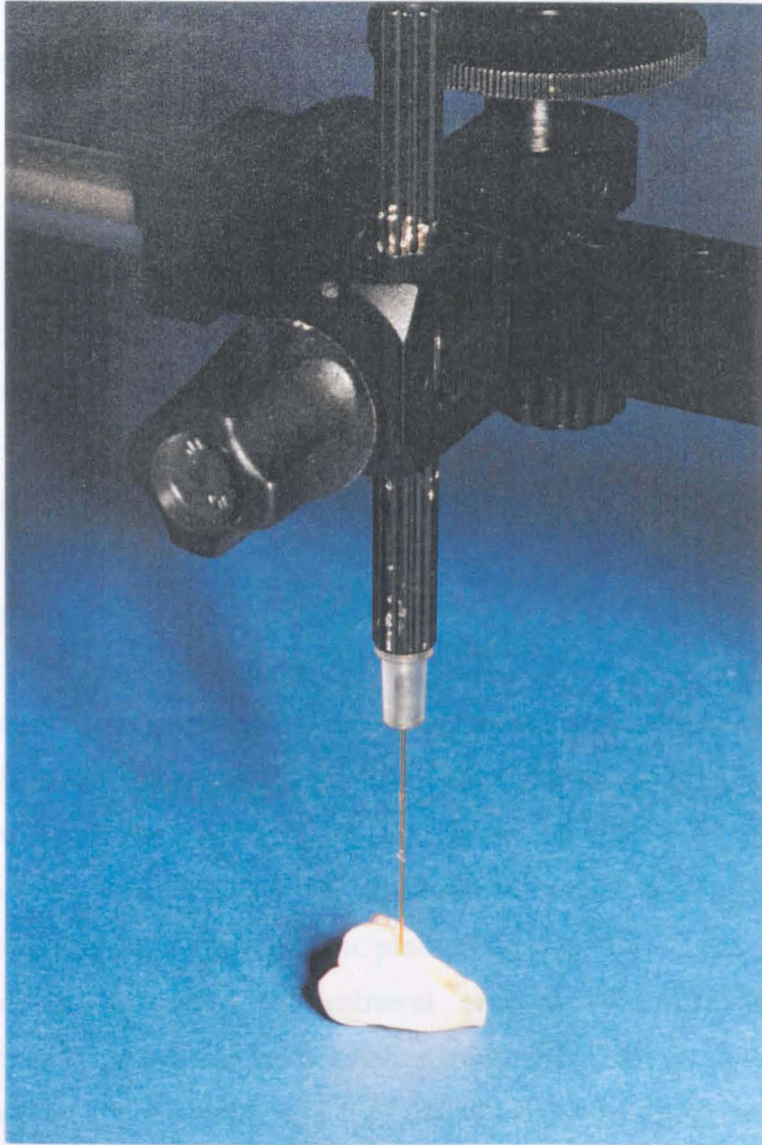


Figure 2.5 The laser handpiece held stationary, in contact with, and perpendicular to the surface to be treated, by an adjustable jig.

whereas, at the lower powers, there was no observable change to the surface of normal enamel. A balance was struck therefore between forming craters, for ease of location of the irradiated area, and causing minimal tissue damage (as described in Section 1.5.3). The laser parameters chosen for Chapters 3 and 4 were within the range recommended for clinical use (Myers, 1991):

Laser energy: 50, 100 and 150 mJ.

Number of pulses per second: 10 and 20 pps.

Treatment duration: 2 and 5 sec.

2.6 Microradiography and Microdensitometry

2.6.1 Introduction

Microradiography, and subsequent microdensitometric analysis of enamel, is based on the fact that absorption of X-rays by an enamel section is dependent on the mineral content of that tissue (as discussed in Section 1.7.2). Demineralised enamel will absorb fewer X-rays than sound enamel, so will appear darker on a radiographic plate. The equation of Angmar *et al.* (1963) is used to calculate the mineral content of the tissue from microdensitometric measurements of enamel microradiographs in correlation with a reference image of known opacity - usually an aluminium step wedge. Further information on the principles of microradiography can be found in Section 1.7.

2.6.2 Microradiography

Sections were mounted between two layers of clingfilm and placed on a Kodak high resolution microradiographic plate (Type 1A) (Eastman Kodak Company, Rochester, New York, USA) alongside an aluminium step-wedge (figure 2.6). The stepwedge consisted of a series of aluminium sheets of known thickness (50 -300 μm) which produce a standard series of grey levels

on the microradiograph (figure 2.7). The step wedge was placed along the y-axis of the plate as Creanor (1987) found variation in X-ray beam homogeneity from the top to the bottom of the plate, whereas horizontally, beam variation was less than 1 %. The sections, plate and step-wedge were placed in a photographic plate holder and exposed to $\text{Cu}(K_{\alpha})$ x-rays for 20 min (20 kV, 30 mA). The microradiographic plates were developed using standard techniques; the sections were removed and stored in thymol until required further.

2.6.3 Microdensitometry

Two microdensitometers were used in this study:

- i) Leitz ASBA image analyser
- ii) Advice image analysis unit (Brian Reece Scientific Ltd, England)

The analysis in Chapter 3 was carried out using the ASBA, whereas all the analyses in Chapters 4 and 5 were performed using the Advice image analysis unit - which only became available in the final part of the project.

The Leitz image analyser system consists of a microscope (Leitz Ortholux II) in conjunction with a stabilised transmitted illumination system (figure 2.8). The image of the microradiograph was recorded by a video camera (ASACA Corporation type 700BE) mounted on the microscope, and transmitted to an analyzer unit (Leitz Image Analyzer). The analyser unit was controlled by a Z8002 microprocessor which digitised the video signals from the camera into 256 grey levels with a resolution of 256 x 256 pixels. Potentiometers on the front panel of the image analyzer enabled the unit to be set up so that the 256 grey levels covered the region of interest. The digitised image was then transferred to a BBC-Master computer for further analysis and storage of results. The software for the BBC-Master computer and the Leitz Image Analyzer was written by Dr. R. Strang and Mr I.P.A. MacDonald (formerly of the Department of Clinical Physics, West of Scotland Health Boards).

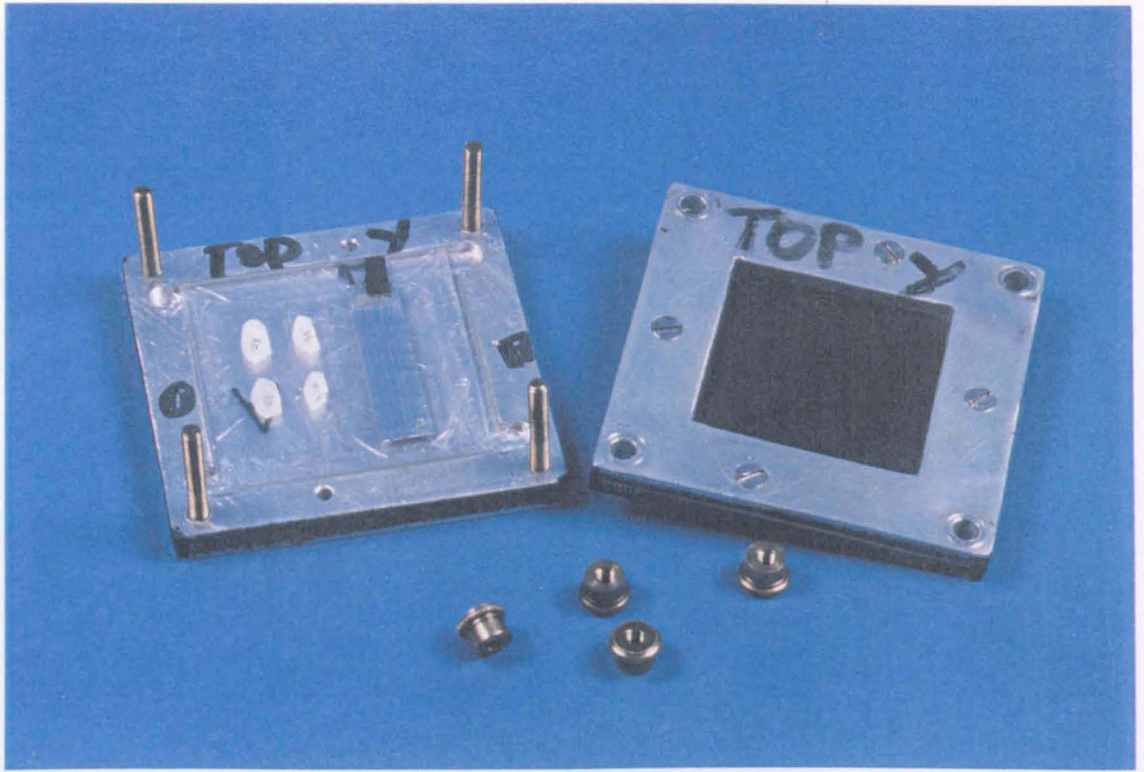


Figure 2.6 Sections mounted in clingfilm covering the glass photographic plate. The aluminium step-wedge is placed alongside the sections. The sections, plate and step-wedge are placed in a photographic plate holder.

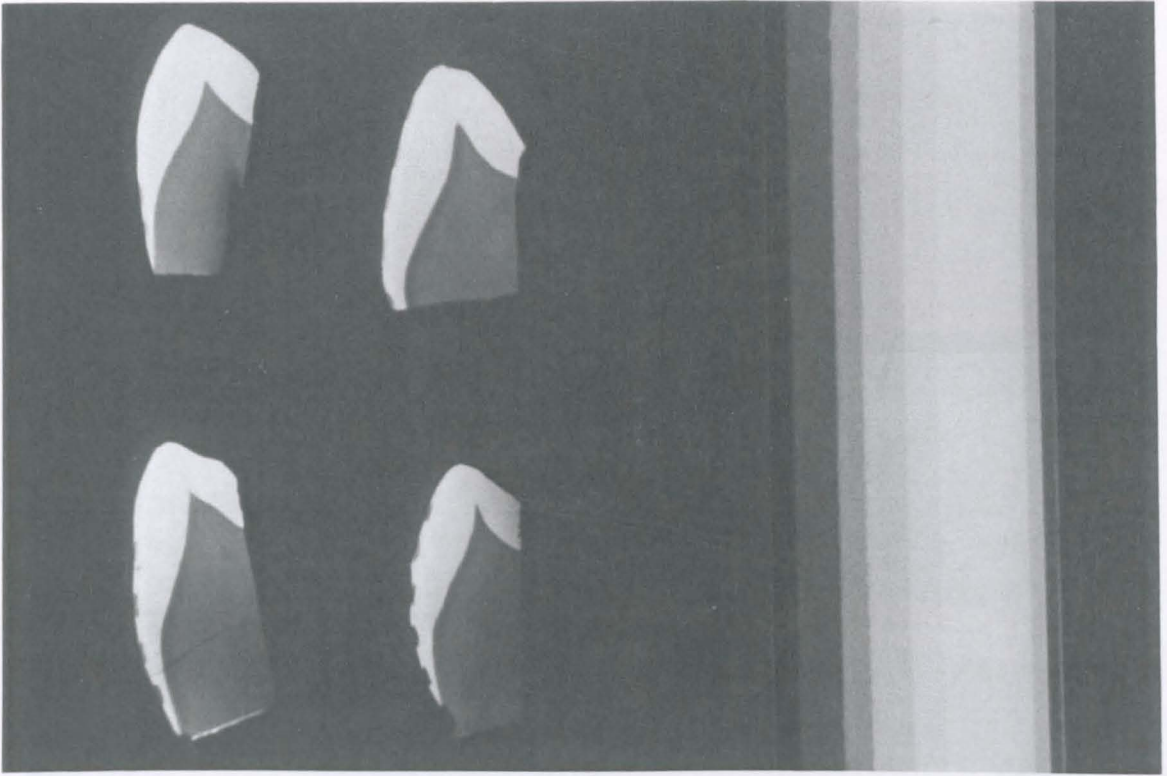
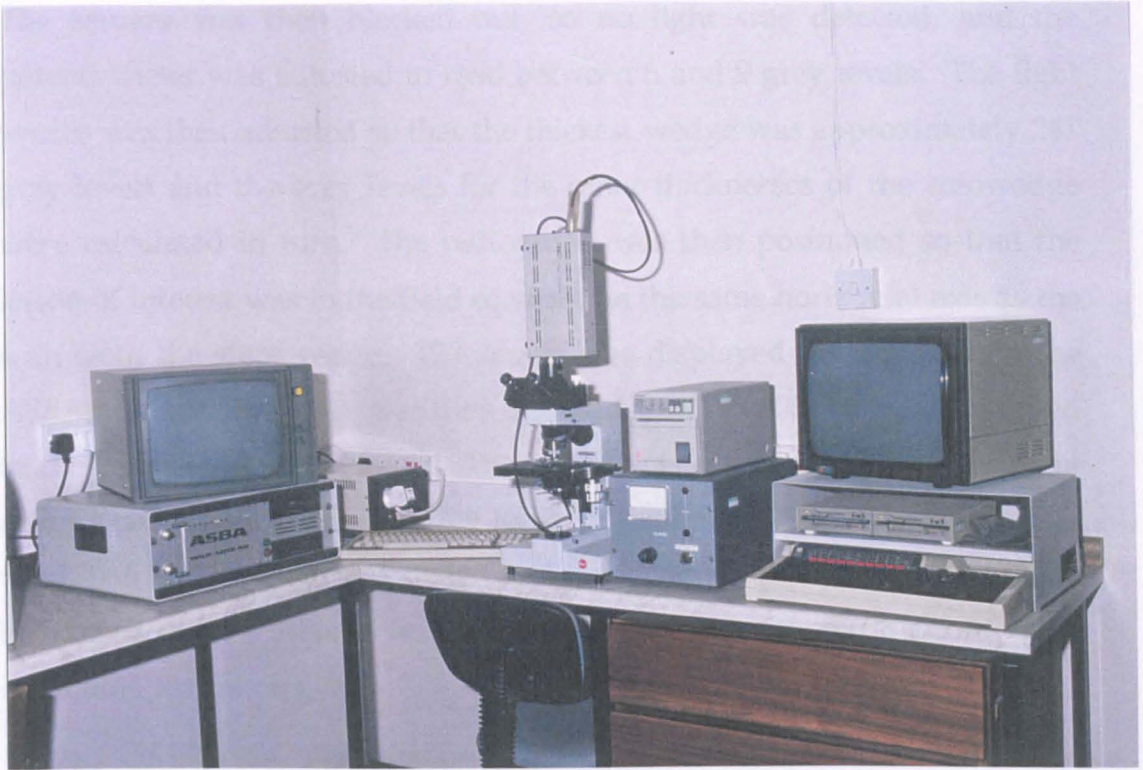


Figure 2.7 Black and white photograph of a developed microradiographic plate showing sections with artificial carious lesions and the aluminium step-wedge.

The system was calibrated using the aluminium step-wedge. The microdensitometric plate was positioned on the microscope stage so that the thickest aluminium wedge was in the field of view. The camera was first saturated with light and the potentiometer adjusted to record 250 grey levels.



A fourth order polynomial curve was fitted to the aluminium step-wedge grey levels and the grey levels of the profile converted to per cent volume mineral using the equation derived by Angmar *et al.* (1963). Appendix I gives a detailed account of the formulae derived by Angmar *et al.* (1963) equating the percent volume mineral with measured optical density of aluminium. The profile information and other relevant data, such as section thickness, were stored on floppy disk for later analysis.

The Advice Image Analysis Unit was used in conjunction with the same microscope as the ASBA system and a new CCD camera (COHU) (figure 2.9).

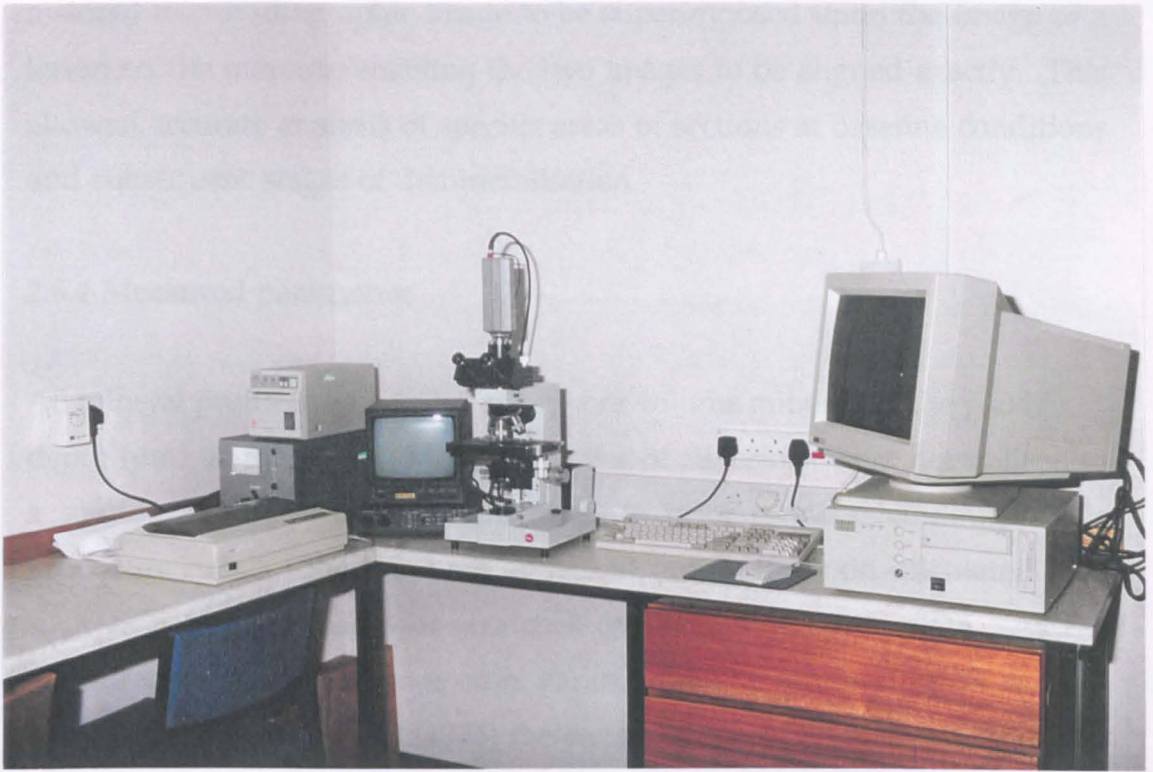
Figure 2.8 The Leitz microdensitometry system, incorporating a Leitz microscope, a video camera, an image analyser unit (ASBA) and a computer to process and store the information obtained.

The system was calibrated using the aluminium stepwedge. The microradiographic plate was positioned on the microscope stage so that the thickest aluminium wedge was in the field of view. The camera was first saturated with light and the potentiometer adjusted to record 250 grey levels. The camera was then blacked out, so no light was detected, and the potentiometer was adjusted to read between 6 and 9 grey levels. The light source was then adjusted so that the thickest wedge was approximately 241 grey levels and the grey levels for the other thicknesses of the stepwedge were calculated in turn. The radiograph was then positioned so that the lesion of interest was in the field of view, on the same horizontal axis as the scan from the step wedge. The image was displayed horizontally on the ASBA monitor; the image was then digitised into 256 x 256 pixels transferred to the BBC computer monitor. The image was displayed in four different colours corresponding to the grey levels of the image. At the magnification used, ($\times 6.2$), 1 pixel corresponded to 3 μm . The width of the lesion area to be recorded was adjustable; an average microdensitometric profile was calculated for this region.

A fourth order polynomial curve was fitted to the aluminium step-wedge grey levels and the grey levels of the profile converted to per cent volume mineral using the equation derived by Angmar *et al.* (1963). Appendix I gives a detailed account of the formula derived by Angmar *et al.* (1963) equating the percent volume mineral with measured optical density of aluminium. The profile information and other relevant data, such as section thickness, were stored on floppy disk for later analysis.

The Advice Image Analysis Unit was used in conjunction with the same microscope as the ASBA system and a new CCD camera (COHU) (figure 2.9). In this case, the advice unit digitised the image into 768 x 576 pixels; at the magnification used 1 pixel corresponded to 0.82 μm . The digitised image was then transmitted to a 486 DX2 PC (Badger) and converted into grey levels. An Excel[®] programme was used to convert the grey levels of the

profile into percent volume mineral as described above. The software for the
"Advice" programme was written by Dr. R. Szarg and Mr S. Freshick (Adviser,
Edinburgh). The major advantages of the Advice image Analysis Unit were
its ease of use and speed of data handling. In addition, the system allowed



accepted range.

The integrated mineral loss (IML) was calculated from the area above the
profile from a point at the 20 % volume mineral level on the initial slope to
a point (S) in sound enamel. Point S was selected by the operator on the
baseline profile and, providing the section was planoparallel, its positioning
in sound enamel was unimportant. In subsequent profiles of the same lesion,
point S was calculated by the computer, to maintain a fixed distance between
this point and the 20 % level on the initial slope. IML is calculated in terms
of fractional mineral content \times depth, and hence has units of microns
(%vol.mineral.ppt).

Figure 2.9 The Advice Image Analysis Unit

The percent volume mineral content of the surface zone was taken as the
maximum mineral content of the surface layer. The minimum lesion mineral

profile into percent volume mineral as described above. The software for the Excel® programme was written by Dr. R. Strang and Mr S. Roebuck (Adolos, Edinburgh). The major advantages of the Advice image Analysis Unit were its ease of use and speed of data handling. In addition, the system allowed a stored microradiographic image to be superimposed upon the image of a lesion on the monitor, enabling the two images to be aligned exactly. This allowed accurate analysis of specific areas of sections at baseline conditions and subsequent stages of demineralisation.

2.6.4 Measured parameters

All mineral profiles were stored as per cent volume mineral on the y-axis and depth (μm) on the x-axis. Mineral profiles of all lesions were normalised to a sound enamel mineral content of 80 % prior to data handling. This procedure reduces the influence of second order effects on calculated data such as accidental marks or scratches on the radiographic plate. As the measured value for normal enamel varies, in the literature, from 78 % to 87 % by volume (Groeneveld, 1974) the chosen value of 80 % was within this accepted range.

The integrated mineral loss (ΔZ) was calculated from the area above the profile from a point at the 20 % volume mineral level on the initial slope to a point (S) in sound enamel. Point S was selected by the operator on the baseline profile and, providing the section was planoparallel, its positioning in sound enamel was unimportant. In subsequent profiles of the same lesion, point S was calculated by the computer, to maintain a fixed distance between this point and the 20 % level on the initial slope. ΔZ is calculated in terms of fractional mineral content x depth, and hence has units of microns (%Vol.mineral. μm).

The percent volume mineral content of the surface zone was taken as the maximum mineral content of the surface layer. The minimum lesion mineral

content was taken as the lowest point on the mineral profile deep to the surface zone. The lesion depth was calculated as being the distance from the 20 % mineral content of the initial slope to an arbitrary cut-off point at approximately 95 % of the value of normal enamel. This arbitrary cut-off point was selected because of the unreliability of determining depths in lesions where the mineral content approaches that of sound enamel asymptotically (Mallon & Mellberg, 1985).

Appendix I outlines the derivation of the formula used to calculate the volume percent mineral from the optical density of the radiographic plate, which takes into account the absorption coefficients and thicknesses of the organic and inorganic elements of the enamel. This is equated against the absorption coefficient of the aluminium.

2.7 Scanning Electron Microscopy

2.7.1 Introduction

From the results of a pilot study - in which lased enamel specimens were dehydrated, placed into a vacuum and sputter coated by a standard SEM preparation procedure - a high proportion of samples exhibited visible cracks on the enamel surface. It was not known whether these cracks were due to the action of the laser irradiation on the enamel, or an artifact of the SEM preparation procedure. It was decided therefore, to use a technique whereby replicas were created of the specimens to be examined (McGadey *et al.*, 1994), and these replicas were subsequently used to produce micrographs (see Section 2.7.4). Thus, the likelihood of cracks occurring in the lased samples, due to the SEM procedure, was minimised.

2.7.2 Replica Creation

Tooth specimens were wiped with a isopropyl alcohol-saturated tissue (Azo-

wipe, Vernon-Carus Limited, England) and dried in air. A small amount of impression material (Unosil, DeTre, Dentsply, Germany) was stippled onto the surface of the specimen using a brush. The specimen was pressed into impression material, contained within a mould, ensuring an accurate impression of the specimen was made and taking care to avoid trapping air bubbles. The impressions were left to set for an hour. The specimens were then removed carefully and examined for artifacts using a dissecting microscope.

Positive impressions (replicas), were produced by gently dripping epofix epoxy resin (Struer Ltd, UK) into the impression mould. These were then covered to exclude dust, and left overnight to polymerise. The replicas were subsequently removed from the impression moulds and again examined for defects. Satisfactory replicas were mounted on 32 mm diameter aluminium stubs (Agar Scientific Ltd.) using a conductive carbon cement (Leit C, TAAB Laboratories Equipment Ltd.).

2.7.3 Sputter Coating

The specimens were placed in the vacuum chamber of a sputter coating machine (Polaron E 5000) and the air was evacuated until a reading of 0.1 Torr was obtained. Argon gas was allowed to bleed slowly into the chamber while it was still being pumped down. A thin film of gold was evaporated from a target situated at the top of the chamber, onto the surface of the specimen, at a voltage of 1.2 kV. This process continued for 5 min. The Argon was present in order to deflect gold particles into inaccessible areas of the specimen, hence ensuring complete coverage of the specimen by the gold particles.

2.7.4 Scanning Electron Microscopy (SEM)

A Jeol T 300 scanning electron microscope was used - operating at an

accelerating voltage of 30 kV and angulation of zero degrees. Micrographs were taken from the laser treated sites at x 250 and x 1000 magnifications using Kodak TP120 film type 6415 (Kodak Ltd. Manchester).

2.8 Infrared Spectroscopy

2.8.1 Introduction

In quantitative analysis, the percentage concentrations of components in a mixture are measured by comparison of absorption intensities. Each component is examined in its pure form at a series of concentrations, which enables the production of a calibration curve of concentration against absorption intensity for a selected band. The concentrations of these components in a mixture may then be obtained by measuring their characteristic band intensity and reading the corresponding concentration from the calibration curve. The basis of the quantitative analysis of enamel carbonate is to make a comparison of the absorption intensities of specific carbonate and phosphate bands. As the use of absolute values for carbonate absorbance would necessitate highly accurate weighing of samples (which is difficult with such small samples) and a uniform particle size, the ratios of values of specific carbonate and phosphate bands were used instead. The method of quantitative carbonate analysis used in this study involved a calibration system devised by Featherstone *et al.* (1984) from a study of the absorption characteristics of a series of synthetic carbonated apatites.

2.8.2 Production of a Standard Curve

The standardising system consisted of calcium phosphate tribasic (CPT, Baker-analysed, Baker No.1436, Sigma Chemical, Dorset) in combination with barium carbonate (BaCO_3 , Sigma Chemical, Poole, Dorset). These two chemicals were blended together in the weight ratios 1:20, 1:10, 1:6, 1.5, 1:3, 2:5, and each blend was ground in an agate mortar and pestle for 15 min.

1.5 mg of each blend was then ground with 150 mg of potassium bromide (KBr Spectroscopic grade, Sigma Chemical, Dorset), for 5 min (the KBr is a carrier matrix for the sample). Each sample was subsequently pressed into transparent discs using a 16 mm diameter KBr die (Specac, Cambridge, UK) with an applied load of 10 000 kg, under a vacuum of 0.5 torr (Beckman 00-25 press, Glenrothes, Scotland) for 1 min. Initially, a disc of pure KBr was placed in the sample chamber of the infrared spectrometer (Mattson 5000 Fourier Transform Infrared Spectrometer, Mattson Instruments inc, USA) and a spectrum was run. This KBr spectrum was then considered to be the background spectrum and was automatically subtracted, by the computer attached to the spectrometer (Genie 4DX33, WinFirst™ Unicam Analytical Systems, Cambridge, UK), from any subsequent sample spectrums. Each standard disc was then placed in turn into the spectrometer chamber and a spectrum was run for each one (32 scans per spectrum, resolution 4.0).

In order to eliminate skew in the spectra, usually stemming from the KBr matrix, and for the purposes of calculating peak sizes, it is necessary to calculate a baseline on each spectra. The principles behind this calculation are shown in figure 2.10. For the peak of interest, of maximum absorbance at frequency ν , a baseline is drawn through ν_1 and ν_2 . The baseline is measured at the same frequency ν , as the peak of interest. The baseline is automatically calculated by the computer using detailed criteria.

From the standard discs, the carbonate band at 1435 cm^{-1} and the phosphate band at 575 cm^{-1} gave strong sharp bands which were satisfactory for standardisation. The extinction (E) of each band was calculated (E_{1435} and E_{575}), from measurement of the baseline transmittance (T_2) and peak transmittance (T_1), using the relationship:

$$E = \log T_2/T_1.$$

A series of E_{1435}/E_{575} values was calculated, and the slope (M) of the line was

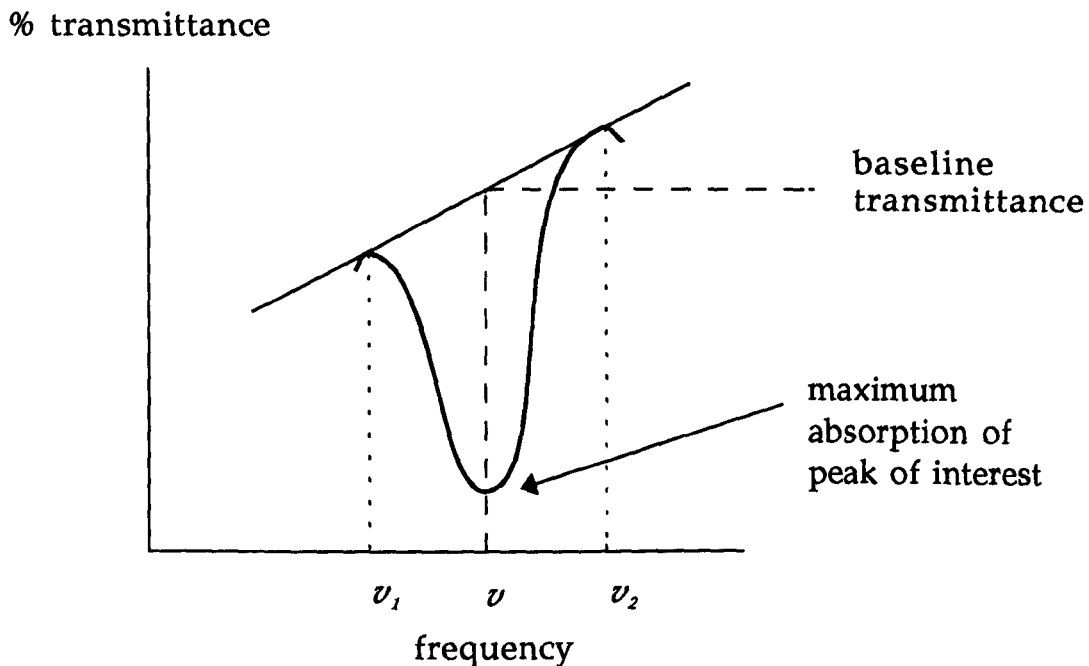


Figure 2.10 Measurement of baseline transmittance (automatically calculated by the computer). For the peak of interest, of maximum absorbance at frequency ν , a baseline is drawn through ν_1 and ν_2 . The baseline is measured at the same frequency (ν) as the peak of interest.

calculated for the relationship:

$$\text{CO}_3/\text{CPT} \times 100 = M(E_{1435}/E_{575}).$$

Featherstone *et al.* (1984) found this relationship gave the best correlation between the extinction ratios of a series of synthetic carbonated apatites and their known carbonate concentration).

2.8.3 Enamel samples

Two blocks of enamel, of surface area approximately 5 mm x 5mm, were cut from the buccal surface of the sample teeth. One block from each pair was irradiated by moving a laser continuously over the enamel surface (see Section 6.2). Each block (lased and nonlased) was attached by superglue (Loctite 454, UK) to an individual glass slide, such that the enamel surface was uppermost and perpendicular to the slide. The slide was placed under a micrometer and the height of the block was measured at specific points. Enamel was removed from the tooth in powder form, by manually scraping the surface with a reinforced steel scraper (NOGA deburring tools, Monks & Crane, Glasgow). The powdered enamel was weighed using a Sartorius MC1 balance (Sartorius, Germany), which has a resolution of 0.1 mg. After 1.5 mg of powdered enamel was obtained, the heights of the same specific points on the enamel block were again measured and the depth to which the enamel had been abraded was recorded. While it is appreciated that this method will only give a rough estimate of the extent of tissue removal from the enamel surface, it has the advantage that there is no sample contamination - which was found to be a problem when abrasive strips (McWilliam, 1995) were used to obtain the sample.

The 1.5 mg of powdered enamel was then ground with 150 mg of KBr in an agate mortar and pestle, for 5 min. This powder mixture was subsequently pressed into discs, as described in Section 2.8.2, and placed in the infrared

spectrometer. The procedure was repeated, this time the enamel coming from further into the tooth (sample 2). An IR spectrum was run for each disc and extinction ratios were calculated as described above (Section 6.2.1) - but this time using the carbonate band at about 1415 cm^{-1} (E_{1415}/E_{575}).

Featherstone *et al.* (1984) calculated the slope ratio between a standard curve (as above) and the percentage carbonate concentrations of the synthetic carbonates to be 1.77. The percent carbonate in the enamel samples is therefore calculated using the equation:

$$\%CO_3 = (M \times 1.77)(E_{1415}/E_{575}).$$

CHAPTER 3 - The Effect of Pulsed Nd:YAG Laser Irradiation on Artificial White Spot Enamel Lesions.

3.1 Introduction

Removal of carious dental enamel using the pulsed Nd:YAG laser has been advocated as a method of treatment for anxious patients (Myers & Myers, 1985a). Ablation of sound and carious enamel, and dentine, has been achieved using CO₂, Er:YAG and excimer lasers (Hibst & Keller, 1989; Tasev *et al.*, 1990; Neev *et al.*, 1996), as well as the Nd:YAG laser. Myers & Myers (1985b) demonstrated that incipient fissure caries in extracted teeth could be debrided using a pulsed Nd:YAG laser. Other reports of laser ablation of carious enamel have concentrated on assessing the underlying surface structure after cavity preparation with the laser. White *et al.* (1994) compared cavities prepared by the pulsed Nd:YAG laser with those made by a dental drill and Chang & Anderson (1994) investigated the use of dyes to enhance laser ablation of white spot lesions. Despite these studies, however, there has been no quantitative assessment of the effect of pulsed Nd:YAG laser irradiation on carious enamel, under various laser conditions.

Whilst it is accepted that the ideal treatment of porous white spot lesions is remineralisation, there is the possibility that re-hardening of the tissue surface may be achieved, equally effectively, by other techniques. The purpose of this study was, initially, to test whether Nd:YAG laser irradiation would fuse and harden the intact surface of carious enamel, possibly making it stronger and more resistant to further caries attack.

The aim of this study was, therefore, to assess and quantify the effects of pulsed Nd:YAG laser irradiation on artificially created white spot lesions in enamel, by means of SEM and microradiography (artificial white spot lesions were chosen in order to minimise the variation in opacity and structure

found in natural white spot lesions - as described in Section 1.6.2).

Firstly, the nature and extent of tissue removal from the artificial white spot lesions were examined, at a range of laser irradiation exposures. The depth of tissue ablation, and the shape of the lased craters, were quantified by microdensitometry (of longitudinal sections cut through the lased areas). Secondly, the surface morphology of the lased enamel and its surrounding unlased area was examined using scanning electron microscopy.

3.2 Method and Materials

Ten caries-free lower molars, extracted for orthodontic purposes, were cleaned (as described in Section 2.2.2) and coated with nail varnish, leaving two exposed enamel windows approximately 1 mm wide on the buccal surface (as shown in figure 2.3.a). The teeth were placed in a demineralising solution (2 mmol/l calcium, 2 mmol/l phosphate, 0.01 ppm fluoride at pH 4.6) for 3 to 5 days until artificial carious lesions were formed on the exposed enamel strips, as described in Section 2.3.4.

The buccal surface of each tooth was divided into quadrants, each containing one half of an artificial carious lesion strip. Each quadrant was lased in one spot on the lesion strip, using 50 or 100 mJ pulses (at 10 pps) for 2 or 5 sec (see figure 3.1). The position of each laser irradiation condition, with respect to the two lesion strips, was rotated between teeth. This was to compensate for regional enamel variation - in particular cervical-incisal carbonate differences which may influence the rate of laser ablation. The normal enamel between the two lesions was lased in one spot, using 100 mJ for 5 sec. The laser fibre, as described in Section 2.5.2, was held using a mechanical jig to ensure that the fibre tip was in fixed contact with the tissue surface; lasing was carried out perpendicular to the enamel surface.

An impression of each tooth surface was taken before and after lasing using

the technique described in Section 2.7. The pre- and post-laser histological replicas were examined on a JEOL scanning electron microscope at magnifications up to $\times 2000$ SEMV at the lowest voltage (5kV) that allowed with the increased magnification the best image quality.



microphotographs were taken of the enamel sections. Microchemical analysis of the lesions on either side of the band after washed, calculation of the lesion mineral content (Angerer *et al.*, 1979; Strong *et al.*, 1987) as described in Section 2.6. The parameters calculated were total mineral loss (ΔZ), volume percent mineral loss of the lesion body (ΔW) and surface area (SA). The depth of the white spot lesion was measured at 1 cm from the band spot. The maximum depth and width of the laser craters were also measured.

Figure 3.1 Four laser spots on the artificial white spot lesion strips. The enamel was carbonised around the periphery of the crater. The craters formed using 100 mJ pulses (left hand side craters) were slightly larger than those formed at 50 mJ (right hand side craters). Pulses were 100 ns. Tissue ablation occurred on laser

the technique described in Section 2.7. The pre- and post-laser irradiation replicas were examined on a Jeol T300 scanning electron microscope at magnifications up to $\times 2000$. SEM's of the lased carious lesions were compared with the corresponding pre-lased samples, and the enamel surfaces were inspected for morphologic changes induced by the various laser treatments. Specimens were examined blindly with the intention of developing an index of surface damage similar to that of Radvar *et al.* (1995). The degree of disruption to the lesion surface was scored on an arbitrary scale from 0 - 3. Criteria for this index were as follows:

- Score 0. No visible change to the enamel surface.
- Score 1. Superficial changes to the enamel including surface melting or surface roughening, but no ablation.
- Score 2. Moderate ablation of enamel lesions.
- Score 3. Extensive ablation of enamel lesions.

Teeth were sectioned through the centre of the lased spots and hand-ground to a thickness of about 140 μm (as described in Section 2.2); baseline microradiographs were taken of the enamel sections. Microdensitometric analysis of the lesions on either side of the lased crater enabled calculation of the lesion mineral content (Angmar *et al.*, 1963; Strang *et al.*, 1987) as described in Section 2.6. The parameters calculated were total mineral loss (ΔZ), volume percent mineral loss of the lesion body (LB) and surface zone (SZ). The depth of the white spot lesion was measured at both sides of the lased spot. The maximum depth and width of the lased craters were also measured.

3.3 Results

On lasing artificial carious enamel, the emission of intense white light and cracking sounds was observed frequently (a plasma); this was particularly evident when 100 mJ pulses were used. Tissue ablation occurred on laser

irradiation at both 50 mJ and 100 mJ, forming a crater area. The enamel surrounding the crater was often carbonised by the laser (see figure 3.1).

3.3.1 Microradiography

The mean microradiographic measurements of the crater depth and width, lesion ΔZ , lesion body, lesion depth and surface zone, at each laser condition, are shown in table 3.1. The raw data is displayed in appendix II, tables a-d.

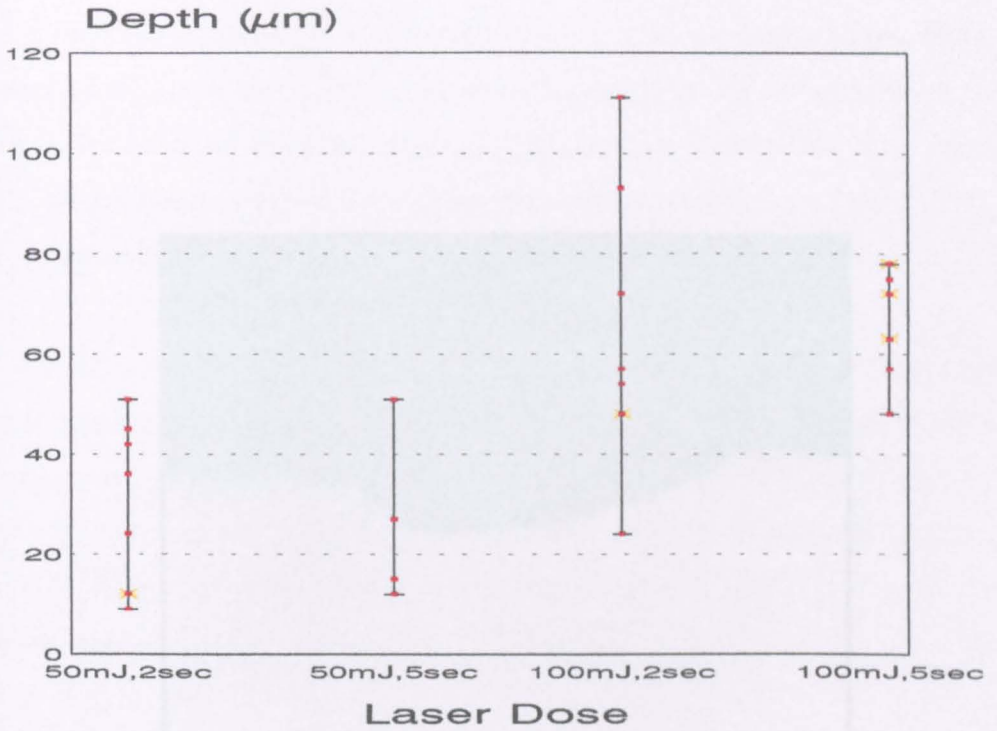
There was much variation in the amount of tissue ablated within each laser condition, as assessed by microradiography. The variation in lased crater depth, for each laser condition, is illustrated in figure 3.2. Most variation occurred using 100 mJ, for a 2 sec exposure, where the crater depth ranged from 24 to 111 μm . All lesions and lased areas were compared using paired t-tests (2-sided). Laser irradiation at 100 mJ resulted in craters which were significantly deeper than those produced by 50 mJ pulses, for both the 2 sec and 5 sec exposure times ($p=0.012$, $p=0.023$ respectively). At 100 mJ the mean depths of the lased craters were 63.4 (sd 27.7) μm and 66.0 (sd 10.14) μm , at 2 and 5 sec respectively, whereas at 50 mJ the crater depths were 28.9 (sd 16.7) μm and 26.3 (sd 17.7) μm respectively.

Most of the artificial lesions exposed to 100 mJ pulses of irradiation were completely ablated and the underlying sound enamel partially disrupted (see figure 3.3). The lased craters formed at 100 mJ (5 sec) were significantly deeper than the original artificial white spot lesions ($p=0.003$). The mean depth of the lased craters at 100 mJ (5 sec) was 66.0 (sd 10.1) μm compared to the mean original lesion depth of 53.1 (sd 5.1) μm . On exposure to 50 mJ pulses, however, complete lesion ablation occurred in only three samples; in each case the sound enamel below the lesion was not disturbed. For the remainder of the 50 mJ samples, the lased craters were on average 40.0 (± 25.7) % and 26.1 (± 11.5) % of the depth of the original lesions, at 2 and 5 sec respectively.

Table 3.1 The mean microradiographic values for each measured parameter of the lesions and lased craters.

Laser Condition mj/s	Lesion measurements			
	ΔZ (%Vol.min. μm)	SZ (%Vol.min.)	LB (%Vol.min.)	depth (μm)
100 / 5	2810 (sd 1508)	59.0 (sd 14.1)	57.6 (sd 13.3)	53.1 (sd 5.1)
100 / 2	2430 (sd 873)	61.3 (sd 6.9)	52.3 (sd 12.3)	53.6 (sd 10.2)
50 / 5	3446 (sd 1626)	66.5 (sd 2.5)	52.2 (sd 11.9)	54.8 (sd 9.6)
50 / 2	2865 (sd 900)	56.1 (sd 10.3)	50.6 (sd 14.9)	64.5 (sd 16.3)

Laser Condition mJ/s	Crater measurements	
	depth (μm)	width (μm)
100 / 5	66.0 (sd 10.1)	537.9 (sd 243.5)
100 / 2	63.4 (sd 27.7)	463.8 (sd 137.1)
50 / 5	28.9 (sd 16.7)	331.3 (sd 129.3)
50 / 2	26.3 (sd 17.7)	464.3 (sd 203.0)

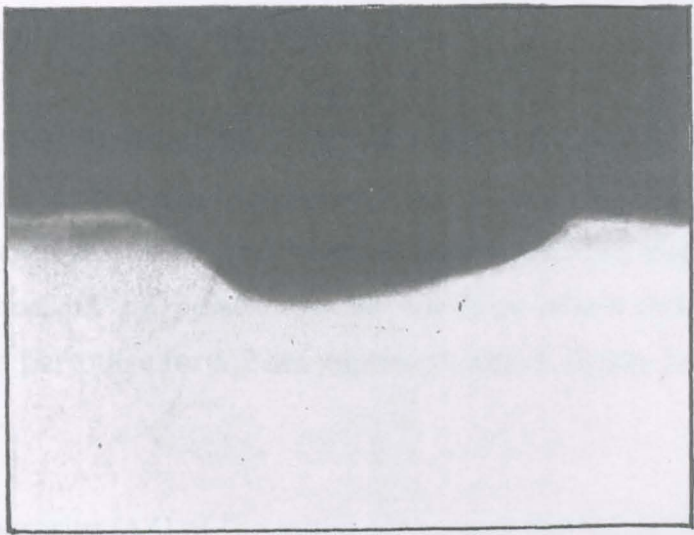


 two specimens of the same depth

Figure 3.2 The maximum depth (μm) of the craters formed by laser irradiation at 50 or 100 mJ, for 2 or 5 sec. \lceil = range of values.

Lased crater width also varied markedly, it ranged from 141 to 972 μm (see figure 3.4). There was no significant difference in the width of the lased craters between any of the treatment groups ($p > 0.05$) between the width of the lased crater and the original lesion width in the lesion (DZ, lesion body mineralisation, fig 3.4, see text for details) ($r < 0.18$), as shown in figure 3.5. There was also no significant difference in crater width and depth.

There was no significant difference in the depth of the lased craters formed at any of the laser parameters. The mean ablation depth of both the 50 and 100 mJ laser craters was 3.17 μm (range 0.5 to 10.0 μm) for a 2 sec exposure.



The depth and position of the lased craters were related to the original lesion, as seen in table 3.1. There was a significant difference in the characteristics of the original lesion (DZ, width, body mineralisation, or depth) and the depth of the lased crater (see figure 3.5).

3.3.2 SEM Analysis

There were no laser ablation effects on surface morphology, porosity, roughness, and no significant changes in surface morphology were observed ($p > 0.05$). The degree of laser disruption to the lesion surface was graded on a 0-3 scale from 0-3, as described in Section 3.2.

Figure 3.3 A typical microradiograph of a crater formed by lasing at 100 mJ for 2 sec. The original lesion on the enamel (seen here at the left of the lased crater) has been completely ablated, and the underlying enamel has been disrupted.

Lased crater width also varied markedly in each condition, the overall range being 141 - 972 μm (see figure 3.4). There was no significant difference in the width of the lased craters between any of the conditions and no correlation between the width of the lased crater and the original characteristics of the lesion (ΔZ , lesion body mineralisation, depth, or surface zone measurements; $r < \pm 0.16$), as shown in figure 3.5. There was also no correlation between the width and depth of the lased craters ($r = 0.33$).

There was no significant difference in terms of depth and width between the craters formed at 2 sec and those formed at 5 sec, for both laser powers. The mean ablation depth per pulse was therefore greater at 2 sec than 5 sec, for both the 50 mJ and 100 mJ pulses. At 100 mJ there was a mean ablation depth of 3.17 μm per pulse for a 2 sec exposure, and 1.32 μm per pulse for a 5 sec exposure.

The depth and porosity (ΔZ) of the initial white spot lesion varied between teeth, as seen in table 3.1. There was no correlation ($r \leq \pm 0.4$) between the characteristics of the original lesion (ΔZ , surface zone thickness, lesion body mineralisation, or depth) and the depth of the lased crater, as shown in figure 3.6.

3.3.2 SEM Analysis

There were no laser ablative effects on sound enamel at the powers used, and no significant changes in surface morphology were observed by SEM. The degree of laser disruption to the lesion surface was scored on an arbitrary scale from 0-3, as described in Section 3.2.

General observations for each group were as follows:

Group 0. No visible change to the enamel surface.

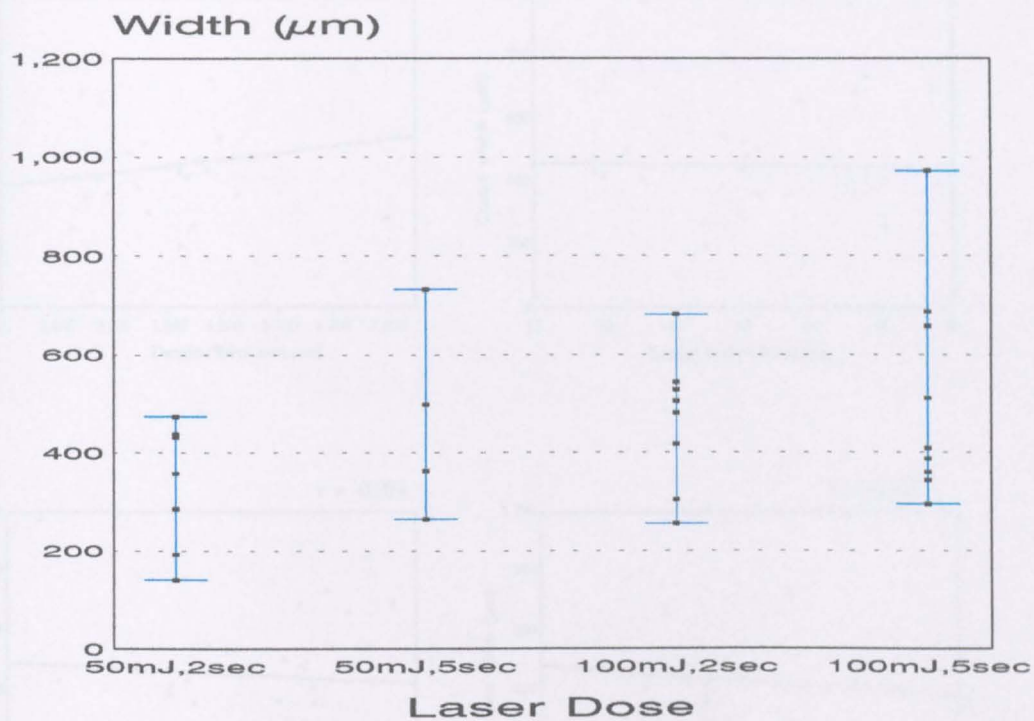


Figure 3.4 The width (μm) of the craters formed by laser irradiation at 50 or 100 mJ, for 2 or 5 sec. I = range of values.

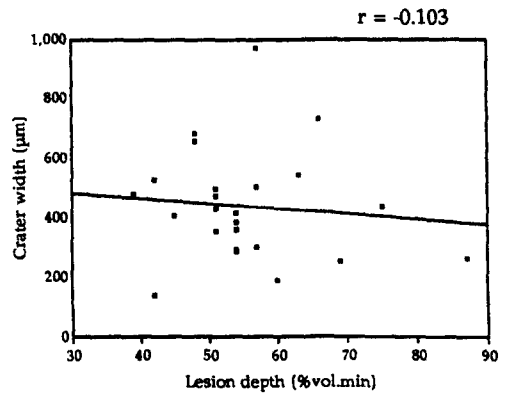
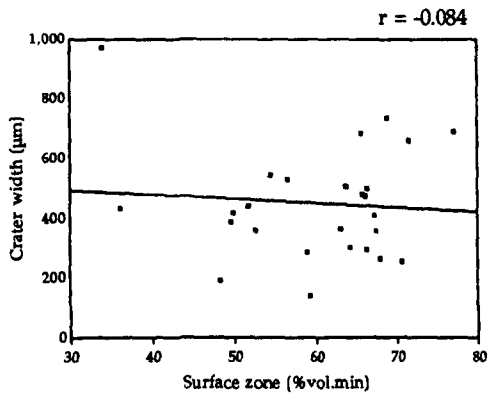
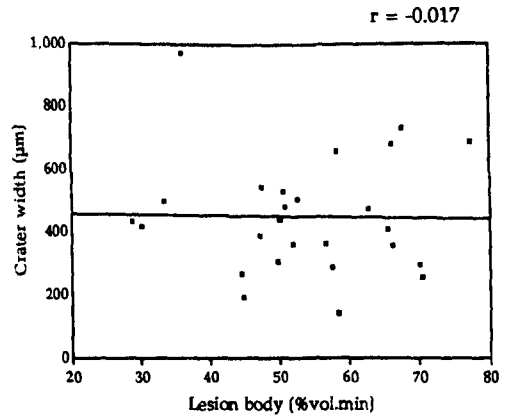
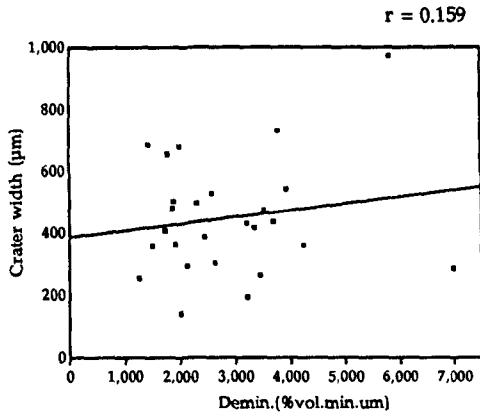


Figure 3.5 Regression graphs of the lased crater widths against the original lesion characteristics.

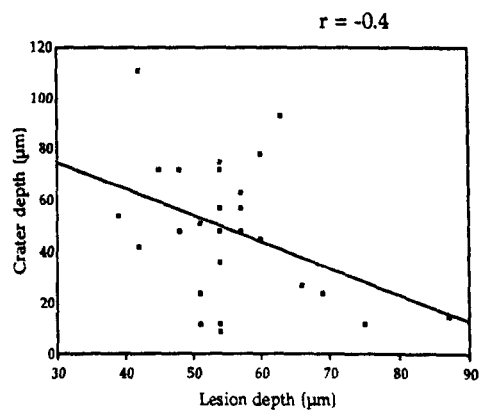
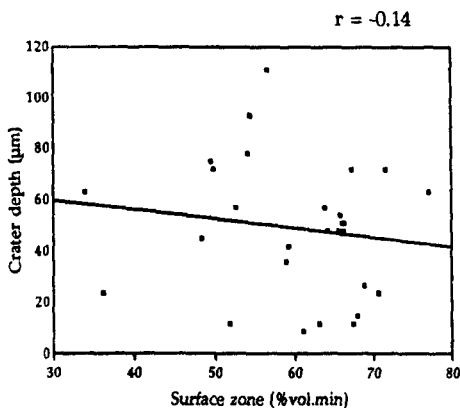
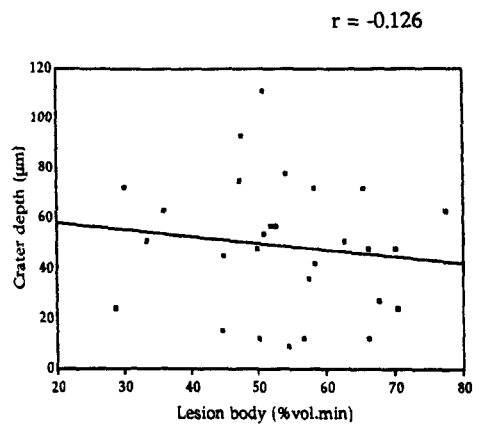
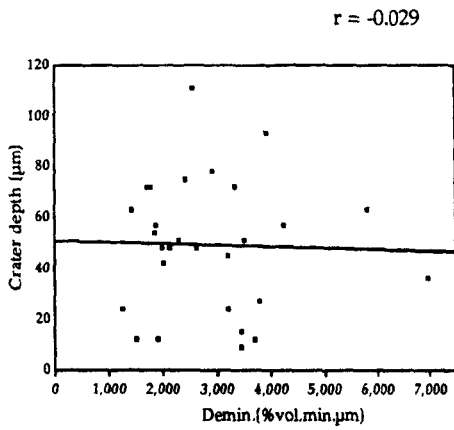


Figure 3.6 Regression graphs of the lased crater depths against the original lesion characteristics.

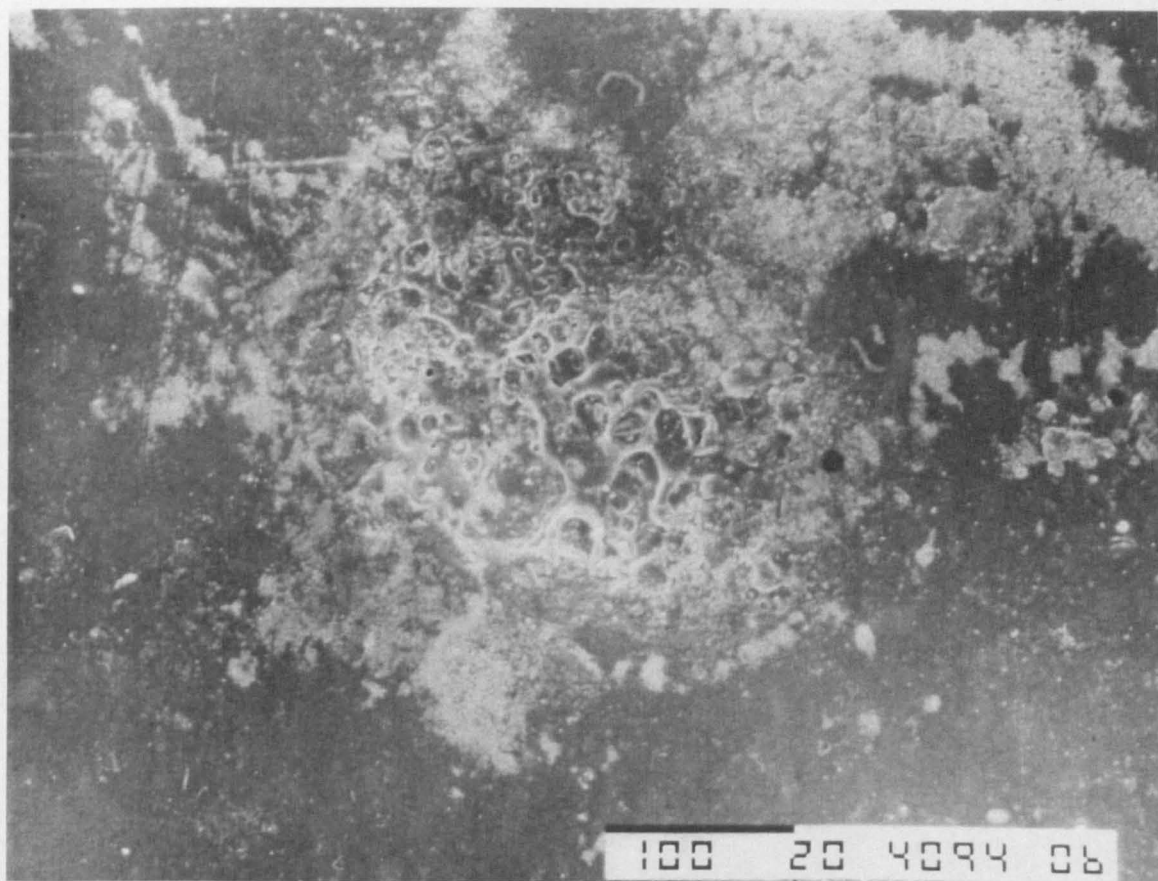
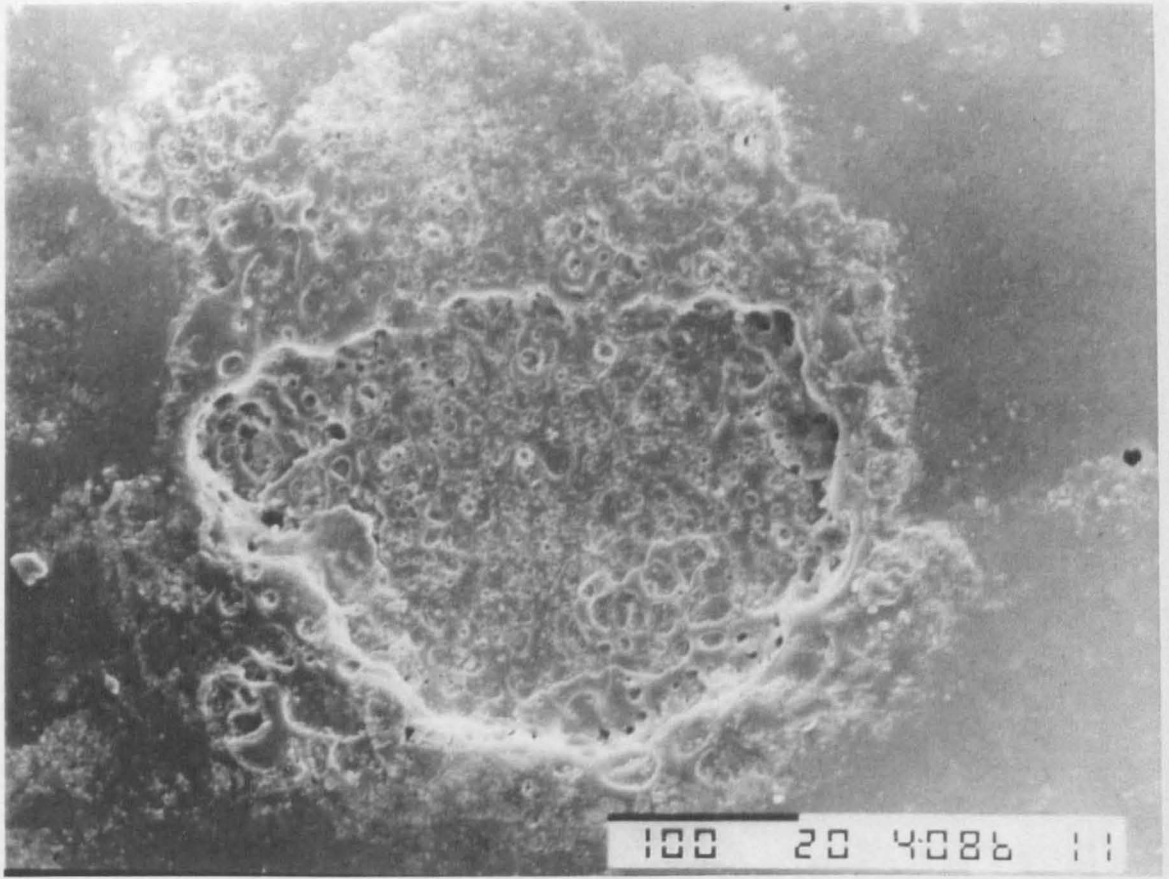
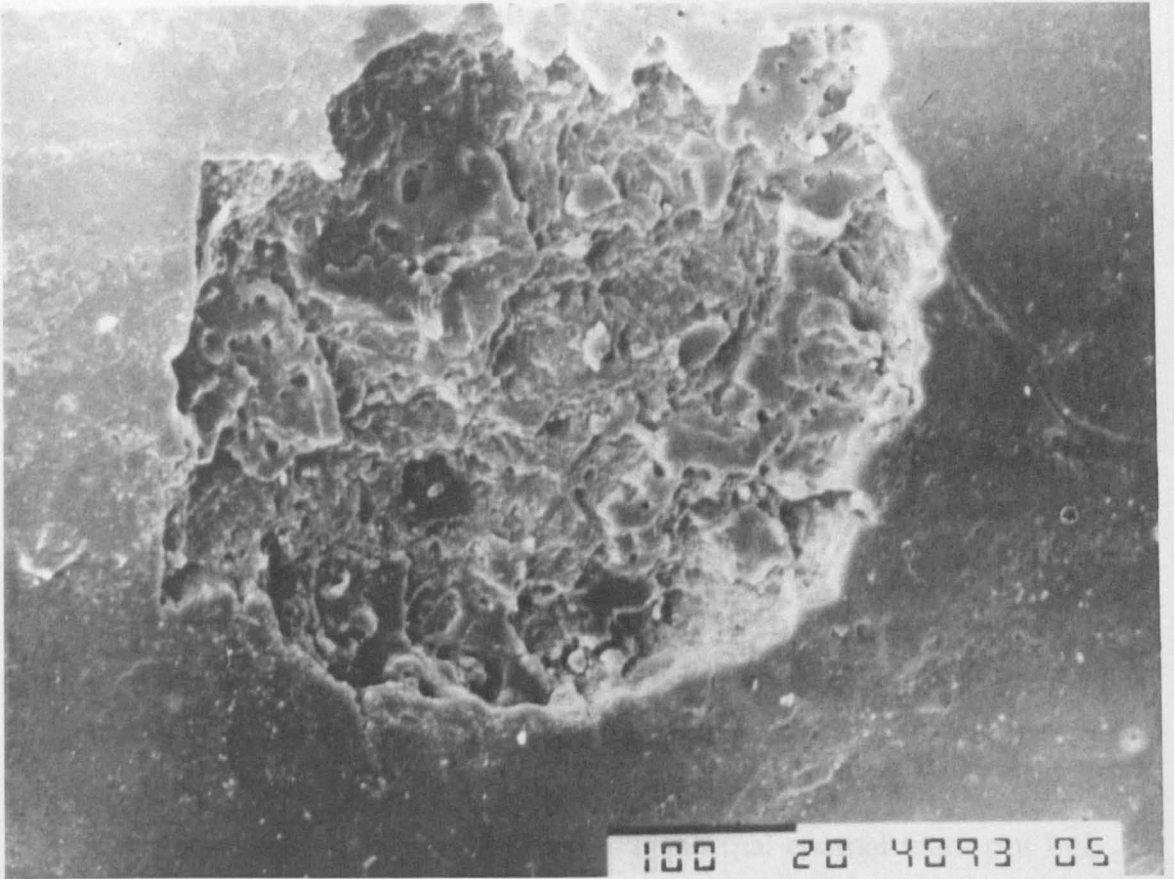


Figure 3.7 Typical SEMs of laser craters, which were arbitrarily scored into three groups a) group 1 - slight superficial melting over a diffuse, large area.



b) Group 2 - A distinct central crater shaped area, with well defined melting around the periphery of the crater onto non-ablated enamel.

Group 2 - Slight, partially superficial, non-irregular ablation deep area. No defined central area was observed and no peripheral melting.



The laser conditions used did not always correlate with the extent of morphological change as determined by SEM analysis. An exception is group 2 where the 50 mJ laser area had a smaller ablation depth area, compared with the 100 mJ condition. It was concluded that the formation of a crater of uniform diameter from a smaller area of energy is possible. Comparison of the microtopography data with the SEM analysis revealed that the laser energy delivered to the tooth surface was not uniform.

c) Group 3 - A central area of deep ablation, with extensive surface melting. Layers of molten enamel are seen and there is little peripheral melting.

As a summary of the ablation of a hot spot lesion by the laser, a specimen was prepared with the power settings used. The amount of material being removed at 100 mJ laser is 50 mJ. Some damage to the tissue occurred within the first two seconds of irradiation.

- Group 1. Slight, possibly superficial, melting over a diffuse, large area. No defined central area was obvious and no subsurface ablation had occurred (see figure 3.7.a).
- Group 2. There was a distinct, central crater shaped area with well defined melting around the periphery of the crater onto non ablated enamel. The total area of melting was much wider than the diameter of the fibre, up to double the fibre width (see figure 3.7.b).
- Group 3. There appeared to be a central area of deep ablation, with extensive surface melting. Layers of molten enamel and large pores were clearly visible in the crater. There was little or no peripheral melting of enamel. The diameter of the crater was similar to that of the optic fibre tip (see figure 3.7.c)

SEM scores are shown in table 3.2, along with the associated laser conditions and measured crater depths. All samples of normal enamel were put into group 0.

The laser conditions used did not always correlate with the extent of morphological change as determined by SEM analysis. An exception is group 2, where the 50 mJ lased areas had a smaller, shallower ablated area, compared with the 100 mJ conditions, which consisted mainly of surface melting. Comparison of the microradiography data with the SEM analysis found no relationship between the actual measured crater depth and the qualitative SEM assessment of laser damage.

In summary, the depth of the ablation of white spot lesions by Nd:YAG laser irradiation was correlated with the power setting used, the extent of ablation being greater at 100 mJ than at 50 mJ. Most damage to the lesion occurred within the first two seconds of irradiation.

Table 3.2 SEM scores of damage to white spot lesions, with the corresponding laser powers and depth measurement from each crater (whereby group 1 is superficial damage, group 2 is moderate ablation, and group 3 is extensive ablation - as described in Section 3.3.2).

SEM score	Laser condition mJ/s	Actual crater depth (μm)
Group 1	50/2	12
	50/2	42
	50/2	45
	50/2	9
	100/2	48
	100/2	54
	100/5	78
Group 2	50/2	51
	50/2	36
	50/2	24
	100/2	57
	100/2	72
	100/5	57
	100/5	75
	100/5	78
	100/5	48
Group 3	50/5	51
	100/2	111
	100/5	63
	100/5	63

3.4 Discussion

Previous investigations of pulsed Nd:YAG laser ablation of intact and carious enamel have focused on clinical comparisons of the laser with dental drills (White *et al.*, 1992, 1994, 1995). As yet, little quantitative data is available. Initially, in this study, it was hoped that Nd:YAG laser irradiation would fuse and harden the intact surface of carious enamel, possibly making it stronger and more resistant to further caries attack. However, from various pilot studies carried out on artificial white spot lesions, it became evident that the laser irradiation caused ablation of tissue even at the lowest powers used (30 mJ).

The purpose of this investigation was, therefore, to examine the ablative effects of a pulsed Nd:YAG laser, at different conditions, on the natural surface of artificial carious enamel. The experimental procedure involved a microradiographic analysis of lased artificial carious enamel and a qualitative assessment by SEM. Lasing in a single spot enabled a uniform amount of power to be applied to a specific area of the tooth. The laser conditions chosen in this portion of the study were within the range recommended for clinical use (Myers, 1991).

Immediately obvious was the amount of variation in lased crater depth, at all laser conditions. Particularly surprising was the lack of correlation between crater depth and the original ΔZ of the lesion; the most demineralised lesions were expected to be more susceptible to laser ablation. Stern *et al.* (1972) found a range of 200 to 700 J.cm⁻² (ruby laser) produced similar laser effects from tooth to tooth and suggested this disparity might be due to inherent differences in lesion colour and opacity. Similarly, variations in chemical structure may contribute to the irregular behaviour of tissue to lasing. In particular, differences in carbonate content may be responsible as this component of enamel appears to be the most susceptible to Nd:YAG laser irradiation (Yamamoto & Ooya, 1974; Yamamoto & Sato,

1980).

As tissue is removed by initial laser pulses and a crater formed, a space may develop between the fibre tip and the lesion surface. Consequently, the larger surface area exposed to the laser beam (ie., a hollow rather than the original flat tooth surface) would reduce the applied laser power, subsequent pulses being less effective in ablating tissue. This would perhaps account for the greater ablative efficiency of a two second application compared with five seconds. As discussed in Section 1.6.3, transmission of energy to the adjacent tissue also decreases the ablative efficiency of the laser.

The observations made from the SEMs were consistent with a process of surface melting and recrystallization (Stern *et al.*, 1972; Sato, 1983; Quintana *et al.*, 1992, Pogrel *et al.*, 1993). There was no evidence of the fracturing or cracking that has been observed with the CO₂ laser (Nelson *et al.*, 1987; Ferreira *et al.*, 1989), caused by the thermal cycles the surface enamel undergoes during pulsed laser irradiation. In group one, the surface melting had a smooth fused appearance, whereas in the higher groups the central ablated area was more rough, possibly due to blow-off of the molten surface enamel (Nelson *et al.*, 1986a). Stern *et al.* (1971) reported the phenomenon whereby ruby laser irradiation seems to be more highly absorbed by the interprismatic areas of the enamel surface rather than by the prism ends. They found, by scanning electron microscopic examination, that interprismatic areas appeared as amorphous depressions which outlined the raised, circular enamel prism ends. In the present study, there was no evidence of this occurrence; the lased area appeared to be uniform and, in most cases, regularly molten. The fact that the ablated area was often larger than the diameter of the optic fibre suggests diffusion of the laser beam at the tooth surface possibly due to its natural curvature. Despite the rigidity of the mechanical jig, there appears to have been slight movement of the optic fibre in a few cases.

Myers & Myers (1985b, 1989) used the Nd:YAG laser to remove carious enamel, without damaging the underlying normal enamel, prior to fissure sealant application. In this study, however, when 100 mJ pulses were used, sound enamel below the lesions was often damaged; at 50 mJ, only carious enamel was usually removed, although not in its entirety. It would seem, therefore, that in order to remove carious enamel selectively, successive applications of 50 mJ pulses are the most suitable, with close examination of the tissue between applications to ensure that all carious enamel is removed (while normal enamel is retained).

The formation of craters on the surface of teeth is to be avoided as they may facilitate plaque stagnation (although the sides of the lased craters sloped inwards towards the base of the craters, as shown in figure 3.3), and for aesthetic reasons. Laser ablation may, however, be more acceptable on the occlusal surfaces, where a small enamel defect would be less obvious, particularly around the pits and fissures.

Although it is feasible, therefore, that low power Nd:YAG laser irradiation may be used to remove carious enamel selectively, while leaving sound enamel intact, it is also recognised that clinical use of this technique would be rare, as carious lesions will preferably be left to remineralise. There is always the possibility, however, that the enamel, carious or normal, left behind after lasing has been altered to such an extent that further caries attack will be negligible. In this case it may not be necessary that all carious enamel is removed. This could be an area of further experimentation. Finally, as the technique of laser ablation does not have any significant sound or vibration it may be an acceptable alternative to the dental handpiece for nervous patients.

CHAPTER 4 - The Effect of Pulsed Nd:YAG Laser Irradiation (Alone and in Conjunction with Fluoride Varnish) on Human Enamel Demineralisation

4.1 Introduction

It is well established that ruby lasers can impart a degree of acid resistance to human enamel (Stern & Sognaes, 1964, 1972; Stern *et al.*, 1966). Significant reductions in the extent of artificial caries formation and enamel solubility have also been observed after argon (Oho & Morioka, 1990, Hicks *et al.*, 1993) and CO₂ laser irradiation of enamel (Nelson *et al.*, 1986, 1987; Featherstone & Nelson 1987; Fox *et al.*, 1992). Yamamoto & Oaya (1974), using a pulsed Nd:YAG laser at energy densities of 10 to 20 J.cm⁻², determined lased enamel surfaces to be more resistant to *in vitro* demineralisation than non-lased enamel.

There is increasing evidence of a synergistic relationship between lasers and fluoride, in terms of imparting increased acid resistance to enamel, as observed using argon (Flaitz *et al.*, 1995) and CO₂ laser irradiation (Goodman & Kaufman 1977; Fox *et al.*, 1992). Yamamoto & Sato (1980) found pulsed Nd:YAG laser irradiation in combination with Ag(NH₃)₂F reduced markedly the rate of subsurface demineralisation when compared with Ag(NH₃)₂F treatment alone or laser irradiation alone. Laser irradiation appeared to facilitate the uptake of fluoride by enamel; the depth of penetration of fluoride into the enamel was estimated to be about 7 µm. However, as the Ag(NH₃)₂F caused discolouration of enamel on lasing, it was considered to be unsuitable for clinical use.

Tagomori & Morioka (1989) found Nd:YAG laser irradiation of enamel, followed by a 24 hr application of APF solution led to a 90 % inhibition of calcium dissolution, as compared to non-treated enamel. Acid resistance was

found to be lower when the APF was used before irradiation - in contrast to Yamamoto & Sato (1980) who found fluoride applied before lasing to be the most effective combination. The 24 hr application time of the APF solution would be difficult to replicate in a clinical situation.

The aim of this part of the study was to quantify, by microradiography, the effects of Nd:YAG laser irradiation on the formation of artificial white spot enamel lesions. The study also aimed to investigate the effect, on enamel lesion formation, of laser irradiation used in conjunction with a topical fluoride varnish (Duraphat[®]; Woelm ICN Pharmaceutical, FRG) - applied as directed for clinical use. Duraphat[®] was chosen due to its having superseded APF gel in clinical use in Glasgow, the APF gel having a detrimental effect on certain porcelain and composite restorations (Ripa, 1990). The advantages of fluoride varnishes, compared with other methods of topical fluoride application, have been discussed further in Section 2.4.1. A single section technique was used to enable direct comparison of lased, and adjacent non-lased enamel areas, whilst minimising consideration of intra-tooth variability.

4.2 Method and Materials

4.2.1 Tooth Selection and Preparation

Fifteen caries free premolars, extracted for orthodontic purposes, were bisected longitudinally and each side cut, using the labcut (as described in Section 2.3.2), to give two longitudinal sections approximately 700 µm wide. It was noted from which tooth each section was cut, the intention being to carry out a paired analysis of sections from the same tooth and hence take into account any inter-tooth variability in the analysis of results.

4.2.2 Fluoride Application and Laser Parameters

A thin layer of fluoride varnish (Duraphat[®]) was applied to the natural

enamel surface of half of the sections, left on for 5 min then wiped off with a tissue and the sections rinsed with de-ionised water - as described in Section 2.4.2. All sections were then lased in two spots on the natural enamel surface; the laser parameters used were 100 mJ (10 pps) or 150 mJ (20 pps) for 5 sec. The laser fibre was held using a mechanical jig to ensure that the fibre tip was in fixed contact with the tissue surface, so standardising the amount of energy applied - as described in Section 2.5.2.

4.2.3 Section Preparation and Lesion Creation

The lased sections were subsequently ground to a thickness of 150 μm , directly through the centre of the lased craters - determined by examination under a light microscope. The sections were then microradiographed (as described in Section 2.6.2) and coated in nail varnish on both ground sides, leaving only the natural enamel surface exposed (see Section 2.6.2). They were then placed in an acidified undersaturated demineralisation solution (2 mmol/l calcium, 2 mmol/l phosphate, 0.01 ppm fluoride at pH 4.6), for 3 to 4 days, until artificial white spot lesions were formed on the natural surface, as described in Section 2.3.4. The demineralising solution was changed each day.

4.2.4 Microradiography and Microdensitometry

The nail varnish was subsequently removed and the sections re-radiographed. Microdensitometric analysis was carried out on each lased area and the adjacent, upper and lower, non-lased areas. The microradiographic images of the demineralised sections were superimposed onto their baseline counterparts, as described in Section 2.6.3, enabling calculation of the mineral content of each specific area, before, and after, demineralisation (Angmar *et al.*, 1963; Strang *et al.*, 1987). The parameters calculated were total mineral loss (ΔZ), volume percent mineral loss of the lesion body (LB) and surface zone (SZ), and lesion depth (LD) - as defined

in Section 2.6.4.

4.3 Results

The first portion of this section will describe general observations pertaining to all samples. The second portion (Section 4.3.2) will compare the lesions formed on lased enamel with those formed on non-lased enamel. In Section 4.3.3, the effects of fluoride treatment on lesion formation will be examined, and in Section 4.3.4, the 100 mJ and 150 mJ treatments will be compared. Finally, in Section 4.3.5, the baseline mineral density of lased and non-lased enamel will be compared (before lesion formation).

4.3.1 General Observations

On laser irradiation of enamel, small craters were formed in all of the 150 mJ samples, approximately the same diameter as the laser fibre. The lased areas often appeared smoother than the surrounding enamel at this laser power and had a white opacity (figure 4.1). At 100 mJ, in some cases there was obvious crater formation and in other samples the lased area was only identifiable by a faint ring of carbonised enamel around its perimeter. Often, under the light microscope, there was no visible change to the surface of the lased enamel.

Due to difficulties in aligning two lased spots when grinding each section, problems in locating the lased areas, leakage down the side of the nail varnish and general breakages, there was a large loss of samples. Hence, the original intention of a paired analysis of sections from the same tooth was not possible. Each lased area was, therefore, taken as an individual sample, having its own control in the form of the adjacent non-lased areas.

The ΔZ and lesion body mineral content values of each specific area on the demineralised sections were subtracted from the corresponding sound enamel values, giving the actual mineral loss, after demineralisation, for the lased

and adjacent non-lased areas. To compensate for vertical-matrix height variation (Cresner et al., 1999), the mean of the upper and lower non-lased areas was calculated in each case. The microtopographical roughness of the change in AZ and LB, and the actual SE and LB, of the second enamel following de-installation, are displayed in table 4.1 and 4.2 (not included).



areas, for both the non-fluoride treated samples at 100 mJ ($p=0.001$) and 150 mJ ($p=0.001$), and the fluoride treated samples at 100 mJ ($p=0.001$) and 150 mJ ($p=0.001$). At 100 mJ (table 4.1), the mean decrease in AZ of the lased area was 759 (sd 255) %Vol./mm² compared to 194 (sd 73) %Vol./mm² for the non-lased area (non-fluoride treated samples) and 394 (sd 204) %Vol./mm² compared to 1596 (sd 305) %Vol./mm² (fluoride treated samples). At 150 mJ, the mean decrease in AZ of the lased area was 1385 (sd 750) %Vol./mm² compared to 2434 (sd 627) %Vol./mm² for the non-lased area (non-fluoride treated samples) and 1024 (sd 418) %Vol./mm² compared to 2227 (sd 977) %Vol./mm² (fluoride treated samples).

Figure 4.1 Enamel lased at 150 mJ often appeared smoother than the surrounding enamel and had a white opacity.

and adjacent non-lased areas. To compensate for cervical-incisal lesion variation (Creanor *et al.*, 1989), the mean of the upper and lower non-lased areas was calculated in each case. The microradiographic measurements of the change in ΔZ and LB, and the actual SZ and LD, of the sound enamel following demineralisation, are displayed in table 4.1 and 4.2 (100 mJ and 150 mJ respectively), and summarised in table 4.3 and figure 4.3a and b (for baseline data see Appendix III, tables 1-4). The extent of lesion formation in the lased and (mean) non-lased areas was compared using anova and two-sample t-tests.

4.3.2 Lased versus Non-Lased Enamel

By initial visual examination, there was an obvious difference in the shape of the lesions formed on the lased versus non-lased areas. The surface zone of the lased area was much larger and the lesion appeared shallower. A typical example of a lesions formed in lased and adjacent non-lased enamel is shown in figure 4.4.

Total demineralisation was significantly lower in lased areas than non-lased areas, for both the non-fluoride treated samples at 100 mJ ($p=0.005$) and 150 mJ ($p=0.003$), and the fluoride treated samples at 100 mJ ($p=0.01$) and 150 mJ ($p=0.001$). At 100 mJ (see table 4.3), the mean decrease in ΔZ of the lased areas was 739 (sd 355) %Vol.min. μm compared to 1984 (sd 771) %Vol.min. μm for the non-lased areas (non-fluoride treated samples), and 594 (sd 204) %Vol.min. μm compared to 1546 (sd 908) %Vol.min. μm (fluoride treated samples). At 150 mJ, the mean decrease in ΔZ of the lased areas was 1035 (sd 750) %Vol.min. μm compared to 2434 (sd 627) %Vol.min. μm for the non-lased areas (non-fluoride treated samples), and 874 (sd 432) %Vol.min. μm compared to 2227 (sd 977) %Vol.min. μm (fluoride treated samples). In all conditions, the extent of demineralisation in the lased enamel was only approximately 40 (± 11.2) % of the extent of demineralisation observed in the non-lased enamel.

Tables 4.1 Mineral content changes of each sample, after demineralisation, for the 100 mJ laser treatment, a) ΔZ , b) SZ, c) LB, d) LD (non-lased data is the mean of the upper and lower non-lased areas).

a) Decrease in total mineral content ΔZ (%Vol.min. μm)

Fluoride Treated		Non-Fluoride Treated	
Lased	Non-Lased	Lased	Non-Lased
727.4	1911.3	1362.0	3304.9
503.9	1144.5	1004.2	2486.6
544.2	1675.9	735.9	1340.3
183.9	451.4	553.2	1535.9
554.3	1028.4	430.6	2619.2
623.0	1461.7	745.0	1120.6
832.2	3508.5	212.9	2100.4
778.8	1186.5	867.6	1361.0

b) Surface zone (SZ) mineral content (%Vol.min.)

Fluoride Treated		Non-Fluoride Treated	
Lased	Non-Lased	Lased	Non-Lased
66.75	58.55	56.44	51.19
69.56	57.53	65.58	51.07
73.26	27.18	69.03	63.99
79.56	60.08	69.04	61.41
64.67	54.99	73.59	61.83
65.61	52.97	71.15	61.51
66.32	12.26	63.34	45.02
65.07	64.19	58.61	44.40

c) Decrease in Lesion Body (LB) mineral content (%Vol.min.)

Fluoride Treated		Non-Fluoride Treated	
Lased	Non-Lased	Lased	Non-Lased
17.34	38.95	32.82	42.53
8.78	33.31	27.41	49.02
27.64	55.60	24.36	31.01
1.61	14.60	23.14	40.12
16.03	23.14	11.93	23.14
27.63	30.08	7.59	30.08
32.97	65.92	14.64	65.92
18.91	24.98	28.45	24.98

d) Lesion Depth (μm)

Fluoride Treated		Non-Fluoride Treated	
Lased	Non-Lased	Lased	Non-Lased
72.28	80.90	104.95	206.56
61.60	69.40	64.88	85.01
62.31	69.81	68.17	74.74
20.87	57.08	46.82	72.69
55.03	63.65	64.06	132.23
53.39	64.06	82.95	80.69
60.78	78.43	47.64	87.06
66.53	68.99	59.96	72.28

Tables 4.2 Mineral content changes of each sample, after demineralisation, for the 150 mJ laser treatment, a) ΔZ, b) SZ, c) LB, d) LD (non-lased data is the mean of the upper and lower non-lased areas).

a) Decrease in total mineral content
ΔZ (%Vol.min.µm).

b) Surface zone mineral content
(%Vol.min.)

Non-Fluoride Treated		Fluoride Treated	
Lased	Non-Lased	Lased	Non-Lased
1779.6	2596.1	762.6	3522.3
2221.9	2796.6	1401.4	4707.5
1743.2	2668.7	391.8	1737.9
529.3	2971.7	377.3	1796.7
545.8	1973.5	1322.6	2073.1
2051.4	3208.8	876.6	1540.3
661.1	2187.3	516.6	1632.7
72.3	2310.0	1190.0	2145.6
1596.3	2595.0	264.4	1346.2
752.1	2901.8	715.0	1482.5
972.9	2270.8	1196.1	2457.2
118.3	1203.7	1468.4	2280.8
2171.1	3250.0		
989.1	3205.7		
81.2	2821.4		
420.1	2110.5		
1577.3	2368.2		
1766.9	2254.3		
876.3	1766.6		
588.6	1539.1		
14.1	1599.4		
1971.2	3437.9		
33.5	1404.8		
1314.5	2977.2		

Non-Fluoride Treated		Fluoride Treated	
Lased	Non-Lased	Lased	Non-Lased
43.74	34.77	69.74	51.78
36.12	34.87	36.10	46.95
37.36	28.84	71.73	49.76
56.54	32.38	60.82	41.25
53.76	40.54	56.44	47.39
35.42	31.51	53.04	47.52
55.10	32.84	71.25	44.80
71.42	30.37	61.73	45.58
51.20	37.59	65.07	44.43
51.47	41.03	68.64	56.90
63.21	31.51	54.95	54.19
75.23	57.58	62.62	41.37
46.17	26.87		
39.98	28.95		
39.25	31.11		
44.53	33.42		
42.07	42.04		
36.72	38.93		
56.66	48.77		
66.87	54.65		
78.58	36.35		
53.14	38.90		
76.21	49.16		
50.34	28.76		

c) Decrease in lesion body mineral content (%Vol.min.)

Non-Fluoride Treated		Fluoride Treated	
Lased	Non-Lased	Lased	Non-Lased
41.87	47.19	11.20	49.81
50.23	49.10	39.71	44.63
46.63	50.28	10.10	36.33
59.02	49.77	10.19	39.20
39.74	41.22	34.68	41.19
44.56	51.99	34.66	31.52
24.66	47.93	18.89	30.78
8.81	51.44	19.83	39.69
44.21	52.28	19.18	30.62
9.99	47.95	12.50	26.61
16.52	60.67	25.83	43.63
2.53	31.66	44.46	42.24
47.92	56.35		
37.98	52.39		
50.64	53.28		
36.10	44.24		
42.06	38.10		
48.77	46.24		
32.21	36.05		
14.51	36.72		
14.99	33.80		
43.52	53.75		
1.03	33.80		
39.80	51.85		

d) Lesion depth (µm)

Non-Fluoride Treated		Fluoride Treated	
Lased	Non-Lased	Lased	Non-Lased
65.70	74.33	82.95	109.23
68.17	72.28	93.63	121.15
64.06	75.56	50.92	64.47
32.02	78.44	50.92	62.01
51.63	68.17	53.39	66.12
87.06	90.76	55.85	63.24
57.49	80.49	65.70	76.79
45.99	79.26	104.31	100.61
78.03	75.97	36.14	71.87
50.92	76.38	62.42	80.90
64.88	73.10	60.78	85.42
33.67	62.83	54.21	67.35
70.63	72.28		
62.42	80.08		
30.39	70.26		
25.46	71.86		
63.24	73.92		
56.67	78.85		
41.89	54.99		
41.89	57.91		
45.17	66.12		
91.17	109.23		
53.39	54.72		
56.67	90.35		

Table 4.3 The mean difference between baseline and demineralised enamel for each measured parameter of the lesions, at the a) 100 mJ and b) 150 mJ laser treatment (non-lased values are the mean of the upper and lower non-lased areas of enamel, adjacent to the lased area).

a) 100 mJ

Enamel		ΔZ (%Vol.min. μm)	LB (%Vol.min.)	SZ (%Vol.min.)	LD (μm)
Non-Fluoride Treated	Lased	739 (sd 355)	21.3 (sd 8.9)	65.9 (sd 6.0)	67.4 (sd 19.1)
	Non-Lased	1984 (sd 771)	38.1 (sd 7.0)	55.1 (sd 8.0)	98.9 (sd 48.1)
Fluoride Treated	Lased	594 (sd 204)	18.9 (sd 10.4)	68.9 (sd 5.2)	57.4 (sd 16.6)
	Non-Lased	1546 (sd 908)	35.8 (sd 17.2)	55.1 (sd 8.0)	69.0 (sd 7.8)

b) 150 mJ

Enamel		ΔZ (%Vol.min. μm)	LB (%Vol.min.)	SZ (%Vol.min.)	LD (μm)
Non-Fluoride Treated	Lased	1035 (sd 750)	33.4 (sd 15.3)	52.4 (sd 13.2)	55.8 (sd 17.1)
	Non-Lased	2434 (sd 627)	46.5 (sd 9.2)	37.6 (sd 9.2)	74.5 (sd 11.8)
Fluoride Treated	Lased	874 (sd 432)	23.4 (sd 10.1)	61.0 (sd 10.1)	64.3 (sd 19.7)
	Non-Lased	2227 (sd 977)	38.0 (sd 6.1)	47.7 (sd 6.1)	80.8 (sd 19.7)

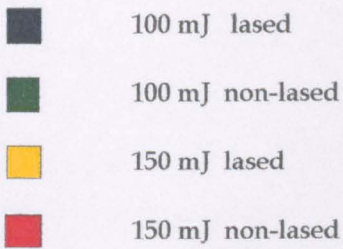
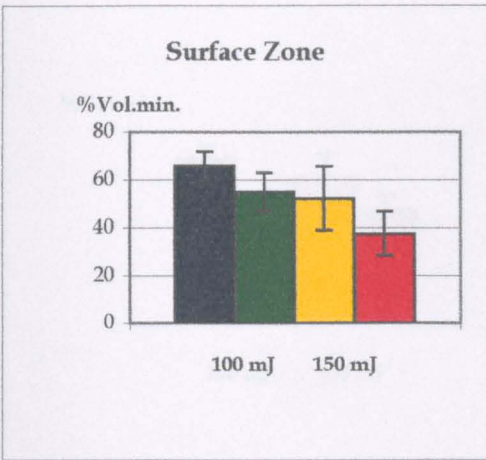
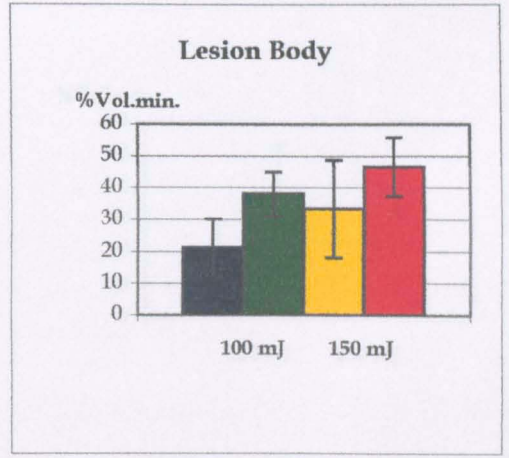
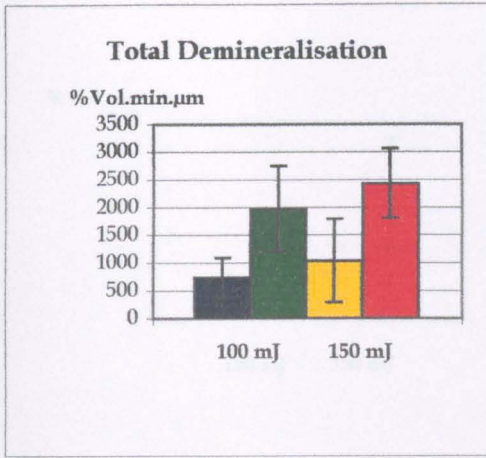
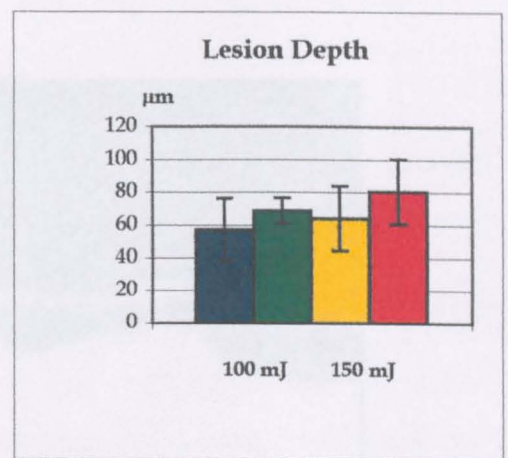
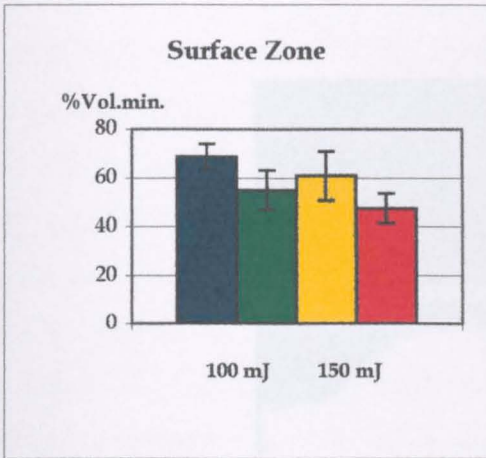
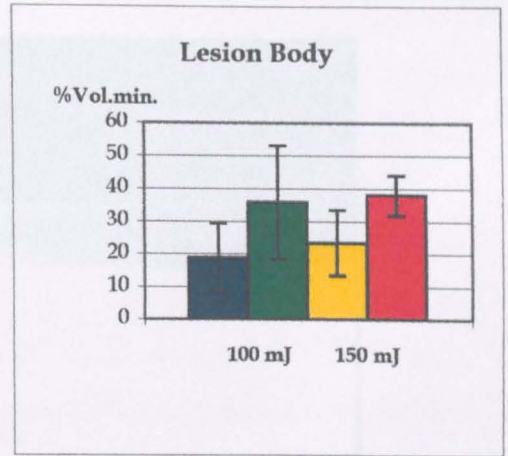
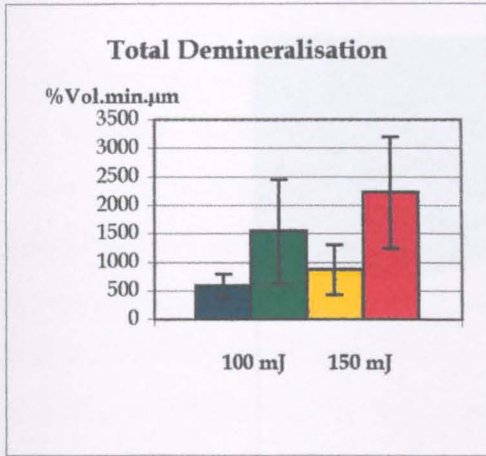


Figure 4.3a The mean measured parameters (± 1 sd) of the lased and non-lased enamel, of the non-fluoride treated samples.



- 100 mJ lased
- 100 mJ non-lased
- 150 mJ lased
- 150 mJ non-lased

Figure 4.3b The mean measured parameters (± 1 sd) of the lased and non-lased enamel, of the fluoride treated samples.

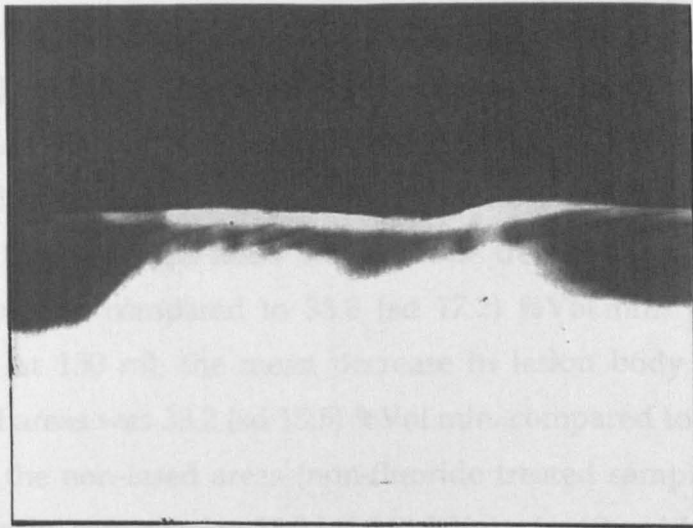
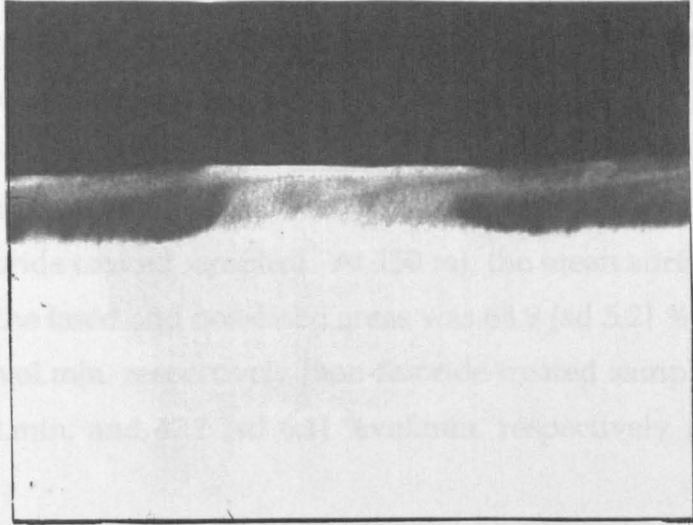


Figure 4.4 A typical example of lesions formed on enamel which has been lased in a specific area. In both cases the lased enamel (150 mJ) is in the centre of the microradiograph, where the thicker surface zone and decreased demineralisation are clearly seen.

Surface zones had a significantly greater mineral content in the lased areas than the non-lased areas, for both the non-fluoride treated samples and the fluoride treated samples, at both 100 and 150 mJ ($p < 0.05$). At 100 mJ the mean surface zone mineral content of the lased areas was 65.9 (sd 6.0) %Vol.min. compared to 55.1 (sd 8.0) %Vol. min. for the non-lased areas (non-fluoride treated samples), and 68.9 (sd 5.0) %Vol.min. compared to 55.1 (sd 8.0) %Vol.min. (fluoride treated samples). At 150 mJ, the mean surface zone mineral content of the lased and non-lased areas was 68.9 (sd 5.2) %vol.min. and 55.1 (sd 8.0) %vol.min. respectively (non-fluoride treated samples), and 61.0 (sd 10.1) %vol.min. and 47.7 (sd 6.1) %vol.min. respectively (fluoride treated samples).

Lesion bodies were significantly less demineralised in the lased areas than the non-lased areas, for both the non-fluoride treated samples at 100 mJ ($p = 0.03$) and 150 mJ ($p = 0.01$), and the fluoride treated samples at 100 mJ ($p = 0.02$) and 150 mJ ($p = 0.03$). At 100 mJ, the mean decrease in lesion body mineral content of the lased areas was 21.3 (sd 8.9) %Vol.min. compared to 38.1 (sd 7.1) %Vol.min. for the non-lased areas (non-fluoride treated samples), and 18.9 (sd 10.4) %Vol.min. compared to 35.8 (sd 17.2) %Vol.min. (fluoride treated samples). At 150 mJ, the mean decrease in lesion body mineral content of the lased areas was 33.2 (sd 15.5) %Vol.min. compared to 46.5 (sd 7.2) %Vol.min. for the non-lased areas (non-fluoride treated samples), and 23.4 (sd 12.2) %Vol.min. compared to 38.0 (sd 6.9) %Vol.min. (fluoride treated samples).

Lesion depths were significantly less in lased areas than non-lased areas, for all treatment groups ($p < 0.05$). At 100 mJ, the mean lesion depth in the lased areas was 67.4 μm (sd 19.1) compared to 98.9 μm (sd 48.1) for the non-lased areas (non-fluoride treated samples), and 57.4 μm (sd 16.6) compared to 69.04 μm (sd 7.8) (fluoride treated samples). At 150 mJ, the mean lesion depth of the lased areas was 55.8 μm (sd 17.1) compared to 74.5 μm (sd 11.8) for the non-lased areas (non-fluoride treated samples), and 64.3 μm (sd 19.7)

compared to 80.8 μm (sd 19.7) (fluoride treated samples).

4.3.3 Fluoride versus Non-Fluoride

In the 100 mJ lased areas, there was no significant difference between the fluoride treated, and non-fluoride treated samples in terms of any lesion parameters. The fluoride treated, 100 mJ, non-lased samples were significantly less demineralised than the samples in all other treatment groups ($p < 0.05$) and had a mean ΔZ of only 1546 (sd 908) %Vol.min.

At 150 mJ, there was no significant difference in total demineralisation between the non-fluoride treated, and fluoride treated enamel, in both the lased and non-lased areas. However, lesion surface zones were significantly larger in the fluoride treated enamel in both the lased and non-lased areas ($p < 0.005$). The mean surface zone mineral content, in the lased and non-lased areas respectively, of the non-fluoride treated samples, was 52.4 (sd 13.2) %Vol.min. and 37.6 (sd 9.2) %Vol.min., compared with the fluoride treated values of 61.0 (sd 10.1) %Vol.min. and 47.7 (sd 6.1) %Vol.min. respectively.

At 150 mJ, lesion bodies were significantly less demineralised in the fluoride treated enamel than in the non-fluoride treated enamel, for both the lased and non-lased areas of enamel ($p < 0.05$). The mean decrease in lesion body mineral content, the lased and non-lased areas respectively, of the non-fluoride treated samples is 33.2 (sd 15.5) %Vol.min. and 46.5 (sd 7.2) %Vol.min., compared with the fluoride treated values of 23.4 (sd 12.2) %Vol.min. and 38.0 (sd 6.9) %Vol.min.

Lesions were significantly deeper in the 150 mJ, fluoride-treated samples than in the non-fluoride treated samples, for both the lased and non-lased areas. Mean lesion depths were 64.3 (sd 19.7) μm and 80.8 (sd 19.7) μm for the fluoride treated samples (lased and non-lased respectively), compared with

55.8 (17.1) μm and 74.5 (11.8) μm for the non-fluoride treated samples.

4.3.4 100 mJ versus 150 mJ

In the non-fluoride treated samples, there was no significant difference in total demineralisation, or lesion depth, between the 100 mJ and 150 mJ treatment groups in both the lased and non-lased areas. However, lesion bodies were significantly less demineralised in the 100 mJ samples than the 150 mJ samples, in both the lased and non-lased samples ($p < 0.05$). The mean decrease of lesion body mineral content in the 100 mJ and 150 mJ samples was 21.3 (sd 8.9) %Vol.min. and 33.2 (sd 15.5) %Vol.min., respectively (lased areas), 38.1 (sd 7.0) %Vol.min. and 46.5 (sd 9.2) %Vol.min. (non-lased areas). Surface zones of the 100 mJ (non-fluoride treated) samples were significantly larger than those of the 150 mJ samples, in both the lased and non-lased areas ($p = < 0.05$). The mean surface zone of the 100 mJ and 150 mJ samples was 65.9 (sd 6.0) %Vol.min. and 52.4 (sd 13.2) %Vol.min. respectively (lased areas), and 55.1 (sd 8.0) %Vol.min. and 37.6 (sd 9.2) %Vol.min. respectively (non-lased areas).

In the fluoride treated samples, the total demineralisation of the 100 mJ, lased and non-lased samples was significantly lower than that of the 150 mJ samples ($p < 0.05$). The mean ΔZ values of the 100 mJ samples were 593.7 (sd 204) %Vol.min. μm , compared with 874 (sd 432) %Vol.min. μm for the 150 mJ samples (lased areas), and 1546 (sd 908) compared to 2227 (sd 977) %Vol.min. (non-lased areas). The surface zones of the 100 mJ samples (fluoride treated), in both the lased and non-lased areas, were significantly larger than those of the 150 mJ samples. The mean surface zone mineral contents of the 100 mJ and 150 mJ samples were 68.9 (sd 5.2) %Vol.min. and 61.0 (sd 10.1) %Vol.min. respectively (lased areas), and 55.1 (sd 8.0) %Vol.min. and 47.7 (sd 6.1) respectively (non-lased areas).

There was no significant difference in lesion body mineral content, or lesion

depth, between the 100 mJ and 150 mJ treatment groups, in the lased and non-lased areas.

4.3.5 Lased vs Non-Lased Enamel at Baseline

At 100 mJ, there was no significant difference in baseline mineral density (ΔZ) between the lased and adjacent non-lased enamel, for both the fluoride and non-fluoride treated samples. At 150 mJ, however, the baseline ΔZ of the lased enamel was significantly larger (and hence the baseline mineral density significantly lower) than that of the adjacent non-lased areas, for both the fluoride and non-fluoride treated samples ($p=0.037$ and $p=0.04$ respectively). The mean baseline ΔZ of the lased and non-lased enamel is 531 (sd 283) %Vol.min. μm and 318 (sd 161) %Vol.min. μm , respectively, for the fluoride treated enamel. The mean baseline ΔZ values of the non-fluoride treated enamel are 566 (sd 207) %Vol.min. μm and 438 (sd 214) %Vol.min. μm , respectively.

4.3.6 Summary

In summary, Nd:YAG laser irradiation of tooth enamel significantly reduced the extent of demineralisation on exposure to an *in vitro* acid challenge, resulting in shallower lesions with larger surface zones and smaller lesion bodies, when compared to non-lased enamel. In all conditions, total demineralisation was approximately 60 % lower in the lased areas than in the non-lased controls. Surface zones of specimens lased at 100 mJ were larger than those of specimens lased at 150 mJ, although total demineralisation was not significantly different. There appeared to be no evidence of a synergistic relationship between laser action and the action of Duraphat® in terms of their effect on total enamel demineralisation. At 150 mJ, however, surface zones were smaller, and lesion bodies were less demineralised in the fluoride treated samples than in the non-fluoride treated samples. At 150 mJ, the initial mineral density (before exposure to demineralising solution) of the

lased enamel was significantly lower than that of the non-lased enamel.

4.4 Discussion

The primary purpose of this investigation was to compare quantitatively the extent of demineralisation in lased human enamel, on exposure to an acid challenge, with that of non-lased enamel. Additionally, in order to investigate the possibility of synergy between laser action and fluoride application, a topical fluoride varnish (Duraphat®) was applied - as directed clinically, to the surface of half of the samples prior to lasing. A single section technique was used to minimise any intra-tooth variability in, for example, tooth opacity and carbonate content. These may influence, respectively, the extent of absorption of Nd:YAG laser irradiation and its subsequent effect on enamel.

It is evident, from this study, that Nd:YAG laser irradiation renders enamel more resistant to demineralisation. In all cases, after exposure to an acid regime, lased enamel was approximately 60 % less demineralised than the corresponding non-lased controls. Surface zones of the lased areas were larger, lesion bodies less demineralised and the lesions shallower, than the non-lased areas. These results are consistent with those of other laser studies (Tagomori & Morioka, 1989; Morioka *et al.*, 1984). Flaitz *et al.* (1995) found, by polarized light evaluation, that argon laser irradiation (100 J.cm⁻²) resulted in a 34 % reduction in lesion body depth, and a two-fold increase in surface zone depth, compared to the control lesions. Yamamoto & Oaya (1974), using an Nd:YAG laser at energy densities of 10 to 20 J.cm⁻², found lased enamel to be more resistant to *in vitro* demineralisation than non-lased enamel. Bahar & Tagomori (1994) found that pit and fissure enamel treated with pulsed Nd:YAG laser irradiation obtained an acid resistance 30 % higher than that of the unlased controls (as measured by the amount of calcium dissolved from a measured area, on acid attack).

Surface zones of the areas lased at 100 mJ were significantly larger than those of the 150 mJ lased areas, although total demineralisation was similar - indicating a difference in the pattern of mineral distribution. At 100 mJ the pulse rate was 10 per sec, at 150 mJ it was 20 per sec. The pulsed Nd:YAG laser has been found to induce microscopic cracks on enamel surfaces, due to the thermal expansion and subsequent contraction of enamel (Nelson *et al.* 1987). At 150 mJ there would be less time for enamel to cool down between successive pulses and possibly less likelihood of cracks forming. Alternatively, the larger energy density imparted at 150 mJ may cause deeper melting of enamel crystals than at 100 mJ. Both of these factors may have affected the dynamics of lesion formation.

The application of fluoride varnish to the enamel surface was found to give little added protection against lesion formation. Lesions formed on the non-lased, Duraphat® - treated enamel had larger surface zones than the equivalent untreated samples, but did not give any other consistent effects. This is, however, in accord with the results of Joyston-Bechal & Kidd (1980), who suggest that topically applied fluoride may exert its maximum effect on initial lesions rather than sound enamel.

Yamamoto & Sato (1980) found laser irradiation in combination with $\text{Ag}(\text{NH}_3)_2\text{F}$ to reduce markedly the rate of subsurface demineralisation, when compared with $\text{Ag}(\text{NH}_3)_2\text{F}$ treatment alone or lasing alone. Electron probe microanalysis revealed intense peaks of fluoride and silver on the lased areas where $\text{Ag}(\text{NH}_3)_2\text{F}$ had been applied. The depth of penetration of fluoride and silver into the enamel was estimated to be 7 μm and 14 μm respectively. Clinical use of $\text{Ag}(\text{NH}_3)_2\text{F}$ is unacceptable, however, because of the brown discolouration produced on lasing. Tagomori *et al.* (1985) in contrast to Yamamoto & Sato (1980), found remarkable acid resistance only when APF solution was used after, and not before, lasing. They suggested that large amounts of fluoride, from the APF, penetrated deep into enamel through cracks caused by laser irradiation, and into spaces between the globular

granules which had been observed by SEM. A large amount of CaF_2 was deposited in enamel treated with the APF solution after laser irradiation (as measured by electron probe microscopy). Again, however, the use of a 24 hr application of an APF solution on teeth prior to, or after, laser irradiation is not clinically practical.

Flaitz *et al.* (1995) found Argon irradiation, in combination with APF gel, to provide more caries resistance than either treatment alone. The topical fluoride would subsequently persist as a calcium fluoride layer on the tooth, or fluoridated apatite. It is probable that some fluoride from the APF gel penetrates into the tooth on lasing, as found with $\text{Ag}(\text{NH}_3)_2\text{F}$ (Yamamoto & Sato, 1980). The laser powers used in the present study (100 mJ & 150 mJ) were higher than those of previous investigations where synergy was observed. Perhaps at the higher powers the fluoride is linked with the more soluble components of the surface melt such as tetracalcium diphosphate monoxide and α or β -tricalcium phosphate.

Although in the present study the fluoride varnish was rinsed off the tooth after the 5 min application time, Duraphat® is known to be difficult to remove. Sorvari *et al.* (1994), by scanning electron microscopy, revealed remnants of Duraphat® varnish on the tooth surface even following vigorous sonication in acetone. There is always the possibility, however, that residual fluoride varnish was burnt off immediately at the high temperature induced by laser irradiation, along with carbonate and water, as has been found to occur with black ink (Tagomori & Iwase, 1995). Alternatively, any beneficial effects of the fluoride varnish on enamel demineralisation may have been counteracted by the varnish acting as an absorptive mediator, increasing the transmission of laser energy to the tooth. The pH of Duraphat® was measured as 4.12, and it must, therefore, be noted that the very application of an acid varnish will subject a tooth to a drop in pH, possibly increasing its susceptibility to further acid attack.

It is important to note that only 1 % of the fluoride available from application of Duraphat® participates in the fluoridation process and that fluoride leaches away relatively fast after application (Djikman & Arends, 1988). After one week *in situ*, Djikman & Arends (1988) found that Duraphat® treated enamel had lost significant amounts of the fluoride originally precipitated in the enamel, and the CaF₂ layer on the enamel surface was at similar levels to non- Duraphat® treated samples. In an *in vitro* study, Edenholm *et al.* (1977) demonstrated a rapid and extensive loss of fluoride from topical fluoride agents if, after application, the tooth was stored in artificial saliva for one week. Koch *et al.* (1982) found a releasing process of fluorine starts 24 hrs after *in vivo* application of Duraphat®. It is perhaps reasonable to expect, therefore, that after 4 days in a demineralising regime there would be no difference between the size of the lesions in Duraphat® treated enamel and untreated enamel. Demineralisation may, however, have been initially slower in the Duraphat® treated enamel, before it leached out of the tooth.

In view of these considerations, a pilot study was carried out whereby Duraphat® varnish was applied to windows of sound enamel, some of which were subsequently lased. The samples were then placed in de-ionised water for set periods of time, after which the solutions were replaced and their fluoride concentration measured. In all cases the amount of fluoride released into solution peaked within the first 15 minutes and decreased rapidly within an hour (see figure 4.5). Although fluoride was released from the lased samples - indicating that the varnish was not completely ablated by the laser irradiation - the amount released after 30 minutes was not significantly different from the control samples (to which no Duraphat® was applied, $p > 0.05$).

The lower baseline mineral density of lased enamel, at 150 mJ, compared to the non-lased enamel, was probably due to the extent of ablation at this power. On examination of the mineral profiles, the initial slope angulation of the lased areas was often greater than that of the non-lased areas. This

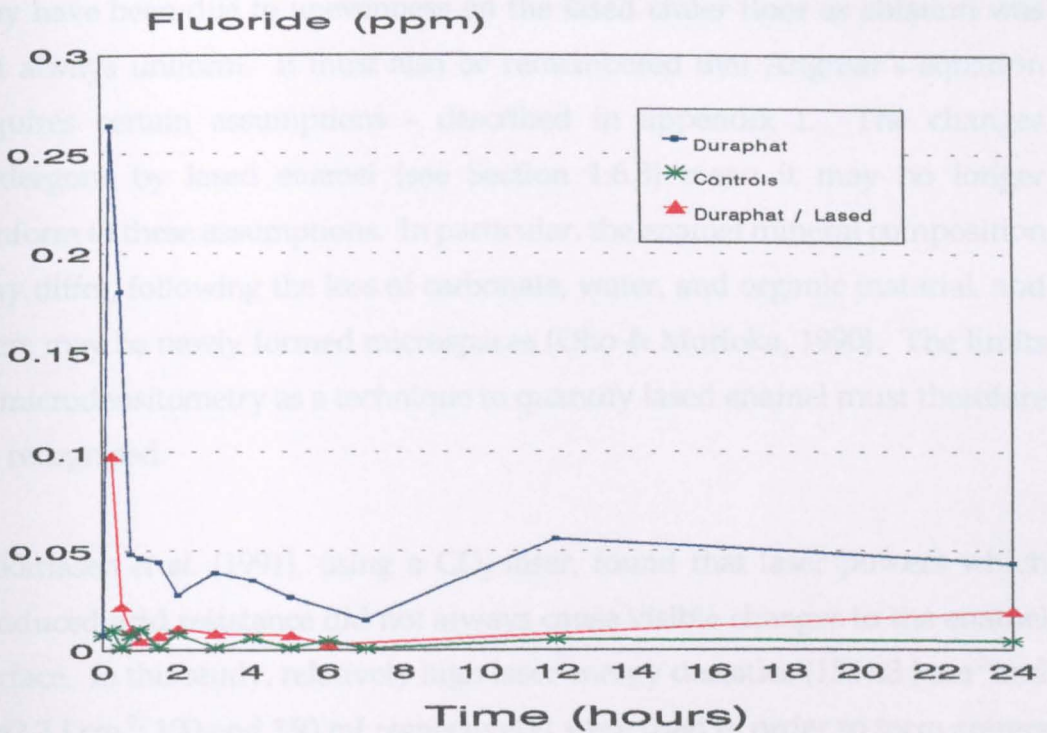


Figure 4.5 The release of fluoride ions from Duraphat[®] applied to enamel surfaces. A thin coat of Duraphat[®] was applied to windows on tooth surfaces (approx. 5 mm x 5 mm), then wiped off and rinsed with de-ionised water (as described in Section 2.4.2). Half of the samples were exposed to Nd:YAG laser irradiation across the whole of the Duraphat[®] covered area. All samples were placed in individual aliquots of de-ionised water and left for measured amounts of time over a 24 hr period. The fluoride concentration of the water was measured after the samples were removed. The controls had no Duraphat[®] applied.

may have been due to unevenness on the lased crater floor as ablation was not always uniform. It must also be remembered that Angmar's equation requires certain assumptions - described in appendix I. The changes undergone by lased enamel (see Section 1.6.3) mean it may no longer conform to these assumptions. In particular, the enamel mineral composition may differ, following the loss of carbonate, water, and organic material, and there may be newly formed microspaces (Oho & Morioka, 1990). The limits of microdensitometry as a technique to quantify lased enamel must therefore be recognised.

Zakariassen *et al.* (1991), using a CO₂ laser, found that laser powers which produced acid resistance did not always cause visible changes to the enamel surface. In this study, relatively high laser energy densities (1554.3 J.cm⁻² and 4662.7 J.cm⁻²; 100 and 150 mJ respectively) were used in order to form craters for ease of location on the enamel surfaces. When lower powers were employed it was difficult to locate the area which had been lased. Obviously, in a clinical situation, it is important that minimal cosmetic or thermal damage is inflicted on the tooth. It does not necessarily follow, however, that a lower extrapolated power will have a corresponding level of acid resistance. There are too many variables to consider, such as thermally induced chemical changes in the enamel (as discussed in Section 1.2.3). Each laser power requires to be evaluated individually to determine its clinical significance.

The ability of laser irradiation to limit the formation of caries-like lesions has been demonstrated clearly in this study. If a suitable power can be established to impart acid resistance, without pulpal injury, then this would be an ideal prophylactic treatment for caries prevention. There was, however, no evidence to suggest that Duraphat[®] varnish, when applied prior to lasing, acts in synergy with the laser action. There appears to be no more advantage to applying fluoride varnish prior to lasing than is obtained after normal prophylactic application of the Duraphat[®]. Further investigations

should focus on the potential of other fluoride vehicles, as laser compatible pre-treatments, and the use of lower, less damaging laser powers. The latter has been addressed in chapter 5, which is an assessment of the acid resistance of enamel irradiated, at various powers, by a laser beam applied in a continuous sweeping motion across its surface.

CHAPTER 5 - The Effect of Pulsed Nd:YAG Laser Irradiation, Applied in a Continuous Motion, on Human Enamel Demineralisation.

5.1 Introduction

It has been seen, in Chapter 4, that pulsed Nd:YAG laser irradiation can induce acid resistance in a tooth surface such that the extent of demineralisation in the lased areas, when exposed to an acid challenge, is only approximately 40 % of that in the non-lased enamel. This ability to limit the formation of caries-like lesions was demonstrated when teeth were irradiated by a laser beam held static, in one position, with the end of the fibre touching, and perpendicular to, the enamel surface. The resultant crater formation on the tooth surface was considered necessary to enable the identification of lased areas. This method also ensured that the dose of irradiation applied to the tooth surface was standardised for an area of 320 μm diameter, so decreasing the number of variables involved in the experiments.

In a clinical situation, however, in order to use the laser as a prophylactic caries treatment, irradiation of larger areas of a tooth surface would be required. The aim of this study was, therefore, to quantify the effects of Nd:YAG laser irradiation, applied in a clinically relevant manner to the tooth surface, on the formation of artificial white spot enamel lesions. Again, as in Chapter 4, microradiography was employed to assess demineralisation, and a single section technique was used to enable direct comparison of lased and adjacent non-lased areas, whilst minimising intra-tooth variability. Laser parameters of 100 mJ and 150 mJ were chosen as they had previously proved to be successful in imparting a degree of acid resistance to enamel samples (Chapter 4).

5.2 Method and Materials

5.2.1 Tooth Selection and Preparation

Thirty caries-free molars, extracted for orthodontic purposes, were first bisected longitudinally, using the lab cut (as described in section 2.3.2), and then an enamel block, approximately 5 mm x 10 mm x 5 mm, was cut from each half. A thin marker groove was cut into the natural enamel surface, such that it bisected the experimental surface, (as shown in figure 5.1). A similar marker was cut horizontally across the cut enamel surface on the left of the block (to enable subsequent identification of the lased area).

5.2.2 Laser Application

The enamel blocks were then lased on the left hand area of the natural surface (the marked side); the laser parameters used were 100 mJ (20 pps), or 150 mJ (20 pps), for 30 sec. The laser fibre was moved, manually, in a continuous motion across the surface of the enamel such that the entire area, from the edges up to the marker groove, was irradiated as evenly as possible during the 30 sec exposure.

5.2.3 Section Preparation and Lesion Creation

The blocks were then bisected longitudinally to obtain a thin section which had the least possible curvature of the enamel surface (see figure 5.1), and each section was ground to a thickness of 150 µm (as described in 2.2.4). The sections were then microradiographed (as described in 2.6.2) and coated in nail varnish on both ground sides, leaving only the natural enamel surface exposed. They were then placed in an acidified undersaturated demineralisation solution (2 mmol/l phosphate, 0.01 ppm fluoride at pH 4.6), for 3 to 4 days, until artificial white spot enamel lesions were formed on the natural surface, as described in section 2.3.4. The demineralising solution

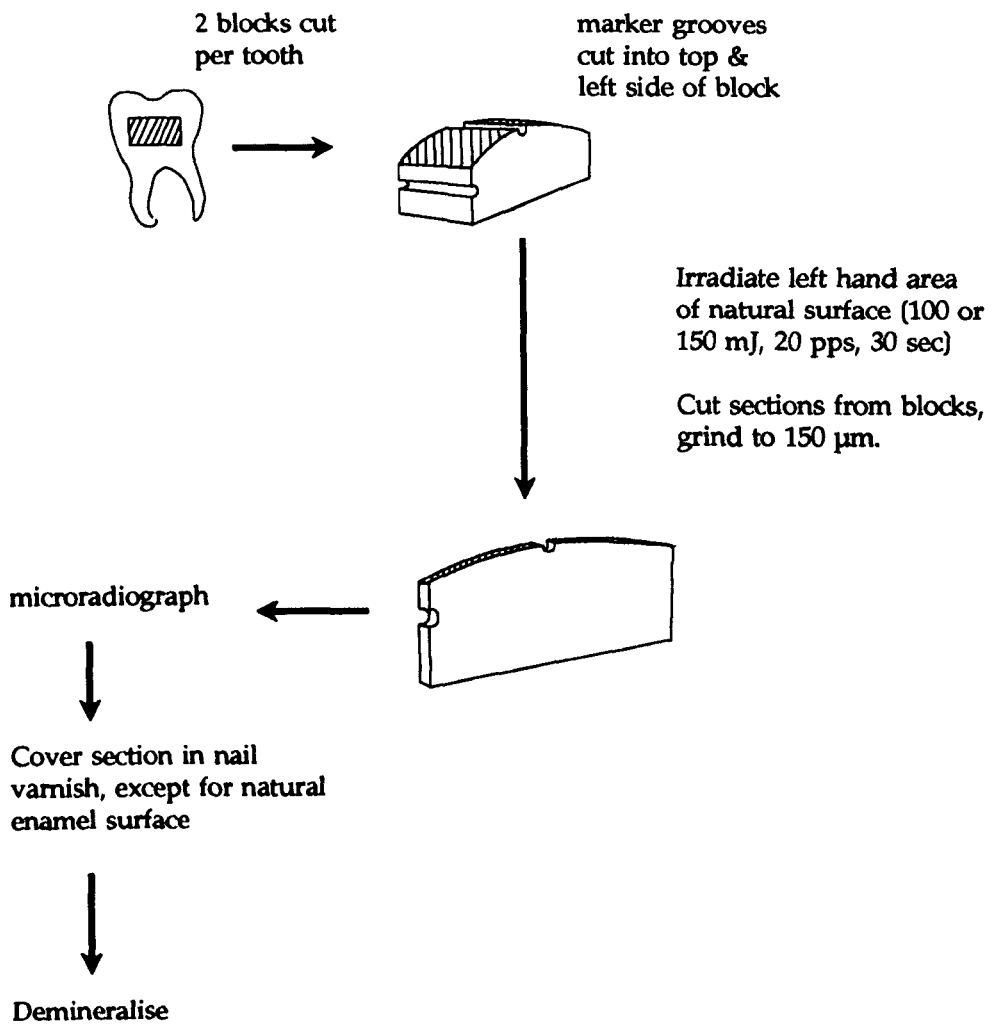


Figure 5.1 The method used to prepare samples for the acid resistance experiment. Laser irradiation was applied in a continuous manner across the tooth surface.

was changed each day.

5.2.4 Microradiography and Microdensitometry

The nail varnish was subsequently removed and the sections re-radiographed. Microdensitometric analysis was carried out on each of the lased and non-lased areas. The microradiographic images of the demineralised sections were superimposed onto their baseline counterparts, as described in Section 2.6.3, by aligning the grooves on the top and sides of the enamel sections. The mineral content parameters of each specific area, before, and after, demineralisation were calculated (Angmar *et al.*, 1963; Strang *et al.*, 1987) in terms of total mineral loss (ΔZ), volume percent mineral loss of the lesion body (LB) the lesion surface zone (SZ) and lesion depth (LD) - as defined in section 2.6.4.

5.3 Results

The first portion of this section will describe general observations pertaining to all samples. The second portion (Section 5.3.2) will compare the lesions formed on lased enamel with those formed on non-lased enamel. In Section 5.3.3 the two laser parameters will be compared. In Section 5.3.4, the baseline mineral density of lased and non-lased enamel will be compared (before lesion formation)

5.3.1 General Observations

On laser irradiation of enamel, using a pulse energy of 100 mJ, there was no evidence, by examination under the light microscope, of any alteration in the ultrastructure of the lased enamel areas. At 150 mJ, in some cases, there was slight plasma formation after about 20 sec, with some smoke and cracking sounds. On examination of the enamel, the lased areas appeared to be slightly opaque compared with the non-lased enamel and had a molten

appearance, with increased surface roughness.

By microdensitometry, it could be seen that demineralisation was not uniform throughout the length of each area (on both the lased and non-lased areas). For this reason, microradiographic measurements were taken from the most demineralised portion of each area. Each section was taken as an individual sample, the non-lased area acting as a control for the lased area.

The ΔZ and lesion body mineral content values of each specific area on the demineralised sections were subtracted from the corresponding sound enamel values, giving the actual mineral loss, after demineralisation, for the lased and non-lased areas. The microradiographic measurements of ΔZ , LB, SZ and LD, of the enamel following demineralisation are displayed in tables 5.1 and 5.2, for the 100 mJ and 150 mJ samples respectively, and summarised in table 5.3 (the baseline data is displayed in appendix IV) and figure 5.2. The extent of lesion formation in the lased and non-lased areas was compared using anova and two-sample t-tests.

5.3.2 Lased versus Non-Lased Enamel

In the 100 mJ samples, following acid challenge, there was no significant difference between the lased and non-lased enamel in terms of ΔZ , lesion body mineral content, surface zone or lesion depth.

(From table 5.1 it can be seen that the values of 6134 and 6324 %Vol.min. μm , for the decrease in total mineral from the 100 mJ lased samples, were much higher than the rest of the results. Although, there was no apparent error in these measurements, the results were taken to be anomalies and were not included in the calculations of mean total demineralisation).

In the 150 mJ samples, total demineralisation was significantly lower in lased areas than non-lased areas ($p=0.003$). The mean decrease in ΔZ of the lased

Table 5.1 Change in mineral content parameters of each sample, after demineralisation, for the 100 mJ laser treatment, ΔZ (%Vol.min. μm), SZ (%Vol.min.), LB (%Vol.min.) and LD (μm).

a) Lased

Decrease in total mineral content		Surface Zone	Lesion depth
ΔZ	LB		
3075.75	45.77	56.14	109.38
1724.84	35.27	65.52	88.82
2381.12	45.46	42.39	87.99
2364.68	40.93	67.73	86.35
3912.07	45.82	55.94	124.18
6134.25	51.25	39.68	152.14
4333.61	50.38	66.89	133.24
6323.92	54.62	70.11	162.00
4476.06	53.93	43.11	131.58
3015.73	38.47	43.15	126.65
2653.96	43.19	52.29	106.91
2376.69	35.47	51.69	119.24
2734.42	50.10	63.06	96.22
1893.26	37.69	60.39	76.48
2959.92	48.39	42.49	87.99
2150.02	45.32	55.82	71.55
426.30	22.17	68.60	60.03
1823.24	33.44	64.41	83.06
2084.76	42.47	67.76	83.88
884.41	28.41	54.94	72.37
1166.49	25.78	66.63	78.98
1947.23	42.88	64.36	76.48
1090.56	25.61	65.42	76.48
2465.68	45.06	59.76	97.86
1886.31	29.46	62.78	115.94

b) Non-lased

Decrease in total mineral content		Surface Zone	Lesion depth
ΔZ	LB		
3538.22	42.52	50.30	135.69
1790.22	38.46	62.57	88.82
1928.80	44.46	67.76	78.13
3353.66	53.42	58.90	102.80
4089.74	48.52	52.33	124.18
3571.74	46.47	44.56	129.93
4035.79	49.75	50.13	125.00
3919.32	32.77	58.67	170.23
2664.59	43.26	50.44	122.53
1535.46	37.05	60.26	72.37
1886.16	39.20	59.01	96.22
1608.94	30.19	53.44	95.40
1394.30	32.99	63.38	68.26
828.32	26.85	63.45	50.99
1803.50	42.27	45.93	76.48
2022.24	47.89	44.50	72.37
1340.23	30.38	68.13	67.43
856.31	19.11	63.82	66.61
1223.73	31.78	66.16	60.03
808.86	27.03	68.93	55.92
2060.68	37.36	61.81	94.57
1714.19	39.30	61.73	72.37
1239.48	23.53	55.83	66.61
3635.66	45.63	66.19	76.81
1204.44	27.99	46.60	83.88

Table 5.2 Change in mineral content parameters of each sample, after demineralisation, for the 150 mJ laser treatment, ΔZ (%Vol.min. μm), SZ (%Vol.min.), LB (%Vol.min.) and LD (μm).

a) Lased

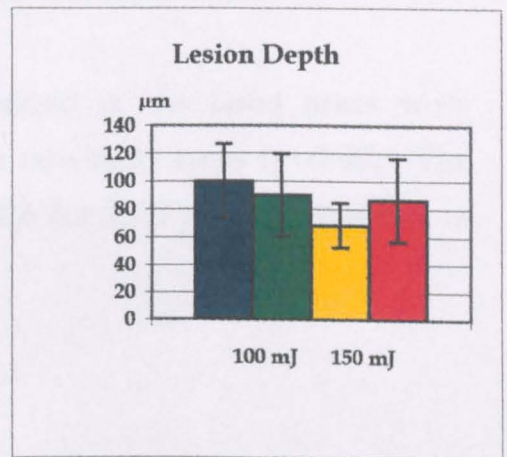
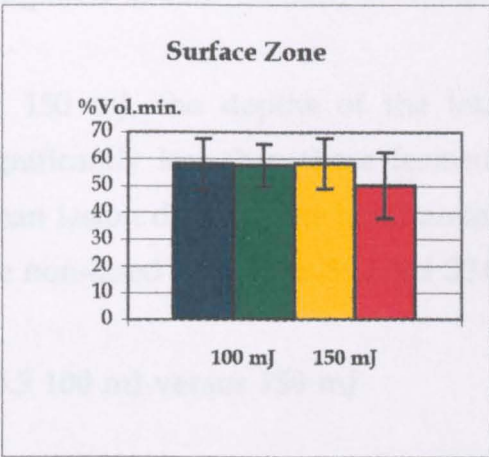
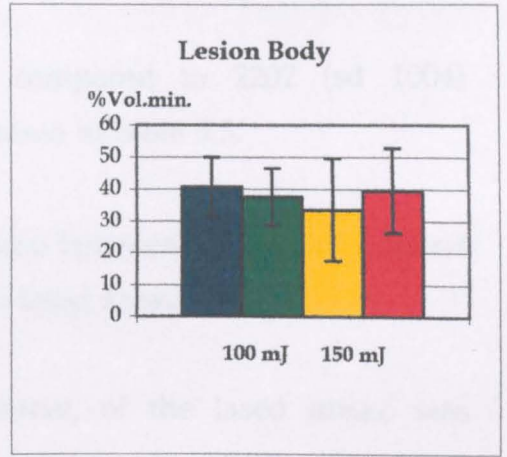
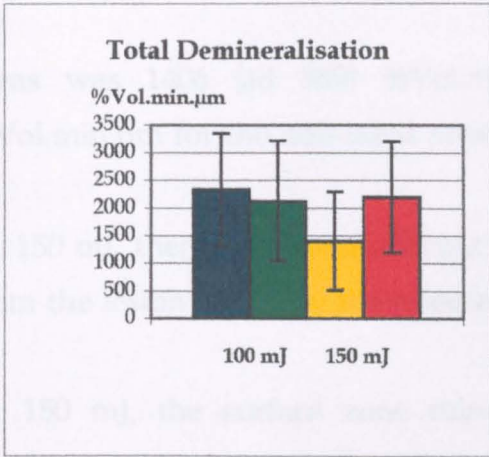
Decrease in total mineral content		Surface zone	Lesion depth
ΔZ	LB		
1305.35	29.14	67.72	71.55
119.51	3.74	47.45	40.30
1841.38	42.80	62.69	80.60
1286.35	32.56	71.23	74.84
2181.98	47.82	48.44	75.66
1603.93	33.49	52.40	83.06
206.72	12.63	67.54	50.16
752.04	17.39	67.28	64.15
949.44	32.70	58.39	51.81
1131.80	15.75	62.19	100.33
167.86	8.53	71.58	50.16
787.93	25.53	61.24	56.74
461.31	17.44	66.86	53.45
606.60	20.04	65.76	49.34
3085.88	43.88	52.52	102.80
1707.17	51.13	45.54	75.66
1277.04	35.01	55.42	70.72
1366.17	39.14	64.78	63.32
2836.37	60.12	49.80	73.19
1000.04	31.34	61.69	59.05
1319.89	40.45	65.67	58.39
1473.92	42.05	61.16	61.68
3281.33	65.63	39.27	91.28
1867.29	36.38	50.11	82.24
2673.13	55.02	42.23	73.19

b) Non-lased

Decrease in total mineral content		Surface zone	Lesion depth
ΔZ	LB		
2212.39	37.82	55.49	115.13
2261.35	30.03	65.43	137.34
1888.88	24.81	54.14	114.31
1600.75	34.26	60.44	80.60
1993.73	43.95	41.80	87.99
4677.96	55.02	47.99	144.74
1651.17	35.46	67.76	80.60
3775.11	33.88	58.67	172.70
406.31	12.01	71.59	43.60
583.60	10.80	67.21	51.81
1225.41	37.34	56.89	67.43
1486.12	34.16	58.37	67.43
600.46	21.04	65.06	63.32
1227.18	37.87	54.97	62.50
2114.90	43.14	44.64	82.24
3626.33	57.37	27.72	92.23
3778.77	54.88	36.86	92.23
2391.28	44.04	43.48	77.30
3437.66	55.95	40.74	80.59
1353.17	34.82	45.40	68.26
2475.33	45.71	41.47	75.66
1584.99	40.78	37.77	62.50
3210.46	54.21	44.18	87.99
3233.32	54.31	44.01	87.99
2253.88	54.49	27.06	68.26

Table 5.3 The mean difference between baseline and demineralised enamel for each measured parameter of the lesions, at the a) 100 mJ and b) 150 mJ laser treatment.

Enamel Treatment		ΔZ (%Vol.min. μm)	LB (%Vol.min.)	SZ (%Vol.min.)	LD (μm)
100 mJ	Lased	2340 (sd 1016)	40.69 (sd 9.2)	58.04 (sd 9.6)	100.2 (sd 26.7)
	Non-lased	2162 (sd 1092)	37.53 (sd 9.0)	57.79 (sd 7.8)	90.1 (sd 29.5)
150 mJ	Lased	1406 (sd 889)	33.59 (sd 16.0)	58.37 (sd 9.4)	68.55 (sd 16.1)
	Non-lased	2202 (sd 1004)	39.53 (sd 13.2)	50.37 (sd 12.3)	86.65 (sd 30.0)



- 100 mJ lased
- 100 mJ non-lased
- 150 mJ lased
- 150 mJ non-lased

Figure 5.2 The mean measured parameters (± 1 sd) of the lased and non-lased enamel samples.

Lased versus Non-Lased Enamel (cont'd)

areas was 1406 (sd 889) %Vol.min.µm compared to 2202 (sd 1004) %Vol.min.µm for the non-lased areas, as shown in table 5.3.

At 150 mJ, there was no significant difference between the loss of mineral from the lesion bodies of the lased and non-lased areas ($p>0.05$).

At 150 mJ, the surface zone mineral content, of the lased areas, was significantly larger than that of the non-lased areas ($p=0.012$). The mean surface zone mineral content of the lased areas was 58.5 (sd 9.3) %Vol.min. compared to 50.4 (sd 12.3) %Vol.min. for the non-lased areas.

At 150 mJ, the depths of the lesions formed in the lased areas were significantly less than those formed in the non-lased areas ($p<0.05$). The mean lesion depth of the lased areas was 68.6 (sd 16.1) µm, whereas that of the non-lased areas was 86.7 (sd 30.0) µm.

5.3.3 100 mJ versus 150 mJ

The total demineralisation of enamel lased at 150 mJ, was significantly less than that of the 100 mJ lased and non-lased enamel samples ($p=0.016$ and $p=0.002$, respectively). The mean total mineral loss (ΔZ) of the 150 mJ lased areas was 1406 (sd 889) %Vol.min. compared to 2340 (sd 1016) and 2162 (sd 1092) %Vol.min. for the 100 mJ lased and non-lased samples respectively.

There was no significant difference in the extent of mineral loss from the lesion bodies at any parameter.

There was no significant difference in the size of the surface zone, between the 100 and 150 mJ lased enamel areas. The surface zones of the non-lased 150 mJ samples were, however, significantly smaller than those of the other

samples ($p=0.018$). The mean surface zone mineral content of the 150 mJ samples was 50.4 (sd 12.3) %Vol.min., compared with 57.8 (sd 7.8) for the 100 mJ samples.

The depth of the lesions formed on the 150 mJ samples was significantly less than those of the 100 mJ samples ($p=0.003$). At 150 mJ, the mean lesion depth was 68.5 (16.1) μm for the 150 mJ samples compared to 100.2 (sd 26.7) μm (lased) and 90.2 (sd 29.5) μm (non-lased).

5.3.4 Lased versus Non-Lased Enamel at Baseline

There was no significant difference in baseline mineral density between any of the sample groups (lased, non-lased, 100 mJ, 150 mJ).

5.3.5 Summary

In summary, on exposure to an *in vitro* acid challenge, enamel samples exposed to laser irradiation at 150 mJ, underwent significantly less total demineralisation than non-lased enamel or enamel exposed to 100 mJ laser irradiation (samples were, on average, approximately 30 % less demineralised). Lesions formed on the 150 mJ samples were also shallower and their surface zones had a significantly larger mineral content. There was no significant difference between the lased and non-lased areas of the 100 mJ samples.

5.4 Discussion

As it has already been demonstrated, in Chapter 4, that Nd:YAG laser irradiation may induce acid resistance in human enamel when focused onto a single spot area, the purpose of this investigation was to quantify further the effect of laser irradiation on enamel demineralisation. In this case, enamel was irradiated by a laser beam passed in a continuous manner over

a relatively large surface area - a method considered to best represent conditions which would be employed in a clinical situation.

Moving a pulsed laser continuously over a relatively large area would give variation in the energy deposited over the sample surface and the dose distribution between samples: some areas would inadvertently receive larger energy doses than others. The microradiographic analysis indicated that demineralisation was not uniform throughout the length of each section. It was important, therefore, that measurements were taken from a reproducible area, which in this study was chosen to be the area of maximum demineralisation in each sample - to give the worst case scenario of acid resistance from a clinical perspective.

The most significant finding from this study was that enamel irradiated at 150 mJ was approximately 30 % less demineralised than the equivalent non-lased enamel and the 100 mJ lased samples. The lesions formed in the lased areas were also shallower and had larger surface zones. In contrast to Chapter 4, enamel lased at 100 mJ was not significantly different from the equivalent non-lased enamel, in terms of demineralisation parameters. Enamel lased at 150 mJ showed an increased surface roughness and opacity, which was not evident in the 100 mJ lased samples.

It may be, therefore, that to impart significant acid resistance to enamel, laser irradiation above a particular threshold value must be used (150 mJ, 450 J.cm⁻², in this study). This may inevitably be associated with a visible alteration to the tooth surface. Hess (1990) found that the total energy output required to modify the tooth structure was reduced by the use of a laser initiator pre-treatment (a layer of black ink on the tooth surface). As the use of low powers of laser irradiation decreases the potential risk of pulp damage (Suda *et al.*, 1995), the use of laser initiators is of interest for further investigation of acid resistance, and will be discussed in Chapter 7.

CHAPTER 6 - An Investigation, by Infrared Spectroscopy, of Enamel Exposed to Pulsed Nd:YAG Laser Irradiation.

6.1 Introduction

It has been seen from Chapters 4 & 5 that enamel exposed to laser irradiation may be more resistant to acid dissolution than normal enamel. A definitive mechanism for laser-induced acid resistance in enamel has not yet been established and there are several possible contributory mechanisms - as discussed in Section 1.6.3. It has been suggested that laser irradiation of enamel causes surface melting, and rapid recrystallisation of various calcium phosphate phases as well as an apatite with a lower carbonate content than normal enamel (Fowler & Kuroda, 1986, Nelson *et al.*, 1987). Nelson *et al.* (1987) determined the carbonate content of surface enamel exposed to CO₂ laser irradiation (50 J.cm⁻²) to be 0.59 (±0.04) %wt/wt, whereas that of non-lased surface enamel from the same tooth was 1.63 (±0.08) %wt/wt. As carbonate-rich mineral is the most soluble component of enamel (Hallsworth, Weatherell & Robinson, 1973), it follows that the lower carbonate content of lased enamel should contribute to its acid resistance.

Conventional carbonate analyses - such as manometric methods (Hülsemann, 1966), the bubble method (Weatherell & Robinson (1968), thermogravimetric methods (Holager, 1970), and gas-chromatography (Nelson & Featherstone (1982) - require specially modified apparatus, specific calibration, or are unsuitable for the small samples required in enamel analysis. Nelson *et al.* (1987) used infrared spectroscopy to quantify the carbonate content of enamel. This technique involves a calibration system for carbohydrate analysis devised by Featherstone, Pearson & LeGeros (1984) - from previously used infrared methods (Arends & Davidson, 1975) - which they claim enables carbonate estimation to better than ±10 % in the range 1-12 %wt/wt. Nelson *et al.* (1987) found that infrared spectroscopy also enabled identification of the

high temperature phase tetracalcium diphosphate monoxide in samples of lased enamel (CO_2 laser irradiation at 50 J.cm^{-2}). This product is, however, more soluble than normal enamel (Fowler & Kuroda 1986) and hence its formation in lased enamel would decrease acid resistance (as discussed in Section 1.6.3).

The aim of this study was to investigate, by infrared spectroscopy, the effects of Nd:YAG laser irradiation on enamel, in order to clarify the mechanism of laser-induced acid resistance. Specifically, the aim was to quantify, using the technique of Featherstone *et al.* (1984), any changes in carbonate content occurring upon laser irradiation, and ascertain whether there is formation of particular calcium phosphate phases, at a range of laser powers. The intention was also to evaluate the use of infrared spectroscopy as a technique to analyse enamel as it has not previously been used in Glasgow for this purpose.

6.2 Method and Materials

As discussed in Section 2.8, this quantitative technique involves the production of a calibration curve of concentration against absorption, for selected carbonate and phosphate bands, to which the enamel samples can be compared.

6.2.1 To produce a standard curve

Barium carbonate (BaCO_3 , Sigma Chemical, Poole, Dorset) and calcium phosphate tribasic (CPT, Baker-analysed, Baker No.1436, Sigma Chemical, Dorset) were blended together in the weight ratios 1:20, 1:10, 1:6, 1.5, 1:3, 2:5. Three blends were made of each weight ratio and each was ground in an agate mortar and pestle for 15 min. 1.5 mg of each blend was then ground with 150 mg of potassium bromide (KBr Spectroscopic grade, Sigma Chemical, Dorset), for 5 min, and subsequently pressed into discs using a 16

mm diameter KBr die (Specac, Cambridge, UK) with an applied load of 10 000 kg, under a vacuum of 0.5 torr (Beckman 00-25 press, Glenrothes, Scotland). Four discs were pressed from each blend.

Initially, a disc of pure KBr was placed in the sample chamber of the infrared spectrometer (Mattson 5000 Fourier Transform Infrared Spectrometer, Mattson Instruments inc, USA) and a spectrum was run. This KBr spectrum was then considered to be the background spectrum and was automatically subtracted, by the computer attached to the spectrometer (Genie 4DX33, WinFirst™ Unicam Analytical Systems, Cambridge, UK), from any subsequent sample spectrums. Each standard disc was then placed in turn into the spectrometer chamber and a spectrum was run for each one (32 scans per spectrum, resolution 4.0).

From the IR spectra of each standard disc the extinction ratios (E) of the carbonate band at about 1435 cm^{-1} to the phosphate band at about 575 cm^{-1} (E_{1434}/E_{575}) were calculated using the relationship $E = \log T_2/T_1$, where E is the extinction of the specific carbonate or phosphate peak, band T_2 is the baseline transmittance (calculated automatically by the spectrometer software) and T_1 is the peak transmittance (as described in Section 2.8.2). Ten successive spectra were run and measured for each standard disc in order that the accuracy of the spectrometer could be ascertained.

Regression was carried out on the E ratios obtained from the standards, in order to calculate the gradient (M) of the line for the relationship:

$$(\text{CO}_3/\text{CPT}) 100 = M (E_{1435}/E_{575}).$$

6.2.2 Enamel Samples

Three caries-free lower molars, extracted for orthodontic purposes, were cleaned (as described in Section 2.2.2) and two blocks, of surface area approximately 5 mm x 5mm, were cut from the buccal surface. One block

from each pair was irradiated by a laser moving continuously over the enamel surface. The powers used were either 150 mJ (20 pps), 100 mJ (10 pps) and 50 mJ (10 pps), for 30 sec. Each block (lased and non-lased) was attached by superglue (Loctite 454, UK) to an individual glass slide, such that the enamel surface was uppermost and perpendicular to the slide. The slide was placed under a micrometer and the height of the block measured. Using the metal scraping tool (NOGA deburring tools, Monks & Crane, Glasgow), 1.5 mg of powdered enamel was then manually scraped from the surface of the block. The height of the enamel block was measured again and the depth to which the enamel had been abraded was recorded. The 1.5 mg of powdered enamel was then ground with 150 mg of KBr in an agate mortar and pestle, for 15 min. This powder mixture was subsequently pressed into discs as described in Section 6.2.1 and placed in the infrared spectrometer. The procedure was repeated, this time the enamel coming from further into the tooth (sample 2). An IR spectrum was run for each disc and extinction ratios were calculated as described above (Section 6.2.1) - but this time using the carbonate band at about 1415 cm^{-1} (E_{1415}/E_{575}).

The percentage carbonate content of each enamel sample was then calculated using the equation:

$$\%CO_3 = (M \times 1.77) (E_{1415}/E_{575}).$$

Where 1.77 is the conversion factor between the standards and the enamel samples (as calculated by Featherstone *et al.*, 1984), and M is the gradient of the standard curve.

6.3 Results

6.3.1 Standards

The raw data of the extinction ratios from each of the standard blends (4 discs per blend, 10 measurements per disc) is shown in Appendix 5. The

mean extinction ratios (E_{1435}/E_{575}), and the percentage errors of the means (standard error as a percentage of the mean) of successive recordings from the same disc of each blend (sample error), is shown in table 6.1. The error in the mean extinction values, between blends, is shown in table 6.2.

As seen in table 6.1, the maximum percentage errors of the means of successive readings of the same samples were 1.14 % (blend 1), 1.58 % (blend 2) and 1.36 % (blend 3).

From table 6.2, the maximum errors in the mean of the mean extinction ratios from the four discs per blend were 1.52 % (blend 1), 3.30 % (blend 2) and 4.10 % (blend 3). In total the maximum error between all blends was 9.89 %.

Using all data from the three blends, the gradient (M) of the line for the relationship $(CO_3/CPT) 100 = M (E_{1435}/E_{575})$, was calculated, by regression, as 14.95 (error = 4.72 %).

6.3.2 Enamel Samples

Typical infrared spectra, of lased and non-lased enamel samples, are shown in figure 6.1.

There were large differences in the baseline transmission between the samples, which indicated differences in the transparency of the discs. There was a lot of sample breakage and discs were not always uniform in intensity, which was reflected in the spectra, which were not completely smooth. Spectral subtraction was carried out between the lased and non-lased enamel samples (using the spectrometer software) in order to identify any differences between the two. There did not appear to be any extra bands in the 510 - 400 cm^{-1} region, of the lased enamel spectra, which would correspond to tetracalcium diphosphate monoxide, even when ordinate expansion was used. There were bands at 2340 cm^{-1} which may correspond to a carbon

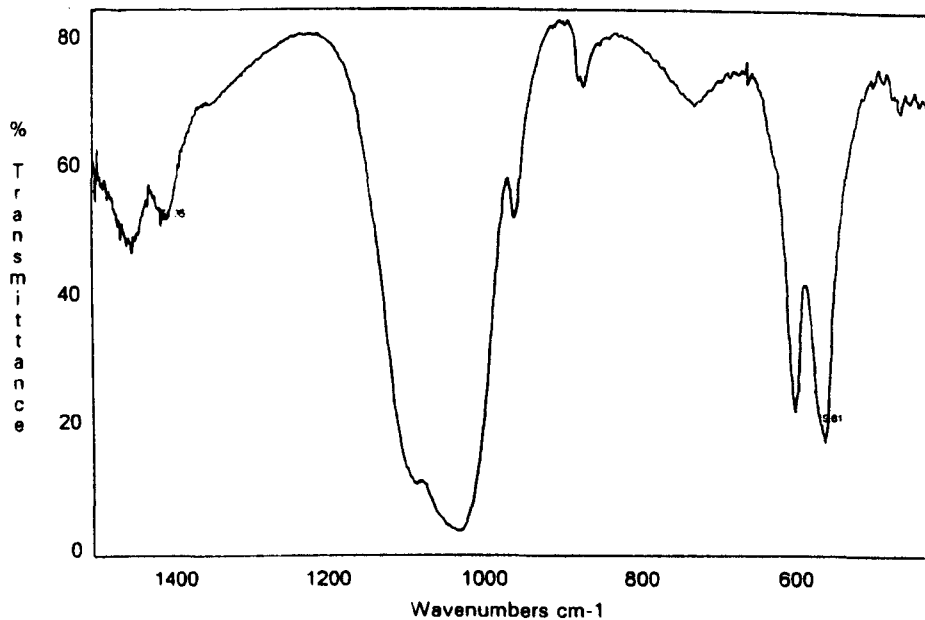
Table 6.1 The mean extinction values (and the percentage error of the mean) of the ten successive readings, from each disc of the three blends.

Standard Weight Ratio	Disc No.	Mean extinction values (% error) per 10 readings		
		Blend 1	Blend 2	Blend 3
1:20	1	0.277 (1.14)	0.202 (0.98)	0.198 (1.28)
	2	0.267 (0.71)	0.207 (0.46)	0.210 (1.36)
	3	0.259 (0.37)	0.191 (1.32)	0.194 (1.30)
	4	0.265 (0.72)	0.178 (1.24)	0.232 (0.88)
1:10	1	0.385 (0.57)	0.345 (0.92)	0.401 (0.32)
	2	0.387 (0.82)	0.345 (0.73)	0.447 (0.92)
	3	0.365 (0.52)	0.375 (1.10)	0.433 (0.44)
	4	0.374 (0.93)	0.331 (0.57)	0.436 (0.58)
1:6	1	0.552 (0.29)	0.600 (0.42)	0.569 (0.33)
	2	0.556 (0.28)	0.587 (0.38)	0.565 (0.28)
	3	0.558 (0.40)	0.557 (0.74)	0.559 (0.40)
	4	0.558 (0.68)	0.583 (0.60)	0.567 (0.28)
1:5	1	0.648 (0.44)	0.696 (0.27)	0.674 (0.24)
	2	0.659 (0.48)	0.714 (0.53)	0.676 (0.28)
	3	0.681 (0.33)	0.715 (0.22)	0.688 (0.32)
	4	0.663 (0.33)	0.720 (0.26)	0.676 (0.23)
1:3	1	1.047 (0.18)	1.090 (0.35)	1.181 (0.13)
	2	1.071 (0.27)	1.100 (0.29)	1.196 (0.13)
	3	1.080 (0.21)	1.102 (0.23)	1.198 (0.32)
	4	1.084 (0.18)	1.097 (0.43)	1.183 (0.13)
2:5	1	1.360 (0.23)	1.359 (0.30)	1.417 (0.22)
	2	1.448 (0.46)	1.328 (0.24)	1.406 (0.43)
	3	1.363 (0.81)	1.440 (1.58)	1.411 (0.18)
	4	1.452 (0.13)	1.395 (0.23)	1.414 (0.13)

Table 6.2 The mean extinction values (and the percentage error of the mean) of the four discs from each blend, and the mean of the values from all three of the blends, at each standard.

Standard Weight Ratio	Mean extinction values (% error) per blend			Mean total values of all 3 blends (% errors)
	Blend 1	Blend 2	Blend 3	
1:20	0.267 (1.40)	0.195 (3.30)	0.209 (4.10)	0.224 (9.89)
1:10	0.378 (1.35)	0.349 (2.66)	0.429 (2.30)	0.385 (6.07)
1:6	0.559 (0.51)	0.582 (1.55)	0.565 (0.38)	0.569 (1.21)
1:5	0.663 (1.04)	0.711 (0.74)	0.679 (0.47)	0.684 (2.06)
1:3	1.071 (0.78)	1.097 (0.24)	1.190 (0.37)	1.119 (3.22)
2:5	1.415 (1.52)	1.381 (1.74)	1.412 (0.17)	1.402 (0.78)

a) lased enamel



b) non-lased enamel

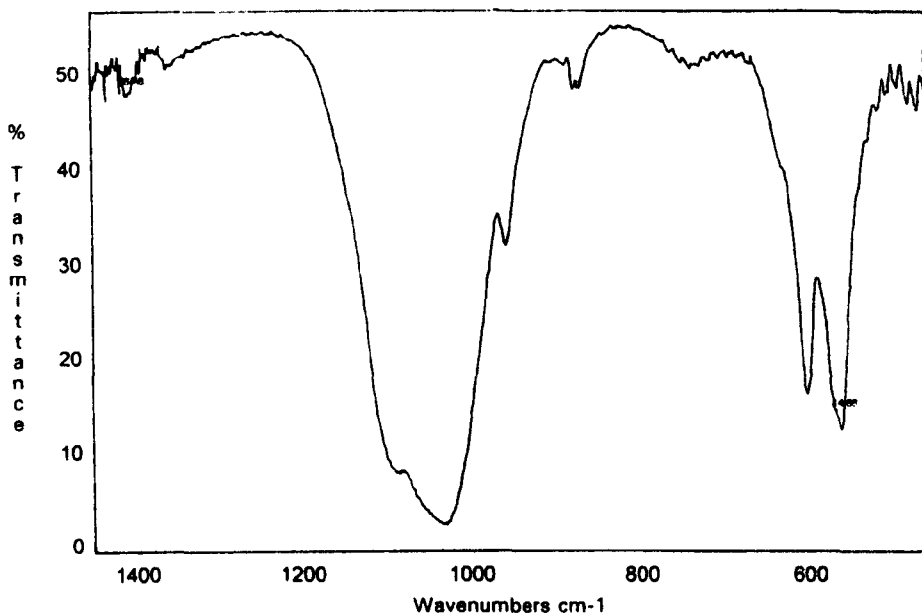


Figure 6.1 Typical infrared spectra of the a) lased and b) non-lased enamel samples. The carbonate content of the enamel was calculated using the extinction ratio of the carbonate bands at 2340 cm^{-1} and the phosphate bands at 575 cm^{-1} .

dioxide peak. These bands were, however, present in both the lased and non-lased samples, and by visual inspection there was no obvious difference in peak size between them.

The carbonate content calculated for each enamel sample, from the equation $\%CO_3 = (M \times 1.77)(E_{1435}/E_{575})$, is shown in table 6.3.

At 50 mJ, the lased enamel in sample 1 had a slightly higher carbonate content than the non-lased sample (1.868 % and 1.370 % respectively). In sample 2, the lased enamel had a much lower carbonate content than the non-lased sample (0.291 % and 2.243 % respectively).

At 100 mJ, sample 1, the carbonate content of the lased enamel is only approximately $\frac{1}{3}$ of the value of the non-lased enamel (1.058 % and 3.130 % respectively). In sample 2, the lased disc broke, but the non-lased sample contained 5.040 % carbonate.

At 150 mJ, sample 1, the lased enamel contained only approximately $\frac{1}{4}$ of the carbonate value of the non-lased sample (0.503 % and 2.021 % respectively). In sample 2, however, the carbonate value of the lased enamel was approximately 6 times greater than that of the non-lased enamel (6.382 % and 1.08 % respectively).

6.4 Discussion

Enamel, being regarded simplistically as a carbonated hydroxyapatite, has been investigated by comparison with synthetic apatites, including hydroxyapatite, whose crystal structure is known (Kay, 1964). Techniques such as X-ray diffraction and infrared spectroscopy have provided detailed information about the positioning of carbonate within the apatite lattice, and its relationship with other crystallite molecules. Carbonate is the most soluble component of enamel (Hallsworth *et al.*, 1973), possibly the first to be

Table 6.3 The carbonate content of the enamel samples, calculated from their IR spectra.

Enamel Sample	Laser Treatment (%CO ₃)		
	150 mJ, 20 pps	100 mJ, 10 pps	50 mJ, 10 pps
1 - Lased	0.503	1.058	1.868
1 - Non-Lased	2.021	3.130	1.370
2 - Lased	6.382	-	0.291
2 - Non-lased	1.080	5.040	2.243

ablated by laser irradiation (Yamamoto & Ooya, 1974; Yamamoto & Sato, 1980) and its loss may contribute to the increased acid resistance of lased enamel. The purpose of this study was to use the technique of infrared spectroscopy, which has been adapted for the analysis of carbonated apatites, to ascertain whether enamel which has been exposed to Nd:YAG laser irradiation contains a lower percentage of carbonate than normal enamel. The aim was also to observe any differences between lased and non-lased enamel, particularly those which may have a bearing on acid resistance such as the formation of tetracalcium diphosphate monoxide.

Nelson & Williamson (1982) found a sample of powdered human enamel to contain 4.1 %wt carbonate (using gas-solid chromatography). In this study, the carbonate content of normal enamel ranged from 1.08 - 5.04 %wt. Although the distribution of phosphate and carbonate in enamel is usually fixed before tooth eruption and generally unaffected by dietary changes, there is much variation in composition both within a single tooth and between different teeth, particularly as a function of depth from the surface (Weatherell, Robinson & Hiller, 1968). Carbonate levels rise markedly from the tooth surface to the ADJ, whereas phosphate levels tend to fall. It was found in this study, that the non-lased enamel showed an increased carbonate content between samples 1 and 2 (ie. as the enamel was obtained from further into the tooth), except in the 150 mJ samples, where the second enamel sample had only approximately half the carbonate content of the first.

Nelson *et al.* (1987) identified, as a recrystallisation product, an apatite with carbonate content lower than the original enamel. They determined the carbonate content of surface enamel exposed to CO₂ laser irradiation (50 J.cm⁻²), to be 0.59 (±0.04) %wt/wt, whereas that of non-lased surface enamel from the same tooth was 1.63 (±0.08) %wt/wt. They did not, however, give any indication of the number of samples they measured. In this study, the carbonate content of the lased enamel, showed no such distinct pattern. At 150 mJ, where it was expected that the most dramatic results would be

obtained, the lased enamel contained less carbonate than the non-lased enamel for sample 1 (surface enamel), however, in sample 2, the lased enamel contained 6.38 % carbonate, which was the highest value observed.

According to Featherstone *et al.* (1984), this infrared spectroscopy method enables reliable estimation of the carbonate content of carbonated apatites to ± 10 % (in the range 1-12 %wt/wt). In this study, the error in the spectrometer (reproducibility between successive readings of each standard disc), was less than 1.6 %. Spectrometer sensitivity is adversely affected by atmospheric fluctuations and the fact that the standards were measured on different days may have caused inconsistencies in instrument performance. Differences between blends may have been due to poor blending, or inaccuracies in measuring. The error in the gradient (M), calculated from all the data, was 4.72 %. The overall error, therefore, in the calculated carbonate concentrations of the enamel samples was only ± 7.6 %. There were large differences in the baseline % transmission between the enamel samples, which indicated differences in the transparency of the discs. This may again be due to a variety of reasons, such as inhomogeneities in grinding, uneven pressing, or the absorption of atmospheric moisture. The discs were very fragile and many shattered when removed from the die, or became cracked, which would have reflected light and affected the light path.

Nelson *et al.* (1987) found the IR spectrum of lased human enamel (CO_2 laser, 50 J.cm^{-2}) contained bands in the $510\text{-}400 \text{ cm}^{-1}$ region (not present in non-lased enamel) which they identified as tetracalcium diphosphate monoxide (TetCP). Kuroda & Fowler (1984), using X-ray diffraction, also identified this compound in enamel lased at 10^4 J.cm^{-2} (CO_2 laser). However, Ferreira *et al.* (1989) were unable to detect, by electron diffraction, either TetCP or a-TCP in lased enamel (CO_2 laser, 120-480 W). As they used very small laser irradiation times (6-520 μs) they suggested that a faster growth rate of apatite relative to the minor a-TCP and TetCP phases may explain the absence of these two compounds; or the relatively low energy densities they used may

not have resulted in a sufficiently high temperature to allow for the formation of measureable amounts of these phases. In this study, there was no evidence of any bands unique to the lased enamel which would correspond to TetCP at $400\text{-}500\text{ cm}^{-1}$. TetCP may only be present in very small amounts, they were only seen by Nelson *et al.* (1987) when ordinate expansion was used. Alternatively, it may be that the absorption characteristics of the Nd:YAG laser mean that formation of TetCP using this type of irradiation was unlikely.

The basis of the quantitative technique of Featherstone *et al.* (1984) is that the extinction ratios of the standards have a linear relationship with the known carbonate concentrations of a series of synthetic carbonated apatites (analysed by gas chromatography). This appears to make the assumption that enamel is a carbonated apatite with a uniform carbonate: phosphate ratio. However, as the carbonate and phosphate content of enamel are known to vary as a function of depth (Weatherell *et al.*, 1968), it cannot be stated unequivocally that measured changes in carbonate are due to a decrease in carbonate in the enamel, and not due to increases in the phosphate content.

Carbonate ions in apatites occur in two crystallographically distinct sites designated A sites (CO_3^{2-} ions replace hydroxyl ions) and B sites (CO_3^{2-} replace PO_4^{3-} ions) (Nelson & Williamson, 1982; Nelson & Featherstone, 1982). Carbonate in enamel is located primarily in B sites; Elliott *et al.* (1985) found only 11 (± 1) % of enamel carbonate ions to be in A sites. There may be other distinct, but thermodynamically unstable, carbonate sites, particularly associated with the hydroxyl ion (Elliott *et al.*, 1985). Different site occupancy has different effects on crystallite unit cell dimensions and hence absorption characteristics due to electrostatic fields from the nearest atomic neighbours. Carbonate ions have four vibrational modes ($\nu 1\text{-}\nu 4$) resulting from: 1) the ionic site occupied (A or B), 2) interactions with vacancies or other ions due to charge compensation mechanisms, 3) different possible orientation of the ion in its site, 4) cluster formation or heterogeneities of distribution in the

solid (Feki *et al.*, 1991). These vibrational modes have been assigned bands by Nelson & Williamson (1982) in a detailed study of infrared spectra. Similarly phosphate ions have six vibrational modes.

The technique used in this study measures differences in the relative intensities of the ν_3 (CO_3) vibrational band (B site carbonate) and the ν_4 (PO_4) band. There is evidence, however, that on the heating of apatites or enamel to 880 °C, type A carbonate bands increase in relative intensity but type B bands decrease, indicating that new A sites become available for ion occupancy (Emerson & Fischer, 1962; El Feki, Rey & Vignoles, 1991; Holcomb & Young, 1980). Holcomb & Young (1980), followed the change and loss of CO_3^{2-} in enamel which was heated in the range 25-1000 °C. They found that, on heating, B site CO_3^{2-} was lost continuously from the outset (beginning at 100 °C), whereas A site CO_3^{2-} first decreased, then increased above 200 °C to a maximum at ~800 °C whereupon it decreased again. They suggested that most of the carbonate ions in B sites transfer partially to A sites through the intermediate CO_2 : a CO_2 band at 2340 cm^{-1} was observed. This may again influence the measurement of carbonate, as changes in B - site carbonate, as measured by Featherstone's technique, may not be a true reflection on the carbonate content of the enamel, some of which been converted to A - site carbonate. The technique does not measure changes in the 11 % of carbonate in the A sites. In the present study, a peak at 2340 cm^{-1} (corresponding to CO_2) was observed in both the lased and non-lased samples, with no significant difference in peak size between the two. Similarly, if there is the formation of TetCP, this implies that some phosphate will have recrystallised into a different lattice position from its origin and hence its band position will have altered. This may again have some influence on the carbonate / phosphate ratio.

Featherstone's standardisation involved synthetic carbonates of 0.2, 3.57, 4.06, and 4.35 %wt/wt and high temperature apatites with carbonate of 0.0, 3.10, and 11.8 %wt/wt, measured using gas-chromatography. Vignoles *et al.*

(1988) found that synthetic carbonates of a low carbonate content contained carbonate mainly in the A sites but as the carbonate content is increased the carbonate exists more in B sites and less remains in the A sites: carbonation in B sites induces a decrease in site A carbonate due to charge compensation. There may therefore, have been slight inaccuracies in the original calibration.

Although it was the intention that the enamel blocks would be measured using a micrometer to determine the depth from which the sample was taken, it proved too difficult to obtain enamel powder in a uniform depth from the surface, using the scraper. The use of the scraper superseded a serial abrasion method (McWilliam, 1995), which proved to be incompatible with IR spectroscopy as it led to sample contamination, and did not allow full sample recovery. The technique could perhaps be used in conjunction with a profilometer to enable exact determination of where the enamel powder was removed from.

Obviously, with the small sample size involved in this study it is difficult to draw any conclusions about the results obtained. There was no convincing pattern to the carbonate content of lased enamel compared with non-lased enamel, and no evidence to suggest the formation of new compounds in lased enamel. As a technique to analyse enamel, infrared spectroscopy has both advantages and disadvantages. Sample preparation is time-consuming, takes a lot of practice and the resulting discs are fragile and absorb moisture easily. Atmospheric conditions may have a large influence on the results. The spectrometer, however, is fully computerised making analysis relatively simple once the sample has been prepared, and the software allows full manipulation of the spectra of interest. In this study the main limitation was access to the spectrometer and time, but ideally the work would be repeated using a larger amount of samples. Most importantly, it must be noted that although this technique may be suitable for analysing normal enamel, the changes induced in enamel upon laser irradiation may mean that it no longer conforms to a carbonate/phosphate structure which is compatible with this

quantitative method.

CHAPTER 7 - Conclusions and Discussion

The overall aim of this thesis was to investigate the interaction of pulsed Nd:YAG laser irradiation with both sound and artificially carious human enamel. More specifically, the aims, as detailed in Chapter 1, were as follows:

1. to characterise the effect of Nd:YAG laser irradiation on artificially created white spot enamel lesions (to simulate the effect of lasing carious enamel).
2. to quantify the effects of pulsed Nd:YAG laser irradiation on enamel demineralisation.
3. to investigate whether there is synergy between the action of pulsed Nd:YAG laser irradiation and fluoride in terms of imparting acid resistance to enamel.
4. to clarify the mechanism by which pulsed Nd:YAG laser irradiation physically interacts with enamel to induce acid resistance.

The first aim was addressed in Chapter 3. Laser irradiation of artificial white spot lesions was found to ablate tissue, even at the lowest powers used (30 mJ). At 50 mJ and 100 mJ, laser irradiation caused crater formation, the depth of which bore no relation to the initial degree of lesion demineralisation (within the range of lesions used). This is significant as natural carious lesions may have different optical properties from artificial lesions and exhibit a larger variation in opacity and structure. Ablation was correlated only with the power used, being greater at 100 mJ than at 50 mJ. SEM examination of the surface morphology of lased enamel, and the surrounding unlased area, was consistent with a process of melting and

recrystallisation as previously described (Quintana *et al.*, 1992; Pogrel *et al.*, 1993)

Previous research has used only visual and explorer examination (Myers & Myers, 1988; Myers & Myers, 1985) to determine whether all carious enamel was removed upon irradiation of lesions. In this thesis, a transverse section through a lased artificial lesion was examined by microdensitometry to determine the depth and extent of ablation for each laser parameter. It is evident, from this investigation, that in order to remove carious enamel selectively, while leaving sound enamel intact, successive applications of low power irradiation (50 mJ) are the most suitable.

The second aim of this thesis has been fulfilled. It has become clear that Nd:YAG laser irradiation imparts a significant degree of acid resistance to the tooth surface. In Chapter 4, laser irradiation of a single spot on a tooth surface, at 100 mJ or 150 mJ (1554.3 J.cm^{-2} and 4662.7 J.cm^{-2} , respectively), led to a 60 % lower mineral loss than non-lased enamel, upon exposure to a demineralising regime. Irradiation at these parameters caused the formation of craters in the enamel surface. The results of the *in vitro* study in Chapter 5, are also of considerable interest. In this case, laser irradiation at 150 mJ, applied in a clinically appropriate manner for 30 sec, over a measured area of a tooth (450 J.cm^{-2}), caused a 30 % inhibition of mineral loss - a level which is still clinically significant. Again, however, the surface of the enamel lased at this power was significantly altered, exhibiting increased surface roughness and opacity, compared with that of normal enamel. Enamel lased at 100 mJ (300 J.cm^{-2}), was not significantly different from non-lased enamel in terms of acid resistance.

Microradiography of single sections was a very good quantitative technique to analyse lased and non-lased enamel, while minimising considerations of intra-tooth variability. This *in vitro* model would be ideal for the further investigation of other laser parameters pertaining to acid resistance, and of

combined preventive protocols such as the use of laser initiators - which may enable a similar degree of acid resistance to be produced using a lower power of irradiation. In addition, this model may be used to investigate other demineralising or remineralising regimes, for example to see if lased, demineralised enamel is more susceptible to remineralisation than non-lased enamel, or if lased carious enamel (as in Chapter 3) is more acid resistant or likely to remineralise, than non-lased enamel.

With regard to the third aim, in Chapter 4 there was no evidence that fluoride acts in synergy with laser irradiation. This is in contrast to previous research and the possible explanations for this discrepancy are discussed below. The lesion formation technique used in this study involved a change of demineralising solution each day, so any residual fluoride, which had leached out of the enamel, was removed each day. Samples were exposed to a demineralising regime for four days, whereas other researchers have simply used a concentrated acid challenge for a very short period of time, 30 sec - 15 min (Fox *et al.*, 1992; Bahar & Tagomori, 1994; Tagomori & Morioka, 1989; Yamamoto & Sato, 1980), or a longer timescale but without changing the demineralising medium regularly (Flaitz *et al.*, 1995). In this case, any fluoride, initially taken up into the lased area, on subsequently leaching out of the enamel, would still be present in the demineralising solution, thus directly affecting lesion formation. Flaitz *et al.* (1995), using polarizing microscopy, compared the lesion depth in lased and non-lased areas, which, as it can be seen in this study, does not reliably indicate the extent of demineralisation. The basis of the investigation in this thesis was its clinical relevance. Lesions were formed in a manner which is more suitable as an oral model than the extreme acid etching methods described above. Duraphat varnish is quick and easy to apply, particularly when compared to studies which used a 24 hr application of APF solution - which is not clinically practical.

Finally, as to the fourth aim, the infrared spectroscopy carried out in Chapter

6 did not clarify the mechanism by which enamel exposed to laser irradiation gains a degree of acid resistance. Infrared spectroscopy was chosen as it has previously been used to quantify the carbonate content of both normal (Featherstone *et al.*, 1984) and lased enamel (Nelson *et al.*, 1987), it was available and relatively simple to use. Although it is appreciated that laser irradiation may decrease the carbonate content of enamel, it was difficult to draw any conclusions regarding carbonate content from this study. Firstly this was because the number of samples was so low. Secondly, it seems that this technique, the basis of which is quantification of the carbonate/ phosphate ratio in enamel, does not take into account any differences in the ratio of these ions due to the melting and recrystallisation of lased enamel. Infrared spectroscopy may therefore only be suitable for analysing the carbonate content of normal enamel, as the changes induced in enamel upon laser irradiation suggest that it no longer conforms to a carbonate/ phosphate structure compatible with this quantitative method.

The work presented in this thesis has indicated the versatility of the Nd:YAG laser as a dental instrument. The laser can be used to ablate carious enamel and has potential as a prophylactic treatment for caries. Clinical application of the laser (for both acid resistance or ablation of carious tissue) may be useful in areas of the mouth where decay is most prevalent, such as in between teeth, or on the occlusal surfaces where crater formation is less of a consideration. Another potential use may be in the preparation of teeth for orthodontic brackets, where the laser can be used for surface roughening, similar to acid etching, but should additionally guard against secondary caries. As yet, there is no adequate quantitative data to indicate the effect of Nd:YAG laser irradiation, at the parameters used in this study, on the dental pulp. This is clearly an area of research which should follow on from this study, in order to define laser parameters which combine safety with a clinically significant level of acid resistance. The most significant aspect of the laser as a strategy to prevent caries, is that it seems to physically alter the structure of enamel so may, therefore, be a method of permanently increasing

tooth resistance to decay.

Appendix I

Derivation of the equation by Angmar *et al.* (1963)

The following equation is used to determine the mineral content of dental hard tissues from a microradiographic image of the hard tissue sample and an aluminium step wedge of known thickness and absorption coefficient:

$$V = \frac{100[(\mu.q)_A \cdot t_A - (\mu.q)_O \cdot t_s]}{[(\mu.q)_M - (\mu.q)_O] \cdot t_s}$$

$(\mu.q)_A$ - the linear absorption coefficient for aluminium (131.5),

$(\mu.q)_O$ - the linear absorption coefficient for organic matter and water (11.3)

t_A - the thickness of the aluminium having the same photographic density as the section at any measure point. This is interpolated from the density curve of the step-wedge.

t_s - the thickness of the section; this is determined individually using a micrometer.

Substituting these values the equation becomes:-

$$V = \frac{52.77 \cdot t_A - 4.54}{t_s}$$

For calculation of the amount of mineral salts from the densitometric data the following assumptions are made:-

- 1 The mineral salts have a density of 3.15.
- 2 The average mineral composition is 37.1 % Ca, 0.5 % Mg, 18.1 % P, 43.3 % O, 0.7 % C and 0.3 % H.
- 3 The Ca:P ratio is 2.05.
- 4 The volume not occupied by mineral salts is filled with organic matter and water.

Appendix II

The microradiographic measurements of crater depth and width, lesion ΔZ , lesion body, lesion depth and surface zone, at each laser condition.

a) 50mJ / 2 seconds

Lesion measurements				Crater measurements	
ΔZ (%Vol.min. μm)	SZ (%Vol.min.)	LB (%Vol.min.)	depth (μm)	depth (μm)	width (μm)
6982	58.91	57.57	54	36	285
1504	67.39	66.29	51	12	357
3516	66.05	62.78	51	51	474
3213	36.16	28.76	51	24	432
3446	60.99	54.47	54	9	-
3205	48.28	44.82	60	45	192
2012	59.19	58.45	42	42	141
3693	51.79	50.16	75	12	438

b) 50 mJ/5 seconds

Lesion measurements				Crater measurements	
ΔZ (%Vol.min. μm)	SZ (%Vol.min.)	LB (%Vol.min.)	depth (μm)	depth (μm)	width (μm)
2301	66.26	33.36	51	51	498
1913	63.03	56.71	54	12	363
3454	67.93	44.53	87	15	264
3791	68.80	67.74	66	27	732

c) 100 mJ/2 seconds

Lesion measurements				Crater measurements	
ΔZ (%Vol.min. μm)	SZ (%Vol.min.)	LB (%Vol.min.)	depth (μm)	depth (μm)	width (μm)
1874	63.69	52.74	57	57	504
1994	65.55	66.26	48	48	681
3339	49.90	30.11	54	72	417
1855	65.72	50.88	39	54	480
2625	64.11	49.88	57	48	303
2566	56.60	50.70	42	111	528
3927	54.43	47.54	63	93	543
1257	70.59	70.49	69	24	254

d) 100 mJ/5 seconds

Lesion measurements				Crater measurements	
ΔZ (%Vol.min. μm)	SZ (%Vol.min.)	LB (%Vol.min.)	depth (μm)	depth (μm)	width (μm)
2126	66.20	70.19	54	48	294
2434	49.59	47.27	54	75	387
1430	77.15	77.38	-	63	687
4245	52.58	52.00	54	57	360
5824	33.92	35.96	57	63	972
2915	54.16	54.08	60	78	>342
1782	71.53	58.35	48	72	657
1720	67.22	65.59	45	72	408

Appendix III

Table 1. Microradiographic measurements of lesions on each area of enamel in the 100 mJ, non-fluoride treated samples.

a) Lased Enamel

ΔZ (%Vol.min. μm)			LB (%Vol.min.)		
Sound Enamel	After Demin	Change	Sound Enamel	After demin	Change
1109.17	3377.77	2268.59	80.00	47.19	32.81
383.66	1387.87	1004.20	80.00	52.59	27.41
929.99	1634.91	735.86	80.34	60.07	24.36
535.29	1088.47	553.19	78.69	55.57	23.12
487.97	918.61	430.64	85.20	73.27	11.93
541.22	1286.18	744.96	78.40	70.81	7.59
911.63	1124.56	212.94	77.98	63.34	14.64
461.78	1329.38	867.59	79.55	51.11	28.45

b) Non-Lased Enamel (Area 2)

ΔZ (%Vol.min. μm)			LB (%Vol.min.)		
Sound Enamel	After Demin	Change	Sound Enamel	After Demin	Change
860.43	4557.72	3697.30	80.42	33.28	47.15
779.28	3372.69	2593.42	79.31	29.66	49.65
481.99	1924.66	1442.67	81.00	48.90	32.11
361.90	1572.03	1210.14	80.00	44.86	35.14
444.58	2610.34	2165.75	80.00	41.92	38.08
523.61	1456.24	932.63	79.81	55.49	24.32
671.84	2710.98	2039.15	78.03	36.83	41.19
814.28	2010.92	1196.65	77.89	47.40	30.49

c) Non-Lased Enamel (Area 3)

ΔZ (%Vol.min. μm)			LB (%Vol.min.)		
Sound Enamel	After Demin	Change	Sound Enamel	After Demin	Change
1133.70	4346.33	3212.63	80.00	42.09	37.91
752.36	3132.13	2379.77	79.64	31.26	48.38
356.09	1596.10	1238.02	80.00	50.09	29.91
529.59	2391.11	1861.58	79.01	33.92	45.10
263.02	3335.72	3072.70	81.60	38.62	42.98
593.48	1901.97	1308.49	78.37	45.69	32.69
880.87	3042.43	2161.55	77.19	35.72	41.46
340.40	1865.68	1525.28	74.75	41.09	33.67

Table 2. Microradiographic measurements of lesions on each area of enamel in the 100 mJ, fluoride treated samples.

a) Lased Enamel

ΔZ (%Vol.min. μm)			LB (%Vol.min.)		
Sound Enamel	After Demin	Change	Sound Enamel	After demin	Change
373.72	1101.14	727.43	78.82	61.48	17.34
368.22	872.07	503.85	77.17	68.39	8.78
1091.78	1636.01	544.23	75.15	47.51	27.64
948.15	764.29	183.86	76.94	78.70	1.76
550.92	1105.26	554.34	80.70	64.67	16.03
492.64	1117.59	624.95	78.22	50.59	27.63
467.61	1299.79	832.19	77.78	44.80	32.97
532.47	1311.31	778.84	76.95	58.04	18.91

b) Non-Lased Enamel (Area 2)

ΔZ (%Vol.min. μm)			LB (%Vol.min.)		
Sound Enamel	After Demin	Change	Sound Enamel	After Demin	Change
499.39	2297.45	1798.07	80.00	45.53	34.47
808.41	2277.06	1468.65	80.41	43.07	37.34
952.17	2667.01	1714.84	80.00	29.98	50.02
467.36	1118.91	651.55	73.33	53.02	20.31
512.39	1764.77	1252.39	77.23	53.56	23.68
299.87	2049.14	1749.27	78.22	47.37	30.85
658.65	3907.15	3248.50	81.68	9.65	72.03
660.04	2048.29	1388.26	76.63	41.57	35.06

c) Non-Lased Enamel (Area 3)

ΔZ (%Vol.min. μm)			LB (%Vol.min.)		
Sound Enamel	After Demin	Change	Sound Enamel	After Demin	Change
307.68	2332.21	2024.53	80.80	37.37	43.44
684.81	1505.16	820.35	75.78	46.50	29.28
752.63	3389.54	2636.91	80.76	19.57	61.18
734.75	985.93	251.19	75.28	66.39	8.88
734.43	1538.89	804.46	78.62	56.02	22.60
511.09	1685.18	1174.09	76.17	29.30	29.30
512.42	4280.99	735.44	72.79	12.97	59.82
393.41	1478.08	1084.67	80.24	65.36	14.89

Table 3

Microradiographic measurements of lesions on each area of enamel in the 150 mJ, non-fluoride treated samples.

a) Lased Enamel

ΔZ (%Vol.min. μm)			LB (%Vol.min.)		
Sound Enamel	After Demin	Change	Sound Enamel	After demin	Change
438.52	2218.11	1779.60	78.24	36.37	41.87
623.01	2844.93	2221.92	80.00	29.77	50.23
620.90	2364.12	1743.21	78.62	31.99	46.63
642.05	1171.39	529.34	80.00	20.98	59.02
643.38	1189.22	545.84	80.16	40.42	39.74
462.10	2513.53	2051.43	80.00	35.44	44.56
865.22	1526.33	661.11	79.02	54.37	24.66
853.99	926.28	72.29	78.09	69.27	8.81
744.90	2341.16	1596.26	83.06	38.84	44.21
420.61	1172.75	752.14	79.73	20.86	9.99
798.85	1771.70	972.85	79.73	63.21	16.52
773.12	891.39	118.27	77.53	75.01	2.53
167.71	2338.80	2171.09	82.36	34.44	47.92
356.70	1345.77	989.07	72.76	34.78	37.98
813.65	894.81	81.16	80.94	30.30	50.64
405.10	825.22	420.12	76.01	39.92	36.10
667.83	2245.14	1577.31	80.00	36.52	42.06
690.09	1456.95	1766.86	76.74	27.94	48.77
531.03	2253.35	876.30	81.02	48.71	32.31
188.46	777.05	588.59	80.00	65.49	14.51
766.78	780.92	14.14	88.02	73.03	14.99
328.66	2299.86	1971.20	78.79	35.26	43.52
381.31	347.84	33.49	80.29	79.29	1.03
394.64	1709.16	1314.52	79.73	39.93	39.80

b) Non-Lased Enamel (Area 2)

ΔZ (%Vol.min. μm)			LB (%Vol.min.)		
Sound Enamel	After Demin	Change	Sound Enamel	After Demin	Change
160.26	2839.80	2679.53	80.00	31.87	48.13
308.56	3196.13	2887.57	79.61	30.84	48.77
789.84	3196.94	2407.10	76.93	27.67	49.27
382.91	3541.12	3158.20	80.74	29354	51.20
337.60	1852.97	1515.38	80.98	46.02	34.96
225.03	3432.08	3207.05	81.39	29.80	51.59
829.53	2881.34	2051.82	79.02	32.38	46.64
942.66	2724.86	1782.20	77.76	30.37	47.39
646.14	3097.66	2451.52	81.78	27.69	54.09
369.50	3143.34	2773.85	80.95	41.31	39.64
853.72	3629.36	2775.64	32.83	22.69	10.14
704.43	1691.26	986.83	79.68	49.86	29.82
136.76	3555.74	3418.99	81.33	23.43	57.90
297.17	3679.36	3382.19	79.19	24.66	54.53
599.14	3453.66	2854.52	80.00	28.05	51.95
186.80	2240.03	2053.23	79.69	28.78	50.91
467.96	2517.31	2049.35	78.69	41.11	37.58
1000.08	3357.02	2356.94	76.68	32.59	44.10
144.18	1974.87	1830.69	80.00	41.85	38.15
144.88	1716.89	1572.01	80.00	41.85	38.15
430.92	2111.11	1680.19	80.00	47.12	32.88
254.66	3376.53	3121.87	81.42	27.42	54.00
353.67	1480.83	1145.16	80.00	47.59	32.41
630.60	3377.90	2747.30	80.00	29.39	50.61

c) Non-Lased Enamel (Area 3)

ΔZ (%Vol.min. μm)			LB (%Vol.min.)		
Sound Enamel	After Demin	Change	Sound Enamel	After Demin	Change
502.12	3014.77	2512.65	78.96	32.73	46.24
214.30	2919.90	2705.59	80.00	30.58	39.42
287.38	3217.59	2930.21	80.70	29.41	51.29
431.23	3215.37	2784.14	80.00	31.66	48.34
386.11	2817.80	2431.68	81.97	34.49	47.48
233.51	3444.14	3210.63	81.83	29.43	52.40
974.44	3297.26	2322.82	80.00	30.78	49.22
841.71	3679.52	2837.81	76.20	20.72	55.48
486.25	3224.80	2738.54	81.00	30.55	50.45
239.58	3269.22	3029.65	81.91	25.66	56.26
516.57	2282.63	1766.05	81.45	20.78	60.67
480.82	1901.36	1420.54	80.00	46.50	33.50
276.28	3357.28	3081.00	80.68	25.90	54.79
414.64	3443.85	3029.21	80.00	29.75	50.25
769.89	3558.13	2788.24	80.98	26.36	54.62
250.36	2418.17	2167.81	80.00	42.43	37.57
216.37	2903.31	2686.94	80.00	41.37	38.63
287.64	2439.22	2151.57	78.81	30.44	48.38
189.18	1819.65	1702.47	80.00	46.05	33.95
169.55	1675.82	1506.27	80.00	44.70	35.30
613.34	2131.93	1518.60	80.00	45.29	34.71
287.67	4033.36	3754.69	80.48	26.98	53.50
402.56	2046.96	1664.40	81.21	46.04	35.18
317.09	3554.17	3237.08	81.00	27.92	53.08

Table 4.

Microradiographic measurements of lesions on each area of enamel in the 150 mJ, fluoride treated samples.

a) Lased Enamel

ΔZ (%Vol.min. μm)			LB (%Vol.min.)		
Sound Enamel	After Demin	Change	Sound Enamel	After demin	Change
823.14	1585.70	762.56	80.24	69.04	11.2
289.46	1690.85	1401.39	74.12	34.41	39.71
854.44	1246.21	391.77	81.05	70.95	10.10
440.17	817.42	377.25	69.81	59.62	10.19
238.30	1560.93	1322.63	77.70	43.02	34.68
815.56	1692.11	876.55	79.00	44.35	34.66
961.79	1478.37	516.58	78.96	60.07	18.89
656.21	1846.19	1189.98	80.33	60.50	19.83
560.33	824.75	264.42	61.02	41.84	19.18
242.59	957.57	714.98	80.00	67.50	12.50
245.69	1441.77	1196.08	74.92	49.09	25.83
241.47	1709.92	1468.44	78.60	34.14	44.46

b) Non-Lased Enamel (Area 2)

ΔZ (%Vol.min.μm)			LB (%Vol.min.)		
Sound Enamel	After Demin	Change	Sound Enamel	After Demin	Change
350.33	2862.58	2512.24	80.00	36.73	43.27
85.25	5580.53	5495.28	80.66	43.22	37.44
218.26	947.89	729.63	81.71	40.41	41.30
222.10	1926.47	1704.37	79.56	32.22	47.34
255.95	2565.55	2309.59	80.00	34.23	45.77
388.11	2178.72	1790.61	77.67	42.83	34.83
874.49	2419.81	1545.32	70.90	44.49	26.40
414.82	2460.44	2045.62	81.00	45.43	35.57
304.51	2041.10	1736.59	78.56	38.73	39.83
199.35	1941.20	1741.85	80.00	51.84	28.16
205.82	2123.19	1917.37	87.66	52.10	35.56
223.18	2642.45	2419.27	79.29	37.03	42.26

c) Non-Lased Enamel (Area 3)

ΔZ (%Vol.min.μm)			LB (%Vol.min.)		
Sound Enamel	After Demin	Change	Sound Enamel	After Demin	Change
140.97	4673.29	4532.32	80.00	23.65	56.35
226.86	4146.57	3919.71	79.67	27.86	51.82
343.79	3089.89	2746.10	80.00	48.65	31.35
135.40	2024.52	1889.12	81.00	49.95	31.05
120.01	1956.55	1836.54	80.00	43.40	36.60
342.77	1632.84	1290.07	78.35	50.16	28.20
558.87	2278.88	1720.01	79.66	44.49	35.17
628.44	2873.94	2245.51	79.67	35.85	43.82
392.00	1347.78	955.784	74.24	52.84	21.40
398.60	1621.83	1223.22	80.00	54.95	25.02
261.81	3258.83	2997.02	82.33	30.62	51.71
351.75	2494.16	2142.41	78.60	36.39	42.21

Appendix IV

Table 1. Microradiographic measurements of lesions in the 100 mJ samples for a) the lased areas and b) the non-lased areas.

a) Lased Enamel (100 mJ)

ΔZ (%Vol.min. μm)			LB (%Vol.min.)		
Sound Enamel	After Demin	Change	Sound Enamel	After demin	Change
663.71	3739.46	3075.75	79.71	33.94	45.77
597.74	2322.59	1724.84	77.24	41.97	35.27
874.69	3255.81	2381.12	79.69	34.23	45.46
340.48	2705.16	2364.68	78.58	37.67	40.93
389.43	4301.50	3912.07	78.19	32.38	45.82
612.54	6746.79	6134.25	77.52	26.27	51.25
418.29	4751.90	4333.61	80.25	29.87	50.38
484.18	6808.10	6323.92	80.29	25.67	54.62
955.55	5431.61	4476.06	80.56	26.63	53.93
1566.57	4582.29	3015.73	69.50	31.03	38.47
853.70	3507.66	2653.96	76.50	33.30	43.19
588.71	2965.40	2376.69	75.52	40.05	35.47
419.40	3153.82	2734.42	81.64	31.54	50.10
289.06	2182.32	1893.26	80.36	42.67	37.69
700.62	3660.54	2959.92	75.17	26.79	48.39
473.49	2623.51	2150.02	76.79	31.46	45.32
588.19	1014.49	426.30	77.90	55.73	22.17
183.27	2069.58	1823.24	80.00	50.54	33.44
136.32	1959.55	2084.76	80.00	46.56	42.47
688.88	2773.64	884.41	78.78	36.31	28.41
614.80	1499.20	1166.49	80.69	52.28	25.78
612.19	1778.68	1947.23	77.43	51.65	42.88
362.53	2309.76	1090.56	80.27	37.39	25.61
857.16	1947.72	2465.68	75.95	50.33	45.06
207.72	2673.4	1886.31	80.00	34.94	29.46

b) Non-Lased Enamel (100 mJ)

ΔZ (%Vol.min. μm)			LB (%Vol.min.)		
Sound Enamel	After Demin	Change	Sound Enamel	After Demin	Change
1238.56	4776.78	3538.22	78.35	35.83	42.52
703.30	2493.52	1790.22	77.99	39.53	38.46
432.14	2360.94	1928.80	79.15	34.69	44.46
531.81	3885.47	3353.66	78.96	25.54	53.42
586.14	4675.88	4089.74	78.20	29.68	48.52
905.44	4477.19	3571.74	79.08	32.61	46.47
861.04	4896.82	4035.79	80.00	30.25	49.75
444.53	4363.85	3919.32	76.07	43.29	32.77
1320.23	3984.83	2664.59	79.48	36.22	43.26
497.00	2032.46	1535.46	79.71	42.66	37.05
922.38	2808.54	1886.16	77.28	38.08	39.20
901.32	2510.26	1608.94	72.42	42.24	30.19
494.45	1888.75	1394.30	82.46	49.47	32.99
463.30	1291.62	828.32	76.22	49.37	26.85
1239.84	3043.34	1803.50	74.26	31.99	42.27
562.12	2584.36	2022.24	76.66	28.77	47.89
317.85	1658.08	1340.23	76.71	46.33	30.38
524.12	1728.56	856.31	77.19	49.20	19.11
634.98	1491.29	1223.73	80	60.89	31.78
165.51	1389.24	808.86	79.23	47.45	27.03
1239.54	1248.40	2060.68	78.4	51.37	37.36
496.11	2556.79	1714.19	77.67	40.31	39.30
430.62	2144.80	1239.48	77.32	38.02	23.53
566.50	1805.98	3635.66	78.30	54.77	45.63
769.45	4405.1	1204.44	80	34.37	27.99

Table 2, Microradiographic measurements of lesions in the 150 mJ samples for a) the lased areas and b) the non-lased areas.

a) Lased Enamel

ΔZ (%Vol.min. μm)			LB (%Vol.min.)		
Sound Enamel	After Demin	Change	Sound Enamel	After demin	Change
333.68	1639.04	1305.35	80	50.86	29.14
1211.63	1331.14	119.51	68.06	64.32	3.74
718.34	2559.72	1841.38	77.27	34.47	42.80
482.71	1769.06	1286.35	76.16	43.60	32.56
532.37	2714.35	2181.98	80.39	32.57	47.82
953.52	2557.45	1603.93	74.58	41.09	33.49
851.06	1057.79	206.72	74.67	62.04	12.63
618.57	1370.62	752.04	73.86	56.47	17.39
413.63	1363.07	949.44	80.00	47.30	32.70
890.46	2022.26	1131.80	77.63	61.88	15.75
931.58	899.44	32.14	75.05	66.52	8.53
502.07	1290.00	787.93	77.87	52.34	23.53
518.56	979.87	461.31	76.02	58.58	17.44
243.88	850.48	606.60	80.00	59.96	20.04
364.49	3450.36	3085.88	77.64	33.76	43.88
591.18	2298.34	1707.17	78.00	26.86	51.13
755.96	2033.00	1277.04	75.57	40.56	35.01
279.79	1645.96	1366.17	79.82	40.68	39.14
318.40	3154.77	2836.37	80.00	19.82	60.12
505.28	1505.32	1000.04	78.53	47.19	31.34
440.39	1760.28	1319.89	78.64	38.18	40.45
335.12	1809.05	1473.92	79.19	37.14	42.05
719.84	4001.17	3281.33	79.50	23.87	65.63
420.04	2287.33	1867.29	79.47	43.09	36.38
327.35	3000.48	2673.13	78.72	23.70	55.02

b) Non-Lased Enamel (150 mJ)

ΔZ (%Vol.min. μm)			LB (%Vol.min.)		
Sound Enamel	After Demin	Change	Sound Enamel	After Demin	Change
1009.88	3222.27	2212.39	78.78	40.97	37.82
372.58	2633.93	2261.35	78.11	48.09	30.03
676.59	2565.47	1888.88	75.00	50.20	24.81
585.94	2186.69	1600.75	75.93	41.67	34.26
960.90	2954.63	1993.73	79.52	35.57	43.95
852.72	5530.68	4677.96	77.26	22.24	55.02
435.81	2086.98	1651.17	75.91	40.45	35.46
723.50	4498.60	3775.11	77.17	43.29	33.88
375.21	781.52	406.31	80.00	67.99	12.01
389.95	973.55	583.60	77.08	66.27	10.80
827.02	2052.43	1225.41	75.36	38.02	37.34
286.00	1772.12	1486.12	79.64	45.49	34.16
708.97	1309.43	600.46	79.49	58.46	21.04
617.05	1844.23	1227.18	80.00	42.13	37.87
443.52	2558.42	2114.90	78.70	35.56	43.14
321.89	3948.22	3626.33	80.00	22.63	57.37
244.05	4022.81	3778.77	78.96	24.08	54.88
373.43	2764.71	2391.28	80.00	35.96	44.04
315.82	3753.48	3437.66	79.54	23.59	55.95
736.01	2089.18	1353.17	77.70	42.88	34.82
236.31	2711.64	2475.33	78.69	32.98	45.71
546.27	2131.26	1584.99	78.55	37.77	40.78
197.52	3407.98	3210.46	80.00	25.79	54.21
198.24	3431.56	3233.32	80.00	25.69	54.31
395.60	2649.48	2253.88	78.97	24.48	54.49

Appendix V

Extinction ratios of the carbonate:phosphate bands (E_{1415}/E_{575} -see Section 6.2.2), for three blends of the standard weight ratios (1:20, 1:10, 1:6, 1:5, 1:3, 2:5), four pressings from each blend, four discs per blend and the Mean value.

a) Blend 1

Extinction Ratios (1:20)				Extinction Ratios (1:10)			
Disc 1	Disc 2	Disc 3	Disc 4	Disc 1	Disc 2	Disc 3	Disc 4
0.275	0.267	0.258	0.271	0.392	0.398	0.364	0.367
0.294	0.259	0.261	0.258	0.382	0.403	0.372	0.371
0.270	0.262	0.258	0.256	0.386	0.384	0.359	0.371
0.259	0.275	0.259	0.268	0.391	0.391	0.364	0.370
0.285	0.270	0.259	0.255	0.372	0.382	0.355	0.367
0.282	0.262	0.254	0.269	0.384	0.381	0.366	0.385
0.267	0.271	0.255	0.266	0.395	0.394	0.373	0.380
0.284	0.275	0.260	0.266	0.378	0.378	0.366	0.381
0.277	0.265	0.260	0.272	0.387	0.371	0.365	0.377
0.273	0.261	0.262	0.268	0.382	0.386	0.370	0.375
0.277 (sd 0.01)	0.267 (sd 0.006)	0.259 (sd 0.003)	0.265 (sd 0.006)	0.385 (sd 0.007)	0.387 (sd 0.01)	0.365 (sd 0.006)	0.374 (sd 0.011)

Extinction Ratios (1:6)				Extinction Ratios (1:5)			
Disc 1	Disc 2	Disc 3	Disc 4	Disc 1	Disc 2	Disc 3	Disc 4
0.557	0.573	0.547	0.552	0.644	0.650	0.679	0.659
0.553	0.571	0.555	0.545	0.634	0.645	0.682	0.657
0.558	0.567	0.551	0.556	0.657	0.657	0.688	0.660
0.551	0.571	0.571	0.576	0.653	0.674	0.678	0.663
0.549	0.561	0.556	0.543	0.662	0.660	0.689	0.657
0.546	0.569	0.557	0.572	0.641	0.657	0.689	0.680
0.547	0.558	0.568	0.572	0.643	0.658	0.672	0.666
0.559	0.563	0.555	0.558	0.656	0.657	0.681	0.656
0.544	0.562	0.559	0.551	0.647	0.656	0.679	0.669
0.557	0.565	0.565	0.556	0.638	0.677	0.670	0.666
0.552 (sd 0.005)	0.566 (sd 0.006)	0.558 (sd 0.007)	0.558 (sd 0.012)	0.648 (sd 0.009)	0.659 (sd 0.010)	0.681 (sd 0.007)	0.663 (sd 0.007)

Extinction Ratios (1:3)				Extinction Ratios (2:5)			
Disc 1	Disc 2	Disc 3	Disc 4	Disc 1	Disc 2	Disc 3	Disc 4
1.042	1.072	1.090	1.075	1.400	1.448	1.343	1.450
1.047	1.071	1.071	1.084	1.388	1.500	1.400	1.464
1.044	1.066	1.071	1.093	1.404	1.430	1.343	1.456
1.046	1.056	1.084	1.092	1.380	1.468	1.420	1.446
1.050	1.068	1.085	1.084	1.394	1.436	1.346	1.443
1.049	1.067	1.078	1.076	1.386	1.440	1.420	1.458
1.055	1.084	1.078	1.077	1.408	1.430	1.336	1.448
1.039	1.074	1.085	1.086	1.410	1.446	1.339	1.450
1.040	1.084	1.071	1.085	1.386	1.438	1.347	1.450
1.057	1.065	1.086	1.084	1.394	1.446	1.338	1.452
1.047 (sd 0.006)	1.071 (sd 0.009)	1.080 (sd 0.007)	1.084 (sd 0.006)	1.395 (sd 0.01)	1.448 (sd 0.021)	1.363 (sd 0.035)	1.452 (sd 0.006)

b) Blend 2

Extinction Ratios (1:20)				Extinction Ratios (1:10)			
Disc 1	Disc 2	Disc 3	Disc 4	Disc 1	Disc 2	Disc 3	Disc 4
0.201	0.208	0.195	0.188	0.335	0.343	0.393	0.324
0.196	0.206	0.198	0.176	0.343	0.343	0.378	0.330
0.193	0.204	0.200	0.175	0.355	0.352	0.391	0.328
0.208	0.210	0.187	0.180	0.332	0.355	0.356	0.343
0.197	0.212	0.190	0.189	0.356	0.341	0.370	0.336
0.200	0.205	0.203	0.172	0.360	0.336	0.379	0.335
0.211	0.206	0.176	0.170	0.345	0.350	0.359	0.332
0.198	0.201	0.182	0.167	0.336	0.345	0.364	0.325
0.209	0.204	0.186	0.180	0.342	0.330	0.374	0.332
0.207	0.210	0.189	0.178	0.349	0.357	0.389	0.328
0.203 (sd 0.006)	0.207 (sd 0.003)	0.191 (sd 0.008)	0.178 (sd 0.007)	0.345 (sd 0.01)	0.345 (sd 0.008)	0.375 (sd 0.013)	0.331 (sd 0.006)

Extinction Ratios (1:6)				Extinction Ratios (1:5)			
Disc 1	Disc 2	Disc 3	Disc 4	Disc 1	Disc 2	Disc 3	Disc 4
0.587	0.595	0.574	0.590	0.691	0.706	0.712	0.718
0.596	0.595	0.537	0.585	0.695	0.724	0.718	0.721
0.601	0.587	0.565	0.582	0.707	0.697	0.707	0.723
0.590	0.576	0.570	0.570	0.685	0.705	0.719	0.720
0.605	0.589	0.550	0.595	0.697	0.709	0.713	0.709
0.606	0.590	0.570	0.587	0.699	0.718	0.708	0.720
0.613	0.578	0.547	0.587	0.698	0.731	0.715	0.724
0.603	0.580	0.554	0.595	0.698	0.703	0.721	0.721
0.600	0.590	0.560	0.570	0.691	0.715	0.716	0.709
0.605	0.585	0.540	0.565	0.697	0.733	0.719	0.730
0.600 (sd 0.008)	0.587 (sd 0.007)	0.557 (sd 0.013)	0.583 (sd 0.011)	0.696 (sd 0.006)	0.714 (sd 0.012)	0.715 (sd 0.005)	0.720 (sd 0.006)

Extinction Ratios (1:3)				Extinction Ratios (2:5)			
Disc 1	Disc 2	Disc 3	Disc 4	Disc 1	Disc 2	Disc 3	Disc 4
1.097	1.085	1.100	1.111	1.345	1.311	1.336	1.400
1.070	1.108	1.108	1.089	1.363	1.338	1.483	1.388
1.102	1.098	1.089	1.103	1.348	1.333	1.507	1.404
1.083	1.090	1.098	1.094	1.342	1.332	1.346	1.380
1.088	1.089	1.107	1.107	1.388	1.338	1.480	1.394
1.111	1.090	1.099	1.084	1.368	1.320	1.484	1.386
1.090	1.108	1.099	1.085	1.359	1.341	1.490	1.408
1.096	1.108	1.119	1.071	1.363	1.316	1.338	1.410
1.077	1.105	1.098	1.118	1.356	1.330	1.438	1.386
1.084	1.114	1.100	1.104	1.358	1.323	1.500	1.394
1.090 (sd 0.012)	1.100 (sd 0.01)	1.102 (sd 0.008)	1.097 (sd 0.015)	1.359 (sd 0.013)	1.328 (sd 0.01)	1.440 (sd 0.072)	1.395 (sd 0.01)

c) Blend 3

Extinction Ratios (1:20)				Extinction Ratios (1:10)			
Disc 1	Disc 2	Disc 3	Disc 4	Disc 1	Disc 2	Disc 3	Disc 4
0.190	0.221	0.188	0.221	0.407	0.443	0.421	0.440
0.198	0.218	0.195	0.228	0.401	0.472	0.431	0.438
0.193	0.197	0.182	0.242	0.399	0.439	0.440	0.451
0.208	0.205	0.203	0.230	0.396	0.452	0.435	0.442
0.187	0.211	0.207	0.227	0.400	0.454	0.432	0.431
0.200	0.213	0.190	0.234	0.405	0.453	0.429	0.435
0.198	0.220	0.191	0.230	0.400	0.451	0.437	0.421
0.188	0.199	0.200	0.240	0.405	0.427	0.443	0.432
0.211	0.209	0.186	0.236	0.403	0.452	0.432	0.441
0.203	0.203	0.197	0.228	0.398	0.429	0.433	0.431
0.198 <i>(sd 0.008)</i>	0.210 <i>(sd 0.007)</i>	0.194 <i>(sd 0.008)</i>	0.232 <i>(sd 0.006)</i>	0.401 <i>(sd 0.004)</i>	0.447 <i>(sd 0.013)</i>	0.433 <i>(sd 0.006)</i>	0.436 <i>(sd 0.008)</i>

Extinction Ratios (1:6)				Extinction Ratios (1:5)			
Disc 1	Disc 2	Disc 3	Disc 4	Disc 1	Disc 2	Disc 3	Disc 4
0.575	0.563	0.561	0.572	0.669	0.672	0.683	0.680
0.570	0.562	0.553	0.573	0.668	0.673	0.691	0.675
0.569	0.569	0.555	0.569	0.673	0.667	0.693	0.673
0.578	0.561	0.550	0.565	0.679	0.675	0.694	0.669
0.571	0.572	0.563	0.557	0.681	0.669	0.687	0.675
0.565	0.556	0.570	0.562	0.683	0.675	0.671	0.674
0.573	0.567	0.557	0.570	0.675	0.682	0.687	0.683
0.560	0.563	0.553	0.571	0.675	0.684	0.694	0.672
0.561	0.563	0.569	0.568	0.674	0.682	0.690	0.684
0.572	0.571	0.558	0.564	0.667	0.680	0.685	0.672
0.569 <i>(sd 0.006)</i>	0.565 <i>(sd 0.005)</i>	0.559 <i>(sd 0.007)</i>	0.567 <i>(sd 0.005)</i>	0.674 <i>(sd 0.005)</i>	0.676 <i>(sd 0.006)</i>	0.688 <i>(sd 0.007)</i>	0.676 <i>(sd 0.005)</i>

Extinction Ratios (1:3)				Extinction Ratios (2:5)			
Disc 1	Disc 2	Disc 3	Disc 4	Disc 1	Disc 2	Disc 3	Disc 4
1.191	1.195	1.200	1.181	1.430	1.402	1.403	1.421
1.180	1.190	1.200	1.185	1.429	1.403	1.417	1.416
1.175	1.192	1.198	1.179	1.409	1.411	1.415	1.409
1.173	1.188	1.200	1.189	1.401	1.405	1.421	1.415
1.182	1.200	1.202	1.183	1.414	1.398	1.402	1.423
1.183	1.201	1.215	1.191	1.411	1.405	1.406	1.412
1.180	1.198	1.176	1.176	1.421	1.413	1.423	1.408
1.179	1.201	1.180	1.182	1.417	1.415	1.409	1.419
1.183	1.192	1.201	1.180	1.427	1.400	1.400	1.407
1.184	1.202	1.212	1.179	1.410	1.403	1.412	1.410
1.181 (nd 0.005)	1.196 (nd 0.005)	1.198 (nd 0.012)	1.183 (nd 0.005)	1.417 (nd 0.01)	1.406 (nd 0.006)	1.411 (nd 0.008)	1.414 (nd 0.006)

BIBLIOGRAPHY

- Amjad, Z. & Nancollas, G.H. (1979) Effects of fluoride on the growth of hydroxyapatite and human dental enamel. *Caries Research*, 13, 250-258.
- Angmar, B., Carlstrom, D. & Glas, J.E. (1963) Studies on the ultrastructure of dental enamel. The mineralisation of normal human enamel. *Journal of Ultrastructure Research*, 8, 12-23.
- Anic, L., Vidovic, D., Luic, M. & Tudja, M. (1992) Laser induced molar pulp chamber temperature changes. *Caries Research*, 26, 165-169.
- Arends, J. & Davidson, C.L. (1975) HPO_4^{2-} content in enamel and artificial carious lesions. *Calcified Tissue Research*, 18, 65-79.
- Arends, J., Schuthof, J. & Jongebloed, W.G. (1980) Lesion depth and microhardness indentations on artificial white spot lesions. *Caries Research*, 14, 190-195.
- Arends, J. & ten Cate, J.M. (1981) Tooth enamel remineralization. *Journal of Crystal Growth*, 53, 135-147.
- Arends, J., Christoffersen, J., Christoffersen, M.R. & Shuthof, J. (1983) Influence of fluoride concentration on the progress of demineralisation in bovine enamel at pH 4.5. *Caries Research*, 17, 455-457.
- Arends, J. & Christoffersen, J. (1986) The nature of early carious lesions in enamel. *Journal of Dental Research*, 65, 2-11.
- Arends, J. & Christoffersen, J. (1990) Nature and role of loosely bound fluoride in dental caries. *Journal of Dental Research*, 69, 601-605.
- Arends, J. & ten Bosch, J.J. (1992) Demineralisation and remineralisation evaluation techniques. *Journal of Dental Research*, 71, 924-928.
- Armstrong, W.D. & Brekhus, P.J. (1938) Possible relationship between the fluorine content of enamel and resistance to dental caries. *Journal of Dental Research*, 17, 393-399.
- Attin, T., Hartman, O., Hilgers, R.D. & Hellwig, E. (1995) Fluoride retention of incipient enamel lesions after treatment with a calcium fluoride varnish *in vivo*. *Archives of Oral Biology*, 40, 169-174.
- Backer Dirks, O. (1974) The benefits of water fluoridation. *Caries Research*, 8, 2-15.

- Bahar, A. & Tagomori, S. (1994) The effect of normal pulsed Nd-YAG laser irradiation on pits and fissures in human teeth. *Caries Research*, 28, 460-467.
- Bakhos, Y., Brudevold, F. & Aasenden, R. (1977) *In vivo* estimation of the permeability of surface human enamel. *Archives of Oral Biology*, 22, 599-603.
- Bennett, D.L. & Murray, J.J. (1973) Factors governing the use of topical fluorides: time and patient acceptability. *Journal of the International Association of Dentistry for Children*, 4, 15-19.
- Bohem, R., Baeschler, T., Webster, J. & Jauke, S. (1977) Laser processes in preventive dentistry. *Optical Engineering*, 16, 493-496.
- Borggreven, J.M.P.M., van Dijk, J.W.E. & Driessens, F.C.M. (1980) Effect of laser irradiation on the permeability of bovine dental enamel. *Archives of Oral Biology*, 25, 831-832.
- Boorsboom, P.C.F., van der Mei, H.C. & Arends, J. (1985) Enamel lesion formation with or without 0.12 ppm F in solution. *Caries Research*, 19, 396-402.
- Brannström, M., Gola, G., Nordenvall, K.J. & Torstenson, B. (1980) Invasion of microorganisms and some structural changes in incipient caries. *Caries Research*, 14, 276-284.
- Brown, W.E., Gregory, T.M. & Chow, L.C. (1977) Effects of fluoride on enamel solubility and cariostasis. *Caries Research*, 11, 118-141.
- Bruun, C. & Givskov, H. (1991) Formation of CaF₂ on sound enamel and in caries-like enamel lesions after different forms of fluoride applications *in vitro*. *Caries Research*, 25, 96-100.
- Brune, D. (1980) Interaction of pulsed carbon dioxide laser beams with teeth *in vitro*. *Scandinavian Journal of Dental Research*, 88, 301-305.
- Caldwell, R.C., Gilmore, R.W., Timberlake, P., Pigman, J. & Pigman, W. (1958) Semiquantitative studies of *in vitro* caries by microhardness tests. *Journal of Dental Research*, 37, 301-305.
- Carlström, D. (1964) Polarization microscopy of dental enamel with reference to incipient carious lesions. *Advances in Oral Biology*, 1, 255-296.
- Chang, Y.H., & Anderson, M.H. (1994) Using the Nd:YAG laser to selectively treat dental carious lesions. *Journal of Dental Research*, 73, 410.

- Christoffersen, J. & Christoffersen, M.R. (1981) Kinetics of dissolution of calcium hydroxyapatite. The effect of some biologically important inhibitors. *Journal of Crystal Growth*, 53, 42-54.
- Clark, D.C., Stamm, J.W. & Tessier, C. (1985) Results of a 32-month fluoride varnish study in Sherbrooke and Lac-Mégantic, Canada. *Journal of the American Dental Association*, 111, 949-953.
- Clarkson, B.H., Wefel, J., Edie, J. & Wilson, M. (1981) SEM and microprobe analyses of enamel-metal fluoride interactions. *Journal of Dental Research*, 60, 1912-1920.
- Clarkson, B.H., Wefel, J.S., Miller, J.S. (1984a) A model for producing caries-like lesions in enamel and dentin using oral bacteria *in vitro*. *Journal of Dental Research*, 63, 1186-1189.
- Clarkson, B.H., Wefel, J.S., Miller, I. & Edie, J. (1984b) Microprobe and SEM analysis of surface coatings on caries-like lesions in enamel after metal ion mordanting and APF application. *Journal of Dental Research*, 63, 106-110.
- Creanor, S.L. (1987) Remineralisation of the incipient enamel lesion. *University of Glasgow - PhD Thesis*, 190.
- Creanor, S.L., Strang, R., Telfer, S., MacDonald, I., Smith, A. & Stephen, K.W. (1986) *In situ* appliance for the investigation of Enamel de- and remineralisation. *Caries Research*, 20, 385-391.
- Creanor, S.L., Strang, R. & Stephen, K.W. (1989) Demineralization in acidified gelatin at different sites on the same enamel surface. *Caries Research*, 23, 345-347.
- Cruz, R., Ögaard, B. & Rölla, G. (1992) Uptake of KOH-soluble and KOH-insoluble fluoride in sound human enamel after topical application of a fluoride varnish (Duraphat) or a neutral 2% NaF solution *in vitro*. *Scandinavian Journal of Dental Research*, 100, 154-158.
- Darling, A.I. (1958) Studies of the early lesion of enamel caries. *British Dental Journal*, 105, 119-135.
- Davidson, C.L., Hoekstra, I.S. & Arends, J. (1974) Microhardness of sound, decalcified and etched tooth enamel related to the calcium content. *Caries Research*, 8, 135-144.
- Dean, H.T., Arnold, F.A. & Elvove, E. (1942) Domestic water and dental caries. Additional studies of the relation of fluoride domestic waters to dental caries experience in 4,425 white children aged 12-14 years of 13 cities in 4 states. *Public Health Report*, 57, 1155-1179.

- De Bruyn, H. & Arends, J. (1987) Fluoride varnishes. *Journal Biologie Buccale*, **15**, 71-82.
- De Josselin de Jong, E. & ten Bosch, J.J. (1985) Error analysis of the microradiographic determination of mineral content in mineralised tissue slices. *Physics in Medicine and Biology*, **30**, 1067-1075.
- De Josselin de Jong, E., ten Bosch, J.J. & Noordmans, J. (1987a) Optimized microcomputer-guided quantitative microradiography on dental mineralised tissue slices. *Physics in Medicine & Biology*, **32**, 887-899.
- De Josselin de Jong, E., van der Linden, A.H.I.M. & ten Bosch, J.J. (1987b) Longitudinal microradiography: a non-destructive automated quantitative method to follow mineral changes in mineralised tissue slices. *Physics in Medicine & Biology*, **32**, 1209-1220.
- Dijkman, T.G. & Arends, J. (1988) The role of 'CaF₂-like' material in topical fluoridation of enamel *in situ*. *Acta Odontologica Scandinavica*, **46**, 391-397.
- Duckworth, R.M. & Morgan, S.N. (1991) Oral fluoride retention after use of fluoride dentifrices. *Caries Research*, **25**, 123-129.
- Edenholm, H., Johnson, G., Koch, G. & Petersson, L.G. (1977) Fluoride uptake and release in deciduous enamel after application of fluoride varnishes. An *in vitro* pilot study. *Swedish Dental Journal*, **1**, 59-64.
- Eisenberg, A.D. & Marquis, R.E. (1980) Uptake of fluoride by cells of *Streptococcus mutans* in dense suspensions. *Journal of Dental Research*, **59**, 1187-1191.
- Ekstrand, J., Koch, G. & Petersson, L.G. (1980) Plasma fluoride concentration and urinary fluoride excretion in children following application of the fluoride containing varnish Duraphat. *Caries Research*, **14**, 185-189.
- El Feki, H., Rey, C. & Vignoles, M. (1991) Carbonate ions in apatites: infrared investigations in the ν_4 CO₃ domain. *Calcified Tissue International*, **49**, 269-274.
- Elliott, J.C., Holcomb, D.W. & Young, R.A. (1985) Infrared determination of the degree of substitution of hydroxyl by carbonate ions in human dental enamel. *Calcified Tissue International*, **37**, 372-375.
- Emerson, W.H. & Fischer, E.E. (1962) The infra-red absorption spectra of carbonate in calcified tissues. *Archives of Oral Biology*, **7**, 671-683.

- Evans, J.R., Robertson, W.G., Morgan, D.B. & Fleisch, H. (1980) Effects of pyrophosphate and diphosphates on the dissolution of hydroxyapatites using a flow system. *Calcified Tissue International*, 31, 153-159
- Featherstone, J.D.B., Duncan, J.F., Cuttress, T.W. (1978) Surface layer phenomenon in *in vitro* early caries like lesions of human tooth enamel. *Archives of Oral Biology*, 23, 397-404.
- Featherstone, J.D.B. & Mellberg, J.R. (1981) Relative rates of artificial carious lesions in bovine, ovine and human enamel. *Caries Research*, 15, 109-114.
- Featherstone, J.D.B. & Rodgers, B.E. (1981) Effect of acetic, lactic and other organic acids on the formation of artificial carious lesions. *Caries Research*, 15, 377-385.
- Featherstone, J.D.B., ten Cate, J.M., Shariati, M. & Arends, J. (1983) Comparison of artificial caries-like lesions by quantitative microradiography and microhardness profiles. *Caries Research*, 17, 385-391.
- Featherstone, J.D.B., Pearson, S. & LeGeros, R.Z. (1984) An infrared method for quantification of carbonate in carbonated apatites. *Caries Research*, 18, 63-66.
- Featherstone, J.D.B. & Nelson, D.G.A. (1987) Laser effects on dental hard tissues. *Advances in Dental Research*, 1, 21-26.
- Ferjerskov, O., Thylstrup, A. & Larsen, M.J. (1981) Rational use of fluorides in caries prevention. *Acta Odontologica Scandinavica*, 39, 241-249.
- Ferreira, J.M., Palamara, J., Phakey, P.P., Rachinger, W.A. & Orams, H.J. (1989) Effects of continuous-wave CO₂ laser on the ultrastructure of human dental enamel. *Archives of Oral Biology*, 34, 551-562.
- Flaitz, C.M., Hicks, M.J., Westerman, G.H., Berg, J.H., Blankenau, R.J. & Powell, G.L. (1995) Argon laser irradiation and acidulated phosphate fluoride treatment in caries-like lesion formation in enamel: an *in vitro* study. *Pediatric Dentistry*, 17, 31-35.
- Fleisch, H., Maerki, J. & Russell, R.G.G. (1966) Effect of pyrophosphate on dissolution of hydroxyapatite and its possible importance in calcium homeostasis. *Proceedings of the Society of Experimental Biology*, 122, 317-320.
- Fowler, B.O. & Kuroda, S. (1986) Changes in heated and in laser-irradiated human tooth enamel and their probable effects on solubility. *Calcified Tissue International*, 38, 197-208.

- Fox, J.L., Yu, D., Otsuka, M., Higuchi, W.I., Wong, J. & Powell, G.L. (1992) Combined effects of laser irradiation and chemical inhibitors on the dissolution of dental enamel. *Caries Research*, 26, 333-339.
- Frazier, P.P., Little, M.F. & Casciani, F.S. (1967) X-ray diffraction analysis of human enamel containing different amounts of fluoride. *Archives of Oral Biology*, 12, 35-42.
- Geddes, D.A.M. & McNee, S.G. (1982) The effect of 0.2 per cent (48 mM) NaF rinses daily on human plaque acidogenicity *in situ* (Stephan curve) and fluoride content. *Archives of Oral Biology*, 27, 765-769.
- Geddes, D.A.M., Weetman, D.A., Featherstone, J.D.B. & Shariati, M. (1986) Rapid *in vitro* mineral loss in human enamel following plaque / sucrose fermentation. *Caries Research*, 20, 169.
- Goodman, B.D. & Kaufman, H.W. (1977) Effects of an argon laser on the crystalline properties and rate of dissolution in acid of tooth enamel in the presence of sodium fluoride. *Journal of Dental Research*, 56, 1201-1207.
- Gordon, T.E. (1967) Single-surface cutting of normal tooth with ruby laser. *Journal of the American Dental Association*, 74, 398-402.
- Groeneveld, A. (1974) Dental Caries. Some aspects of artificial caries lesions examined by contact microradiography. *Ph.D Thesis*, University of Utrecht, The Netherlands.
- Hallsworth, A.S., Weatherell, J.A. & Robinson, C. (1973) Loss of carbonate during the first stages of enamel caries. *Caries Research*, 7, 345-348.
- Hamberg, L. (1971) Controlled trial of fluoride in vitamin drops for prevention of caries in children. *Lancet*, 1, 441-442.
- Hamilton, I.R. (1990) Biochemical effects of fluoride on Oral bacteria. *Journal of Dental Research*, 69, 660-667.
- Harvey, K., Slater, P.J. & Rodger, M.N. (1982) Natural white spot remineralisation *in vitro*. *Journal of Dental Research*, 61, 243.
- Herkströter, F.M. & ten Bosch, J.J. (1990) Wavelength-independent microradiography: A method for non-destructive quantification of enamel and dentin mineral concentrations using polychromatic X-rays. *Journal of Dental Research*, 69, 1522-1526.
- Hess, J.A. (1990) Scanning electron microscopic study of laser-induced morphologic changes of a coated enamel surface. *Lasers in Surgery and Medicine*, 10, 458-462.

- Hibst, R. & Keller, U. (1989) Experimental studies of the application of the Er:YAG laser on dental hard substances. *Lasers in Surgery and Medicine*, 9, 345-352.
- Hicks, M.J., Flaitz, C.M., Westerman, G.H., Berg, J.H., Blankenau, J.L. & Powell, G.L. (1993) Caries-like lesion initiation and progression in sound enamel following argon laser irradiation: An *in vitro* study. *Journal of Dentistry for Children*, 42, 201-206.
- Holager, J. (1970) Thermogravimetric examination of enamel and dentin. *Journal of Dental Research*, 49, 546-548.
- Holcomb, D.W. & Young, R.A. (1980) Thermal decomposition of human tooth enamel. *Calcified Tissue International*, 31, 189-201.
- Hülsemann, J. (1966) On the routine analysis of carbonates in unconsolidated sediments. *Journal of Sedimentary Petrology*, 36, 624-625.
- Ingram, G.S. & Fejerskov, O. (1986) A scanning electron microscope study of artificial caries lesion formation. *Caries Research*, 20, 32-39.
- Joyston-Bechal, S. & Kidd, E.A.M. (1980) Histopathological appearance of artificially produced caries-like lesions of enamel treated with APF during lesion formation *in vitro*. *Caries Research*, 14, 45-49.
- Kantola, S., Laine, E. & Tarna, T. (1973) Laser induced effects on tooth structure, 6 and 7. *Acta Odontologica Scandinavica*, 31, 369-388.
- Kay, M.I., Young, R.I. & Posner, A.S. (1964) Crystal structure of hydroxyapatite. *Nature*, 204, 1050.
- Kidd, E.A.M., Thylstrup, O., Fejerskov, O. & Silverstone, L.M. (1978) Histopathology of caries-like lesions created *in vitro* in fluorosed and sound enamel. *Caries Research*, 12, 268-274.
- Kidd, E.A.M. (1983) The histopathology of enamel caries in young and old permanent teeth. *British Dental Journal*, 155, 196-198.
- Kirkegaard, E. (1977) *In vitro* fluoride uptake in human dental enamel from four different dentifrices. *Caries Research*, 11, 24-29.
- Knoop, F.E., Peters, G.C. & Emerson, W.N. (1939) A sensitive pyramidal diamond tool for indentation measurements. *Journal of Research for the National Bureau of Standards*, 23, 39-61.
- Koch, G., Petersson, L.G., Gleeurup, A. & Lowstedt, E. (1982) Kinetics of fluorine in deciduous enamel after application of fluoride-containing varnish (Duraphat). *Swedish Dental Journal*, 6, 39-44.

- Koch, G., Hakeberg, M. & Petersson, L.G. (1988) Fluoride uptake on dry versus water-saliva wetted human enamel surfaces *in vitro* after topical application of a varnish (Duraphat) containing fluoride. *Swedish Dental Journal*, 12, 221-225.
- Koulourides, T., Feagin, F. & Pigman, W. (1965) Remineralisation of dental enamel by saliva *in vitro*. *Annals of the New York Academy of Sciences*, 131, 751-57.
- Koulourides, T. & Pigman, W. (1960) Studies on the rehardening of artificially softened enamel. *Journal of Dental Research*, 39, 198.
- Kuroda, S. & Fowler, B.O. (1984) Compositional, structural and phase changes in *in vitro* laser-irradiated human tooth enamel. *Calcified Tissue International*, 36, 361-369.
- Larsen, M.J. (1990) Chemical events during tooth dissolution. *Journal of Dental Research*, 69, 575-580.
- Larsen, M.J. & von der Fehr, F.R. (1976) Effect of fluoride on the saturation of an acetate buffer with respect to hydroxyapatite. *Archives of Oral Biology*, 21, 723-728.
- Larsen, M.J. & Jensen, S.J. (1985) An X-ray diffraction and solubility study of equilibration of human enamel-powder suspensions in fluoride-containing buffer. *Archives of Oral Biology*, 30, 471-475.
- Larsen, M.J. & Jensen, S.J. (1989) The Hydroxyapatite solubility product of human dental enamel as a function of pH in the range 4.6-7.6 at 20°C. *Archives of Oral Biology*, 34, 957-961.
- Launey, Y., Mordon, S. & Cornil, A. (1987) Thermal effects of laser on dental tissues. *Lasers in Surgery and Medicine*, 7, 473-477.
- Maiman, T.H. (1960) Stimulated optical radiation in ruby. *Nature*, 187, 493.
- Mallon, D.E. & Mellberg, J.R. (1985) Analysis of dental hard tissue by computerised microdensitometry. *Journal of Dental Research*, 64, 112-116.
- Margolis, H.C. & Moreno, E.C. (1985) Kinetic and thermodynamic aspects of enamel demineralisation. *Caries Research*, 19, 22-35.
- Margolis, H.C., Moreno, E.C. & Murphy, B.J. (1986) Effect of low levels of fluoride in solution on enamel demineralization *in vitro*. *Journal of Dental Research*, 6, 523-9.

- Marquis, R.E. (1990) Diminished acid tolerance of plaque bacteria caused by fluoride. *Journal of Dental Research*, 69, 672-675.
- Marthaler, T.M. (1969) Caries-inhibiting effect of fluoride tablets. *Helvetica Odontologica Acta*, 13, 1-13.
- McGadey, J., Payne, A.P., Creanor, S.L., Foye, R.H. & Whitters, C.J. (1994) An *in vitro* investigation to determine the effects of the pulsed Nd:YAG laser on artificial enamel white spot lesions. *Journal of Dental Research*, 73, 847.
- McWilliam, J. (1995) A laminated assessment of fluoride in white spot lesions after either *in situ* or *in vitro* fluoride exposure. *Journal of Dental Research*, 14, 10.
- Melcer, J., Chaumette, M.T., Melcer, F., Dejardin, J., Hasson, R., Meraud, R., Pinaudeau, Y. & Weill, R. (1984) Treatment of dental decay by CO₂ laser beam: Preliminary results. *Lasers in Surgery and Medicine*, 4, 311-421.
- Mellberg, J.R. (1992) Hard-tissue substrates for evaluation of cariogenic and anti-cariogenic activity *in situ*. *Journal of Dental Research*, 71, 913-919.
- Mellberg, J.R., Laakso, P.V. & Nicholson, C.R. (1966) The acquisition and loss of fluoride by topically fluoridated human tooth enamel. *Archives of Oral Biology*, 11, 1213-1220.
- Mellberg, J.R. & Loertscher, K.L. (1974) Comparison of *in vitro* fluoride uptake by human and bovine enamel from acidulated phosphate fluoride solutions. *Journal of Dental Research*, 53, 64-67.
- Morioka, T., Suzuki, K. & Tagomori, S. (1984) Effect of beam absorptive mediators on acid resistance of surface enamel by Nd-YAG laser irradiation. *Journal of Dental Health*, 34, 40-44.
- Myers, T.D. & Myers, W.D. (1985a) *In vivo* caries removal utilizing the YAG laser. *Journal of the Michigan Dental Association*, 67, 66-69.
- Myers, T.D. & Myers, W.D. (1985b) The use of a laser for debridement of incipient caries. *Journal of Prosthetic Dentistry*, 53, 776-779.
- Myers, T.D. & Myers, W.D. (1988) *In vitro* caries removal. *Californian Dental Association Journal*, 16, 9-11.
- Myers, T.D. (1991) Clinical procedures performed with the American Dental Laser. *The Institute for Laser Dentistry*, 16-22.

- Neev, J., Pham, K., Lee, J.P. & White, J.M. (1996) Dentin ablation with three infrared lasers. *Lasers in Surgery and Medicine*, 18, 121-128.
- Nelson, G.A. & Featherstone, J.D.B. (1982) Preparation, analysis, and characterization of carbonated apatites. *Calcified Tissue International*, 34, 69-72.
- Nelson, D.G.A. & Williamson, B.E. (1982) Low-temperature laser Raman spectroscopy of synthetic carbonated apatites and dental enamel. *Australian Journal of Chemistry*, 35, 715-727.
- Nelson, D.G.A., Featherstone, J.D.B., Duncan, J.F. & Cuttress, T.W. (1983) Effect of carbonate and fluoride on the dissolution behaviour of synthetic apatites. *Caries Research*, 17, 200-211.
- Nelson, D.G.A., Jongebloed, W.L., & Arends, J. (1984) Enamel surface treated with topical fluoride agents. TEM and XRD considerations. *Journal of Dental Research*, 6, 36-12.
- Nelson, D.G.A., Jongebloed, W.L. & Featherstone, J.D.B (1986a) Laser irradiation of human dental enamel and dentine. *New Zealand Dental Journal*, 82, 74-77.
- Nelson, D.G.A., Shariati, M., Glena, R., Shields, C.P. & Featherstone, J.D.B. (1986b) Effect of pulsed low energy infrared laser irradiation on artificial caries-like lesion formation. *Caries Research*, 20, 289-299.
- Nelson, D.G.A., Wefel, J.S., Jongebloed, W.L. & Featherstone, J.D.B. (1987) Morphology, histology and crystallography of human dental enamel treated with pulsed low-energy infrared laser radiation. *Caries Research*, 21, 411-426.
- Ögaard, B., Rölla, G. & Helgeland, K. (1984) Fluoride retention in sound and demineralised enamel *in vivo* after treatment with a fluoride varnish (Duraphat). *Scandinavian Journal of Dental Research*, 92, 190-197.
- Ögaard, B. Seppa, L. & Rölla, G. (1994) Professional topical fluoride applications - clinical efficacy and mechanism of action. *Advances in Dental Research*, 8, 190-201.
- Oho, T. & Morioka, T. (1990) A possible mechanism of acquired acid resistance of human dental enamel by laser irradiation. *Caries Research*, 24, 86-92.
- Palamara, J. Phakey, P.P. Orams, H.J. & Rachinger W.A. (1992) The effect on the ultrastructure of dental enamel of excimer-dye, argon-ion and CO₂ lasers. *Scanning Microscopy*, 6, 1061-1071.

- Patel, P.R. & Brown, W.E. (1975) Thermodynamic solubility product of human tooth enamel: powdered sample. *Journal of Dental Research*, **6**, 728-736.
- Pogrel, M.A., Muff, D.F. & Marshall, G.W. (1993) Structural changes in dental enamel induced by high energy continuous wave carbon dioxide laser. *Lasers in Surgery and Medicine*, **13**, 89-96.
- Poole, D.F.G., Mortimer, K.V., Darling, A.I. & Ollis, W.D. (1961) Molecular sieve behaviour of dental enamel. *Nature*, **189**, 998-1000.
- Purdell-Lewis, D.J., Groenveld, A. & Arends, J. (1976) Hardness tests on sound enamel and artificially demineralized white spot lesions. *Caries Research*, **10**, 201-215.
- Quintana, E., Marquez, F., Roca, I., Torres, V. & Salgado, J. (1992) Some morphologic changes induced by Nd:YAG laser on the noncoated enamel surface: A scanning electron microscopy study. *Lasers in Surgery and Medicine*, **12**, 131-136.
- Radvar, M., Creanor, S.L., Gilmour, W.H., Payne, A.P., McGadey, J., Foye, R.H., Whitters, C.J. & Kinane, D.F. (1995) An evaluation of the effects of an Nd:YAG laser on subgingival calculus, dentine and cementum. *Journal of Clinical Periodontology*, **22**, 71-77.
- Rentsch, H., Merte, K., Zschau, H.E., Plier, F., Otto, G. & Vogt, J. (1990) Fluoride and mineral redeposition in outermost layers of bovine enamel during surface softening. *Caries Research*, **24**, 97-100.
- Retief, D.H., Bradley, E.L., Holbrook, M. & Switzer, P. (1983) Enamel fluoride uptake, distribution and retention from topical fluoride agents. *Caries Research*, **17**, 44-51.
- Ripa, L.W. (1990) An evaluation of the use of professional (operator-applied) topical fluorides. *Journal of Dental Research*, **69**, 786-796.
- Robinson, C., Weatherell, J.A. & Hallsworth, A.S. (1981) Distribution of magnesium in mature dental enamel. *Caries Research*, **15**, 70-77.
- Robinson, C., Weatherell, J.A. & Hallsworth, A.S. (1983) Alterations in the composition of permanent human enamel during carious attack. In *Demineralisation and Remineralisation of the Teeth*, ed. Leach, S.A. & Edgar, W.M., pp. 209-223. IRL Press, Oxford.
- Rölla, G., Ögaard, B. & De Almeida Cruz, R. (1993) Topical application of fluorides on teeth. New concepts of mechanisms of interaction. *Journal of Clinical Periodontology*, **20**, 105-108.

- Rölla, G. & Saxegaard, E. (1990) Critical evaluation of the composition and use of topical fluorides with emphasis on the role of calcium fluoride in caries inhibition. *Journal of Dental Research*, 69, 780-785.
- Sato, K. (1983) Relation between acid dissolution and histological alteration of heated tooth enamel. *Caries Research*, 17, 490-495.
- Saxegaard, E. & Rölla, G. (1988) Fluoride acquisition on and in human enamel during topical application *in vitro*. *Scandinavian Journal of Dental Research*, 96, 523-535.
- Schamschula, R.G., Angus, H., Charlton, G., Duppenhaler, J.L. & Un, P. (1979) Associations between fluoride concentration in successive layers of human enamel and individual dental caries experience. *Archives of Oral Biology*, 24, 847-859.
- Schatz, B. (1955) Speculation on lactobacilli & acid as possible anticaries function. *New York Dental Journal*, 22, 161.
- Shellis, R.P. (1984a) Relationship between human enamel structure and the formation of caries-like lesions *in vitro*. *Archives of Oral Biology*, 29, 975-981.
- Shellis, R.P. (1984b) Variations in growth of the enamel crown in human teeth and a possible relationship between growth and enamel structure. *Archives of Oral Biology*, 29, 697-707.
- Shellis, P. & Duckworth, R.M. (1994) Studies on the cariostatic mechanisms of fluoride. *International Dental Journal*, 44, 263-73.
- Shellis, R.P. & Hallsworth, A.S. (1987) The use of scanning electron microscopy in studying enamel caries. *Scanning Microscopy*, 1, 1109-1123.
- Shellis, R.P. & Poole, D.F.G. (1985) Modified procedure for the quantitative estimation of pore volumes in carious enamel by polarizing microscopy. *Archives of Oral Biology*, 30, 865-868.
- Shern, R.J., Driscoll, W.S. & Korts, D.C. (1977) Enamel biopsy results of children receiving fluoride tablets. *Journal of the American Dental Association*, 95, 310-314.
- Silverstone, L.M. (1966) The translucent zone of enamel caries and artificial caries-like lesions. *British Dental Journal*, 120, 461-471.
- Silverstone, L.M. (1967) Observations on the dark zone in early enamel caries and in artificial caries-like lesions. *Caries Research*, 1, 261-274.

- Silverstone, L.M. (1968) The surface zone in carious and caries-like lesions produced *in vitro*. *British Dental Journal*, 125, 145-157.
- Silverstone, L.M. (1973) The structure of carious enamel. *Oral Science Review*, 41, 0-60.
- Silverstone, L.M. (1981) Enamel Caries. In *Dental caries: aetiology, pathology and prevention*, ed. Silverstone, L.M., Johnson, N.W., Hardie, J.M., Williams, R.A.D, p.142. Macmillan, London.
- Silverstone, L.M., Wefel, J.S., Zimmerman, B.H., Clarkson, B.H. & Featherstone, M.J. (1981) Remineralisation of natural and artificial lesions in human dental enamel *in vitro*. *Caries Research*, 15, 138-157.
- Silverstone, L.M. (1983) Remineralisation and enamel caries: significance of fluoride and effect on crystal diameters. In *Demineralisation and Remineralisation of the Teeth*, ed. Leach, S.A. & Edgar, W.M., pp. 185-205. IRL Press, Oxford.
- Sognaes RF, & Stern, R.H. (1965) Laser effect on dental hard tissue. *Journal of the Southern California Dental Association*, 33, 17-19.
- Sorvari, R., Meurman, J.H., Alakuijala, R. & Frank, R.M. (1994) Effect of fluoride varnish and solution on enamel erosion *in vitro*. *Caries Research*, 28, 227-232.
- Stephen, K.W. & Campbell, D. (1978) Caries reduction and cost benefit after 3 years of sucking fluoride tablets daily at school. *British Dental Journal*, 144, 202-206.
- Stephen, K.W., Boyle, I.T., Campbell, D., McNee, S., Fyffe, J.A., Jenkins, A.S. & Boyle, P. (1981) A 4-year double-blind fluoridated school milk study in a vitamin D deficient area. *British Dental Journal*, 151, 287-292.
- Stern, R.H. (1971) Dentistry and the Laser. In *Laser Applications in Medicine & Biology*, ed. Wohlsbarsht, M.E. pp. 361-388. Plenum Press, New York, London.
- Stern, R.H. & Sognaes, R.F. (1964) Laser beam effect on dental hard tissues. *Journal of Dental Research*, 43, 873.
- Stern, R.H., Sognaes, R.F. & Goodman, F. (1966) Laser effect on *in vitro* enamel permeability and solubility. *Journal of the American Dental Association*, 73, 838-843.
- Stern, R.H. & Sognaes, R.F. (1972) Laser inhibition of dental caries suggested by first tests *in vivo*. *Journal of the American Dental Association*, 85, 1087-1090.

- Stern, R.H., Vahl, J. & Sognaes, R.F. (1972) Lased enamel: ultrastructural observations of pulsed carbon dioxide laser effects. *Journal of Dental Research*, 51, 455-460.
- Strang, R., Macdonald, I.P.A. & Creanor, S.L. (1986) Mineral content variations in demineralised enamel. *Caries Research*, 20, 185.
- Strang, R., Damato, F.A., Creanor, S.L. & Stephen, K.W. (1987) The effect of baseline lesion mineral loss on *in situ* remineralisation. *Journal of Dental Research*, 66, 1644-1646.
- Strang, R., Damato, F.A. & Stephen, K.W. (1988) Comparison of *in vitro* demineralisation of enamel sections and slabs. *Caries Research*, 22, 348-349.
- Suda, H., Tokita, Y. & Sunakawa, M. (1995) The effects of pulsed Nd:YAG laser on the dental pulp. *Journal of Dental Research*, 74, 409.
- Suzuki, K., Morita, K. & Morioka, T. (1982) An increment of acid-resistance of dental enamel with the irradiation of various types of laser beam. *Journal of the Japanese Society of Laser Medicine*, 3, 613-618.
- Tagomori, S. & Iwase, T. (1995) Ultrastructural change of enamel exposed to a normal pulsed Nd:YAG laser. *Caries Research*, 29, 513-520.
- Tagomori, S. & Morioka, T. (1989) Combined effects of laser and fluoride on acid resistance of human dental enamel. *Caries Research*, 23, 225-231.
- Tanaka, M., Moreno, E.C. & Margolis, H.C. (1993) Effect of fluoride incorporation into human dental enamel on its demineralization *in vitro*. *Archives of Oral Biology*, 38, 863-869.
- Tasev, E., Delacretaz, G. & Wolste, L (1990) Drilling in human enamel and dentin with lasers: a comparative study. *SPIEE Laser Surgery: Advanced Characterisation, Therapeutics, and Systems II*, 1200, 437-445.
- Taylor, R., Shklar, G. & Roeber, F. (1965) The Effects of Laser radiation on teeth, dental pulp, and oral mucosa of animals. *Oral Surgery, Oral Medicine & Oral Pathology*, 19, 786.
- Ten Bosch, J.J. & Angmar-Mansson, B. (1991) A review of quantitative methods for studies of mineral content of intra-oral incipient caries lesions. *Journal of Dental Research*, 70, 2-14.
- Ten Cate, J.M. (1990) *In vitro* studies on the effects of fluoride on de- and remineralization. *Journal of Dental Research*, 69, 614-619.

- Ten Cate, J.M. (1992) Patient selection and appliance design in intra-oral models. *Journal of Dental Research*, 71, 908-910.
- Ten Cate, J.M. & Duijsters, P.P.E. (1982) Alternating demineralization and remineralization of artificial carious lesions. *Caries Research*, 16, 201-10.
- Ten Cate, J.M. & Duijsters, P.P.E. (1983a) Influence of fluoride in solution on tooth demineralisation, I. Chemical data. *Caries Research*, 17, 193-199.
- Ten Cate, J.M. & Duijsters, P.P.E. (1983b) Influence of fluoride in solution on tooth demineralisation, II. Microradiographic data. *Caries Research*, 17, 513-519.
- Toth, K. (1976) A study of 8 years domestic salt fluoridation for prevention of caries. *Community Dentistry & Oral Epidemiology*, 4, 106-110.
- Varughese, K. & Moreno, E.C. (1981) Crystal growth of calcium apatites in dilute solutions containing fluoride. *Calcified Tissue International*, 33, 431-439.
- Vignoles, M., Bonel, G., Holcomb, D.W. & Young, R.A. (1988) Influence of preparation conditions on the composition of type B carbonated hydroxyapatite and on the localization of the carbonate ions. *Calcified Tissue International*, 43, 33-40.
- Vogel, G.L., Carey, C.M., Chow, L.C., Gregory, T.M. & Brown, W.E. (1987) Ultramicro analysis of the fluid in human enamel during *in vitro* chemical attack by hydrochloric acid. *Caries Research*, 21, 310-325.
- Vogel, G.L., Carey, C.M., Chow, L.C., Gregory, T.M. & Brown, W.E. (1988) Micro-analysis of mineral saturation within enamel during lactic acid demineralisation. *Journal of Dental Research*, 67, 1172-1180.
- Weatherell, J.A. & Hargreaves, J.A. (1965) The micro-sampling of enamel in thin layers by means of strong acids. *Archives of Oral Biology*, 10, 139-142.
- Weatherell, J.A. & Robinson, C. (1968) Micro determination of carbonate in dental enamel. *Analyst*, 93, 244-249.
- Weatherell, J.A., Robinson, C. & Hiller, C.R. (1968) Distribution of carbonate in thin sections of dental enamel. *Caries Research*, 2, 1-9.
- Weatherell, J.A., Robinson, C., Strong, M. & Nakagaki, H. (1985) Micro-sampling by abrasion. *Caries Research*, 19, 97-102.

- Weatherell, J.A., Robinson, C. & Hallsworth, A.S. (1983) Formation of lesions in enamel using moist acid vapour. In *Demineralisation and Remineralisation of the Teeth*, ed. Leach, S.A. & Edgar, W.M., pp. 225-241. IRL Press, Oxford.
- Wefel, J.S. (1990) Effects of fluoride on caries development and progression using intra-oral models. *Journal of Dental Research*, 69, 626-633.
- Wei, S.H.Y. (1988) Time dependence of enamel fluoride acquisition from APF gels II. *In vivo study*. *Pediatric Dentistry*, 10, 173-176.
- Wespi, H.J. (1948) Gedanke zur frage der optimalen ernahrung in der Schwangerschaft. Salz and brot als trager zusatzlicher nahrungsstoffe. *Schweizerische Medizinische Wochenschrift*, 78, 153-155.
- White, D.J., Faller, R.V. & Bowman, W.D. (1992) Demineralisation and remineralisation evaluation techniques - added considerations. *Journal of Dental Research*, 71, 929-933.
- White, J.M., Goodis, H.E., Adame, S., Balcome, K.E., (1992) Caries removal and restoration in enamel using a Nd:YAG laser. *Journal of Dental Research*, 71, 140.
- White, J.M., Goodis, H.E., Hennings, D.R. & Ho, W. (1993) Dentin ablation rate using Nd:YAG and Er:YAG lasers. *Journal of Dental Research*, 73, 318.
- White, J.M., Goodis, H.E. & Pham, K. (1994) Ablation characteristics of nanosecond pulsed Nd:YAG laser on dentin. *Journal of Dental Research*, 73, 341.
- White, J.M., Goodis, H.E., Sekandari, N. & Fraser, D. (1994) Caries removal and restoration using a Nd:YAG laser. *Journal of Dental Research*, 73, 2465.
- White, J.M., Laurell, K.A., Goodis, H.E., Eakle, W.S., Cipra, D.L., Gegauff, A.G. & Setcos, J.C. (1995) Combined effects of Nd:YAG laser for caries removal in enamel. *Journal of Dental Research*, 74, 476.
- Wilson, P.R. & Beynon, A.D. (1989) Mineralisation differences between human deciduous and permanent enamel measured by quantitative microradiography. *Archives of Oral Biology*, 34, 85-88.
- Wong, L., Cutress, T.W. & Duncan, J.F. (1987) The influence of incorporated and adsorbed fluoride on the dissolution of powdered and pelletized hydroxyapatite in fluoridated and non-fluoridated acid buffers. *Journal of Dental Research*, 66, 1735-1741.

- Yamamoto, H. & Ooya, K. (1974) Potential of yttrium-aluminium-garnet laser in caries prevention. *Journal of Oral Pathology*, 3, 7-15.
- Yamamoto, H. & Sato, K. (1980) Prevention of dental caries by Nd:YAG laser irradiation. *Journal of Dental Research*, 59, 2171-2177.
- Zahradnik, R.T., Moreno, E.C. & Burke, E.J. Effect of salivary pellicle on enamel subsurface demineralisation *in vitro*. *Journal of Dental Research*, 55, 664-670.
- Zakariasen, K.L., Macdonald, R. & Boran, T. (1991) Spotlight on lasers: a look at potential benefits. *Journal of the American Dental Association*, 122, 58-62.
- Zero, D.T., Rahbek, I., Fu, J., Proskin, H.M. & Featherstone, J.D.B. (1990) Comparison of the iodide permeability test, the surface microhardness test and mineral dissolution of bovine enamel following acid challenge. *Caries Research*, 24, 181-185.

